Universität Bremen

Regulation of mycorrhiza induced genes:

Identification of *cis* elements

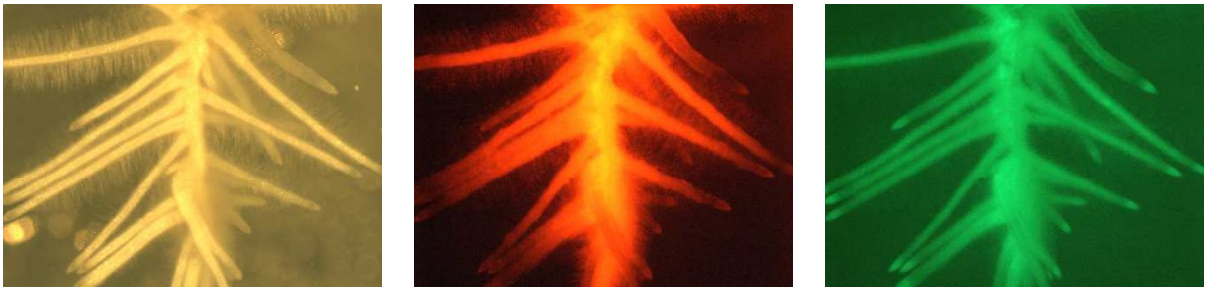

Dissertation

zur Erlangung des Grades eines

Doktors der Naturwissenschaften (*Dr. rer. nat.*)

im Fachbereich 2 (Biologie/Chemie)

vorgelegt von

Jana Müller

Bremen, Januar 2023

1. Examiner: Professor Dr. Uwe Nehls

2. Examiner: Professor em. Dr. Friederike Koenig

Tag des öffentlichen Kolloquiums: 17.03.2023

Table of contents

I. Zusammenfassung

Ektomykorrhiza ist eine mutualistische Interaktion zwischen höheren Landpflanzen und bestimmten Pilzen. Der pilzliche Partner erhält Kohlenhydrate von seinem Pflanzenpartner und liefert im Gegenzug verwertbaren Stickstoff und andere Nährelemente. Über die Mechanismen der Entstehung der Mykorrhizastruktur und welche Signale eine Rolle spielen damit beide Partner sich erkennen ist nicht viel bekannt. Allerdings wurde eine Reihe von Genen gefunden die in Abhängigkeit von Mykorrhizierungen differentiell reguliert sind. RNAsequencing und Mikroarray Analysen in der Arbeitsgruppe Nehls und anderen haben gezeigt, dass viele Gene in Wurzeln von Pappeln in Abhängigkeit von Mykorrhiza differentiell reguliert sind.

Es war das Ziel dieser Arbeit Mykorrhiza abhängige Elemente in den Promotersequenzen von zwei Genen, *Potrx6G1673* und *Potrx6G0093*, zu identifizieren. Dafür wurden entsprechende Promoterfragmente aus genomischer DNA amplifiziert und in transgenen Pappeln getestet. Hergestellt wurden Komposit Pappeln bei denen nur die Wurzeln transgen sind, nicht aber der Spross (Neb et al. 2017).

In dieser Arbeit wurden verschiedene visuelle Marker auf ihre Tauglichkeit überprüft, die entsprechenden Promoterfragmente in den Wurzeln zu visualisieren um eine differentielle Expression dieser Fragmente nachzuweisen. Als visuelle Marker wurden fluoreszierende Proteine ausgewählt, da diese Analysen *in vivo* ermöglichen. Zum Einen wurde super yellow fluorescent protein (sYFP) mit verschiedenen Promoterfragmenten in Pappelwurzeln getestet, allerdings ergaben sich aufgrund der geringen Größe des Fluoreszenzproteins nicht zufrieden stellende Ergebnisse im Bereich der Visualisierung. Diese Probleme traten sowohl bei sYFP mit Kernlokalisationssequenz als auch bei sYFP mit Peroxisomenlokalisationssequenz auf. Deswegen wurde double green fluorescent protein (dGFP) als Fluoreszenzmarker zur Visualisierung der Promoterfragmentaktivität etabliert. Im Verlauf der Arbeit zeigte sich, dass der ursprünglich ausgewählte binäre Vektor zur Pflanzentransformation, pGreen, nicht geeignet zur Lösung der Fragestellung dieser Arbeit war, weswegen die hergestellten Konstrukte in einen weiteren binären Pflanzentransformationsvektor, pCXUN, kloniert wurden. Dieses System aus binärem Vektor und dGFP als visuellem Marker wurde in verschiedenen

Versuchen etabliert und anschließend erfolgreich zur Untersuchung der differentiellen Expression von entsprechenden Pappel-Promoterfragmenten verwendet. Erste Ergebnisse deuten darauf hin, dass die beiden untersuchten Promotoren unterschiedlichen regulatorischen Mechanismen zu unterliegen scheinen.

II. Summary

Ectomycorrhiza is a mutualistic interaction between higher land plants and certain fungi. The fungal partner receives carbohydrates from its plant partner and in return provides usable nitrogen and other nutrients. Not much is known about the mechanisms of the formation of the mycorrhizal structure and which signals play a role in both partners recognising each other. However, a number of genes have been found to be differentially regulated depending on mycorrhization. RNAsequencing and microarray analyses in the research group of Nehls and others have shown that many genes in poplar roots are differentially regulated depending on mycorrhiza.

The aim of this work was to identify mycorrhiza-dependent elements in the promoter sequences of two genes, *Potrx6G1673* and *Potrx6G0093*. For this purpose, corresponding promoter fragments were amplified from genomic DNA and tested in transgenic poplars. Composite poplars were produced in which only the roots are transgenic, but not the shoots (Neb et al. 2017).

In this work, different visual markers were tested for their suitability to visualise the corresponding promoter fragments in the roots in order to detect differential expression of these fragments. Fluorescent proteins were chosen as visual markers because they allow *in vivo* analyses. On the one hand, super yellow fluorescent protein (sYFP) was tested with different promoter fragments in poplar roots, but due to the small size of the fluorescent protein, the visualisation results were not satisfactory. These problems occurred with both sYFP with nuclear localisation sequence and sYFP with peroxisomal localisation sequence. Therefore, double green fluorescent protein (dGFP) was established as a fluorescent marker for visualising promoter fragment activity. In the course of the work, it became apparent that the originally selected binary vector for plant transformation, pGreen, was not suitable for answering the research question of this work, so the produced constructs were cloned into another binary plant transformation vector, pCXUN. This system of binary vector and dGFP as visual marker was established in various experiments and subsequently successfully used to study the differential expression of corresponding poplar promoter fragments. Initial results indicate that the two promoters investigated appear to be subject to different regulatory mechanisms.

1 Introduction

1.1 The Rhizosphere

Soil is one of the most populous habitats on earth. Among plant roots, insects and other macroscopic life forms, myriads of microorganisms, bacteria and fungi are present (Curtis et al. 2002; Buée et al. 2009). Whenever different organisms occupy the same habitat, they have to cope with each other. Thus it is not surprising, that already in 1904, the term “rhizosphere” was introduced by Lorenz Hiltner to describe a zone around the root in which plants and microorganisms interact with each other (Hiltner 1904). In order to survive in this hotspot of competition, plants need to distinguish between “friends”, mutualistic organisms that can contribute to plant health, nutrition, defence and stress tolerance upon interaction, and “foes”, pathogenic organisms with negative effects on plant growth, health and nutrition status (for reviews, see Yu et al. 2019; Berendsen et al. 2012; Bakker et al. 2013; Pieterse et al. 2016).

One of these mutualistic interactions between the roots of higher land plants and fungi is called mycorrhiza.

1.2 Mycorrhiza

Colonisation of land by the first plants 500 million years ago was likely only possible due to their associations with fungi (Field and Pressel 2018). This mutualistic interaction between plants and fungi is called mycorrhiza, a term which was first used in 1885 by Frank and is a word composition of the greek words *mýkēs*, "fungus" and *rhiza*, "root" to describe the extensive interaction between plant roots of higher land plants and certain soil borne fungi (Frank 1885; Trappe 2005). In 1991, it was proposed that plants associating with mycorrhiza fungi predominate their habitats because the fungi contribute to plant nutrition (Read 1991). Since then, this hypothesis has been further supported (for reviews, see Varma et al. 2017; Read and Perez-Moreno 2003; Mohammadi et al. 2011; Guerrero-Galán et al. 2019; Gahan and Schmalenberger 2014) and might explain why a majority of terrestrial plants form mycorrhiza (Smith and Read 2008). Brundrett (2009) reviewed mycorrhizal literature and summarised that roughly 95 % of angiosperms form mycorrhiza in some way and only angio-

sperms with parasitic or carnivory survival strategies, plants with cluster roots or plants adopted to disturbed, nutrient rich environments do not.

Mycorrhizas have been found in nearly all ecosystems and have a huge impact on plant growth and productivity. Where mycorrhiza are present, they play fundamental roles in carbon, nitrogen and phosphorus cycling and thus impact whole ecosystems (for a review, see van der Heijden et al. 2015).

Mycorrhizas are quite variable in structure, since a vast amount of different fungi and plant partners are involved. In their majority they all have two common features: An interface between plant and fungal cells for substrate and metabolite exchange and extraradical hyphae in the soil surrounding the root for substrate acquisition (Johnsen and Gehring 2007). These extraradical hyphae expand the nutrient uptake capacity of plant roots by far since they have a much higher surface for nutrient absorption and can proliferate into smaller soil pores than plant fine roots (Johnsen and Gehring 2007).

There are only four main characterised types of mycorrhiza: arbuscular mycorrhiza, ectomycorrhiza, orchid mycorrhiza and ericoid mycorrhiza (Smith and Read 2008). Arbuscular and orchid mycorrhiza are termed endomycorrhiza. Ericoid mycorrhiza show structures of both ecto- and endomycorrhiza (Smith and Read 2008). As the focus of this work is on ectomycorrhiza, only this type will be further introduced.

1.2.1 Ectomycorrhiza (ECM)

Ectomycorrhiza are frequently characterised by a thick hyphae mantle covering the whole colonised root and a Hartig net, where hyphae are growing in the apoplastic space of colonised root epidermal and cortex cells (Smith and Read 2008). Colonised roots do not develop root hairs since their function is overtaken by the hyphae.

There are roughly 20 000 fungal species known, mainly from the phyla Basidiomycota and Ascomycota, which form mycorrhiza with approximately 6000 plant species, mostly woody perennials (Smith and Read 2008; Brundrett 2009; van der Heijden et al. 2015). Ectomycorrhiza association is the dominant type in temperate and boreal forests and play an important role in carbon and nitrogen cycling and thus forest productivity (Smith and Read 2008). Ectomycorrhizal fungi obtain up to 20 % of photosynthates from their host plant (Hobbie

2006) and in turn can increase plant nitrogen supply by up to 80 % (Hobbie and Hobbie 2006). In addition to nitrogen, the fungus can also provide a range of macronutrients, including phosphate, potassium, calcium, magnesium, sulphur, and micronutrients, such as iron, zinc, copper, and manganese (for a review, see Becquer et al. 2019).

In order to establish a symbiotic or mutualistic relationship, plants and fungi need to communicate with each other. Although recent studies elucidated some of the factors necessary for successful establishment of ectomycorrhizas, most aspects are not known so far. The majority of answers known today come from the mycorrhiza interaction of *Populus spec.* / *Laccaria bicolor* and *Eucalyptus spec.* / *Pisolithus spec.*

For the ECM fungus *Laccaria bicolor*, genes coding for small secreted proteins termed Myccorhizal Induced Small Secreted Proteins (MISSPs) are highly upregulated in mycorrhiza (Martin et al. 2008). *MISSP7* encodes for an effector protein necessary for the formation of ectomycorrhiza (Kang et al. 2020) and is secreted by the fungus upon sensing the flavonoid rutin from plant host roots (Plett and Martin 2012). *Laccaria bicolor* mutants with lower *MISSP7* expression have been shown to be incapable in forming the Hartig net in their plant host (Plett et al. 2011). It also has been elucidated that MISSP7, once located in the nucleus of the host plant cell, interferes with the jasmonate signalling pathway by interacting with the transcriptional repressor Jasmonate Zim Domain protein 6 (JAZ6) and thus reduces plant defence responses (Plett et al. 2014a, 2014b). Other MISSPs, like MISSP8, putatively modulating hyphae aggregation in early stages of symbiosis, have also been found to be crucial for the establishment of symbiosis (Pellegrin et al. 2019).In total, it has been found that *Laccaria bicolor* expresses a core gene regulon during colonisation of different hosts (Plett et al. 2015).

Recent studies hint to the involvement of the common symbiosis signalling pathway in the establishment of ectomycorrhiza (Cope et al. 2019). The common symbiosis signalling pathway is an evolutionary conserved network of genes required for the establishment of arbuscular mycorrhiza and plant-rhizobia interactions (for reviews, see Geurts et al. 2016; Delaux et al. 2015; Martin et al. 2017). It was found that *Laccaria bicolor* produces lipochitooligosaccharides (Cope et al. 2019), signalling molecules which were first found in rhizobia (Lerouge et al. 1990). Cope et al. (2019) showed, that lipochitooligosaccharides of *Laccaria bicolor* induce CASTOR/POLLUX-dependent calcium spiking in *Populus*. In arbuscular mycorrhiza, calcium

spiking activates downstream protein kinases which in turn phosphorylate and thus activate certain transcription factors necessary for the development of symbiosis (for a review, see Luginbuehl and Oldroyd 2017).

Additionally to effector molecules produced by the fungal partner of ectomycorrhiza symbiosis, the plant partner is also capable of altering gene expression in the fungus. For *Populus trichocarpa*, there are also known small secreted proteins (SSPs) capable of translocating into the nucleus of *Laccaria bicolor* during symbiosis and altering gene expression (Plett et al. 2017). Plett et al. 2017 showed that SSPs of *Populus trichocarpa* can influence hyphal branching in *Pisolithus microcarpus*, *Suillus granulatus* and *Laccaria bicolor*.

All these examples show that ectomycorrhiza formation is a tightly controlled process where both the fungal and the plant partner influence each other to form a symbiotic unit. Research has come a long way and many pieces of the symbiosis puzzle have been found, but still the exact mechanism of ectomycorrhiza formation is not known so far.

1.3 Model organisms

1.3.1 Ectomycorrhiza fungi

1.3.1.1 Amanita muscaria

Amanita muscaria, the fly agaric, is a member of the phylum Basidiomycota. *A. muscaria* is native to temperate and boreal forests and capable in ectomycorrhiza formation with a broad host range (Trappe 1987). It can be propagated easily under sterile laboratory conditions (Chambers et al. 1999). There is strong evidence that *Amanita muscaria* is actually a species complex with cryptic speciation events and strong inter and intra continental phylogeografic structuring (Geml et al. 2006, 2008). The genome of *A. muscaria* var. *guessowii* , native to the East Coast of North America, has been sequenced (Kohler et al. 2015). It has been shown that *Amanita muscaria*, among other ECM forming *Amanita* species, has lost several genes in decomposition pathways, like cellulases necessary for the breakdown of plant cell walls, making it highly likely that ECM *Amanita* species will rely solely on carbon from the host plant (Wolfe et al. 2012).

1.3.1.2 Pisolithus microcarpus

Pisolithus microcarpus is a globally distributed ECM forming fungus of the phylum Basidiomycota. *Pisolithus* species show a wide range of ectomycorrhiza formation with different host plants (Chambers et al. 1999). A lot of studies focused on the relationship between *Pisolithus* and *Eucalyptus* species (e.g. Alves et al. 2010; Dauphin et al. 2006, 2007; Plett et al. 2020). The genome of *P. microcarpus* has been sequenced (Kohler et al. 2015), giving more insights into ectomycorrhiza formation.

P. microcarpus is easily maintained and propagated under sterile conditions (Chambers et al. 1999) and can be transformed via *Agrobacteria* (Pardo et al. 2005).

1.3.2 Plants

1.3.2.1 Nicotiana benthamiana

Next to *Arabidopsis thaliana*, *Nicotiana benthamiana* nowadays is one of the most popular model plants. Primary used as a testing system for different viruses, it emerged to be used in many different applications such as plant microbe interaction testing, vaccine production, metabolic pathways elucidation, gene silencing, protein localisation and protein expression (for reviews, see Goodin et al. 2008; Bally et al. 2018). In this study, *Nicotiana benthamiana* was used as a system for sub cellular protein localization as well as for pre-screenings of different vector systems using *Agrobacterium* mediated leaf infiltration.

1.3.2.2 Populus

The genus *Populus* (poplar/aspen/cottonwood) in the order Malpighiales (family Salicaceae) contains roughly 30 tree species native to the Northern hemisphere. Poplar wood is used extensively by mankind for pulp and paper, veneer, excelsior wood wool, construction material, lumber and energy, but trees are also planted as windbreaks, for erosion control and phytoremediation (Bradshaw et al. 2000).

Populus species are "dual-mycorrhiza" plants, capable of forming arbuscular as well as ectomycorrhiza with respective fungal partners (Teste et al. 2020; Jansson and Douglas 2007).

Poplar is one of the best studied tree model organisms and *Populus trichocarpa* was the first tree species to be fully sequenced (Tuskan et al. 2006). Recently, the genome of *Populus alba* has also been unravelled (Ma et al. 2019). Poplars have some characteristics making them

good model organisms to study various questions. They are relatively fast growing trees and vegetative propagation in vitro is possible. Their genome size is moderate (550 MB) and they are amenable for different transformation techniques (for reviews, see Bradshaw et al. 2000; Brunner et al. 2004; Jansson and Douglas 2007).

Because *Populus trichocarpa* does not grow well under sterile laboratory conditions (Nehls, personal communication), two hybrid poplars, *Populus tremula x tremuloides* (T89, Tuominen et al. 1995) and *Populus tremula x alba* (No. 7171-B4, Institut de la Recherche Agronomique, INRA) were used in this study. For *P. tremula x alba*, there is a draft genome sequence available (Mader et al. 2016).

1.4 Plant transformation

Plant transformation is a process, in which DNA is transferred into plant cells. Stable plant transformation results in stable transgenics, meaning the introduced DNA will be incorporated into the host's genome and will be inherited by the offspring. Fully transgenic plants are usually retrieved from tissue cultures or single transformed cells (for a review, see Hansen and Wright 1999). Thus, stable plant transformation often is a time consuming process, taking some months to years depending on the plant species. Transformation however can also be done transiently, meaning the expression of the transgene will only last for a few days to weeks and DNA copies are not integrated into the genome (for a review, see Krenek et al. 2015). Transient transformation techniques generate transgenic plants much faster (usually within a few days) than stable transformation strategies, but no stable genetic lines can be generated.

Often, *N. benthamiana* leaves are used for heterologous transient gene expression. However, in heterologous expression systems, it is possible that certain elements needed for the functionality of the gene of interest are missing. Also, if the promoter of interest is not expressed anymore in an organ specific manner it might cause tissue specific artefacts (Hernandez-Garcia and Finer 2014). Furthermore, artefacts may arise due to the high gene expression since high copy numbers are brought into the cells (Li 2011).

Another method to obtain transgenic plants in a shorter amount of time compared to stable transformation are composite plants. Composite plants consist of untransformed shoots and a transformed root system, making it an ideal test system for root centred biological questions. *Agrobacterium rhizogenes* has been used in many approaches to generate composite plants (Kan 2006). Studies on microbe/root interactions, mycorrhiza formation, metabolism, promoter analyses and gene function, among others, can be performed (Hansen et al. 1989; Kan 2006; Veena and Taylor 2007). Compared to traditional generation of transgenic plants by *Agrobacterium tumefaciens*, composite plants are obtained much faster (a few weeks compared to a few months). In contrast to root tissue culture based transformation, no specific equipment or specialised infrastructure is needed for the generation and maintenance of composite plants (Collier et al. 2005). Visual markers, such as β-Glucuronidase or fluorescence proteins can be used to study protein function or localisation and promoter analyses in the composite plant (Veena and Taylor 2007). However, transformed roots cannot be selected by antibiotic resistances, since the shoot remains untransformed and therefore is not gaining antibiotic resistance. Furthermore, while transgenic roots always carry the tDNA from the native *A. rhizogenes* Ri plasmid, they do not necessarily harbour the tDNA from a binary vector by which *A. rhizogenes* has been transformed (see 1.4.2). While some roots are co-transformed with both tDNAs others are not and co-transformation frequently can differ substantiously. Thus, identification of desired transgenic roots must be performed. Also, it has to be taken into consideration that each emerging root is a single transformation event and no root will be genetically identical to another root since the tDNA will not integrate always at the same positions.

Plant transformation techniques are nowadays used for a vast amount of different reasons. Stable transformation can increase agronomic traits and plant productivity as well as the nutritional value of selected plants. Transient transformation is used for the fast and reliable production of pharmaceuticals or recombinant proteins, metabolic functioning assays and functional protein studies (for a review, see Newell 2000).

Plant transformation can be achieved via direct techniques (e.g. particle bombardment, protoplast transformation, tissue electroporation) or via indirect techniques like *Agrobacterium* mediated transformation.

1.4.1 *Agrobacterium* mediated transformation

Agrobacterium is a genus of gram negative plant pathogenic bacteria inducing tumours in plant tissues (Smith and Townsend 1907). 70 years after the discovery of this plant pathogen, it was elucidated that this genus is capable of horizontal gene transfer from the bacterium to the plant, making it the only organism capable of natural gene transfer between kingdoms of life (Fürner et al. 1986; Tzfira and Citovsky 2008). This phenomenon led to the establishment of *Agrobacterium* as a powerful tool for genetic engineering of plants.

The genus *Agrobacterium* has been reassessed several times and species within the genus were added or removed. Also, there is an ongoing debate on whether or not *Agrobacterium* should be merged with the genus *Rhizobium* due to their close relationship (Tzfira and Citovsky 2008). Species within the genus are often described based on their disease symptoms and host range. The type of symptoms an *Agrobacterium* species causes is determined by the plasmid it harbours. A rough classification of these plasmids is whether they induce tumours (tumour inducing (Ti) plasmids, *Agrobacterium tumefaciens*) or roots (Root inducing (Ri) plasmids, *Agrobacterium rhizogenes*). Exchange of Ti and Ri plasmids easily changes the disease type of species (Gelvin 2003). The genus *Agrobacterium* is able to infect certain hosts in nature and the compatibility seems to depend on certain genes on the Ti/Ri plasmid like *virC* and *virF* (virulence genes C and F), but also on the interaction with Ti/Ri plasmids and the chromosomal background of the *Agrobacterium* species and multiple genetic factors in the plant host (Gelvin 2003). Under laboratory conditions, the host range of *Agrobacterium* is extended to many more plant species and even fungi (Veena and Taylor 2007).

Agrobacteria are capable of integrating part of their DNA into the genome of their host. The DNA that is transferred is called transfer DNA (tDNA). This tDNA is flanked by short 24 bp long direct repeats, called borders. The tDNA usually contains genes for the synthesis of plant phytohormones (like auxin) and opines or for genes modulating their reception. After integration of the tDNA into the genome of the plant host, the plant will start producing the phytohormones, thus altering its phytohormone composition, which will lead to the formation of tumours or roots. It will also start to produce opines, which the *Agrobacteria* use as a carbon and nitrogen source. *Agrobacteria* thus hijack the protein synthesis machinery of the plant to generate a safe living environment and stable nutrient supply.

The mechanism of interaction between *Agrobacteria* and their plant hosts has been studied intensively in the past years and can be described by the following steps (McCullen and Binns 2006):

I.) Chemical recognition of the plant host lead to the activation of virulence genes; movement towards potential host

II.) Physical interaction of bacterium and host.

III.) Synthesis of transfer machinery and substrates to be transferred.

IV.) Transfer of substrates.

V.) Transfer of substrates to the nucleus, integration of tDNA into the genome.

VI.) Expression of tDNA.

Two virulence genes, *virA* and *virG*, are constitutively expressed at low levels and are highly upregulated upon sensing certain plant exudates (e.g. phenols like acetosyringone). Additionally, higher sugar concentration and a low pH are needed for the induction of signalling cascades further inducing the production of the virulence cassettes. Sugars associated with cell wall synthesis, a low pH and phenolic compounds are all associated with wounding in plant cells, and these wounding sites are usually entry sites for *Agrobacteria*. VirG activates the transcription of other *vir* genes (McCullen and Binns 2006). Among them *vir*D1 and *vir*D2 encode for endonucleases cutting the tDNA at the border sequences, generating a single stranded tDNA. VirD2 stays attached to the 5' end of the tDNA, stabilising the complex and protecting it from plant endonucleases. Additionally, the virD2 carries a nuclear localisation signal, which will lead the virD2/tDNA complex to the plant cell nucleus. This complex is transferred through a type 4 secretion system comprised of virB and virD4 proteins into the plant cell. VirE2, which is also transferred into the plant cell through the virB/virD4 channel, is then attached to the virD2/tDNA complex, attaching another nuclear localisation signal and further stabilising the complex (Permyakova et al. 2009). This virD2/tDNA/virE2 complex is then transferred to the plant nucleus, where the tDNA is integrated into the plant genome. Earlier, it was postulated that the tDNA is integrated favourably into actively transcribed and promoter regions of the genome, but later studies found that these results possibly can be attributed to a bias from used selection markers in analysed tissues (for a review, see Gelvin 2017). However, there is evidence that proteins involved in chromatin modifica-

tion might play a role in the integration process of the tDNA and this indicates that tDNA preferably integrates into euchromatic regions (for a review, see Gelvin and Kim 2007). It was shown that *Arabidopsis* plants with a tDNA integration into the 3'-UTR of *HTA1*, a core histone protein, are resistant to stable transformation with *Agrobacterium* but transient transformation is not impaired, indicating that certain core histone proteins play a crucial role in tDNA integration (Mysore et al. 2000). Wherever the tDNA is integrated into the plant genome, transgene expression then is mediated by the surroundings, e.g. chromatin structure and expression of adjacent genes. Koncz and Schell (1986) showed that a promoterless *nptII* gene positioned near the tDNA borders leads to up to 30 % of *nptII* expressing plants in experiments with *Arabidopsis* and tobacco. This indicates that genes on the tDNAs are influenced by adjacent promoters in the plant genome. On the other hand, subsequent transgene silencing due to tandem repeat integrations or DNA methylation might also occur (Gelvin 2003; Gelvin and Kim 2007).

1.4.1.1 Agrobacterium rhizogenes

Infection of plants via *Agrobacterium rhizogenes* causes the so called hairy root disease (Riker et al. 1930). Newly developed roots are formed by infected plant cells which are structurally similar to wild type roots. However the roots caused by *A. rhizogenes* infection are frequently longer, more branched and have an agravitropic phenotype (Veena and Taylor 2007). Hairy roots maintain classical root functions and stably transformed plants can be recovered from infected root tissue (Tepfer 1984). Specific for *Agrobacterium rhizogenes* is the Ri plasmid. The tDNA on this plasmid contains *rol* genes (root oncogenic loci), which presumably alter hormone perception of host plants and therefore are thought to be indirectly responsible for the hairy root phenotype (Bahramnejad et al. 2019).

Under laboratory conditions, *A. rhizogenes* is capable of transforming over 450 plant species, depending on the strain (Veena and Taylor 2007). Among them, *A. rhizogenes* K599 (NCPPB2659) is a hypervirulent strain of the cucumopine type, capable of infecting a variety of different plant species (Savka et al. 1990; Veena and Taylor 2007). It was shown to be capable of generating composite poplar in previous studies (Neb et al. 2017).

1.4.2 Binary vector systems

Every gene located between the left and the right border in the tDNA of the Ti and Ri plasmids of *Agrobacteria* is incorporated into the host plant cell genome. However, direct manipulation of the Ti or Ri plasmids is difficult, since they are usually at least 200 kb in size (Gordon and Christie 2014), are present in low copy numbers in *Agrobacterium* and do not replicate in *E. coli* (Lee and Gelvin 2007). But it was found that the *vir* genes required for the DNA transfer and the tDNA itself could be present on different replicons. This led to the development of binary vector systems for *Agrobacterium* mediated transformation (Lee and Gelvin 2007). The vector containing the *vir* genes is termed the vir helper plasmid and is usually present in the *Agrobacterium* strain used for plant transformation. A second, much smaller plasmid is designed such that the genes of interest are integrated between artificial left and right borders. This plasmid is called binary vector and usually contains antibiotic resistances to screen for the presence of this vector in bacteria (Hellens et al. 2000). For cloning purposes, the binary vector contains origins of replication for *E. coli* as well as for *Agrobacteria*. For easier identification of transgenic cells later in plant experiments, the tDNA on the binary vector can also contain visual markers or antibiotic resistance genes (Hellens et al. 2000; Lee and Gelvin 2007).

In this study, two different binary vector systems were used.

pGREEN based vectors (Hellens et al. 2000) are based on a relatively small backbone (approximately 3 kb) and harbour a *pColE1 ori*, making them high copy vectors in *E. coli*. For the replication in *Agrobacterium*, the *pSA ori* is used. Such *pSA ori* require the activity of *repA* in *Agrobacterium*. *RepA* is present in *trans* on a helper plasmid, (e.g. pSOUP) and is needed for all *Agrobacterium* strains that do not carry an intrinsic *repA*. All pGREEN vectors have a kanamycin resistance gene for the selection of transformants. Different vectors were generated by De Rybel et al. (2011) for promoter studies with different combinations of promoter and fluorescent reporter genes. All vectors contain a multiple cloning site and a ligation independent cloning (LIC) site (De Rybel et al. 2011).

Additionally, pCAMBIA vectors based on pCXUN-FLAG (Chen et al. 2009) were used as a basis for construction. The pCXUN vector backbone is approximately 6 kb in size and carries the *pBR ori* for replication in *E. coli*, the *pVS1 STA* replicon for replication in *Agrobacterium*, as

well as a kanamycin resistance gene for the selection of positive transformants in *E.coli*. The vector also contains a multiple cloning site and a LIC-site.

1.5 Ligation Independent Cloning (LIC)

Ligation independent cloning (LIC) is a technique for inserting DNA fragments of interest in a defined orientation without the need of particular restriction sites at their ends (Aslanidis and de Jong 1990).

For this technique, a vector with a special LIC site is required containing a blunt end restriction endonuclease recognition site which is flanked at both ends by 16 bp long sequence stretches, the LIC adapters. Within this LIC adapter sequences, one particular nucleotide is only present at position 16 counting from the endonuclease cleaving site (**Figure 1**A). The fragment of interest is PCR amplified with primers containing compatible LIC adapter sequences containing a unique nucleotide prior to the DNA of interest (**Figure 1**C). Linearised vector and amplified fragment of interest are treated independently with T4 DNA polymerase, which possesses 3'-5' exonuclease activity. Only the respective unique nucleotide is added to the reaction causing the DNA polymerase to stop DNA degradation at this position due to its polymerase activity. This way, vector and insert obtain long compatible overhangs (**Figure 1**B & D) that anneal at room temperature (**Figure 1**E). The annealed construct then is directly transformed into *E. coli* and the internal *E. coli* DNA repair machinery will close the nicks, so that an intact circular plasmid is generated in *E. coli*.

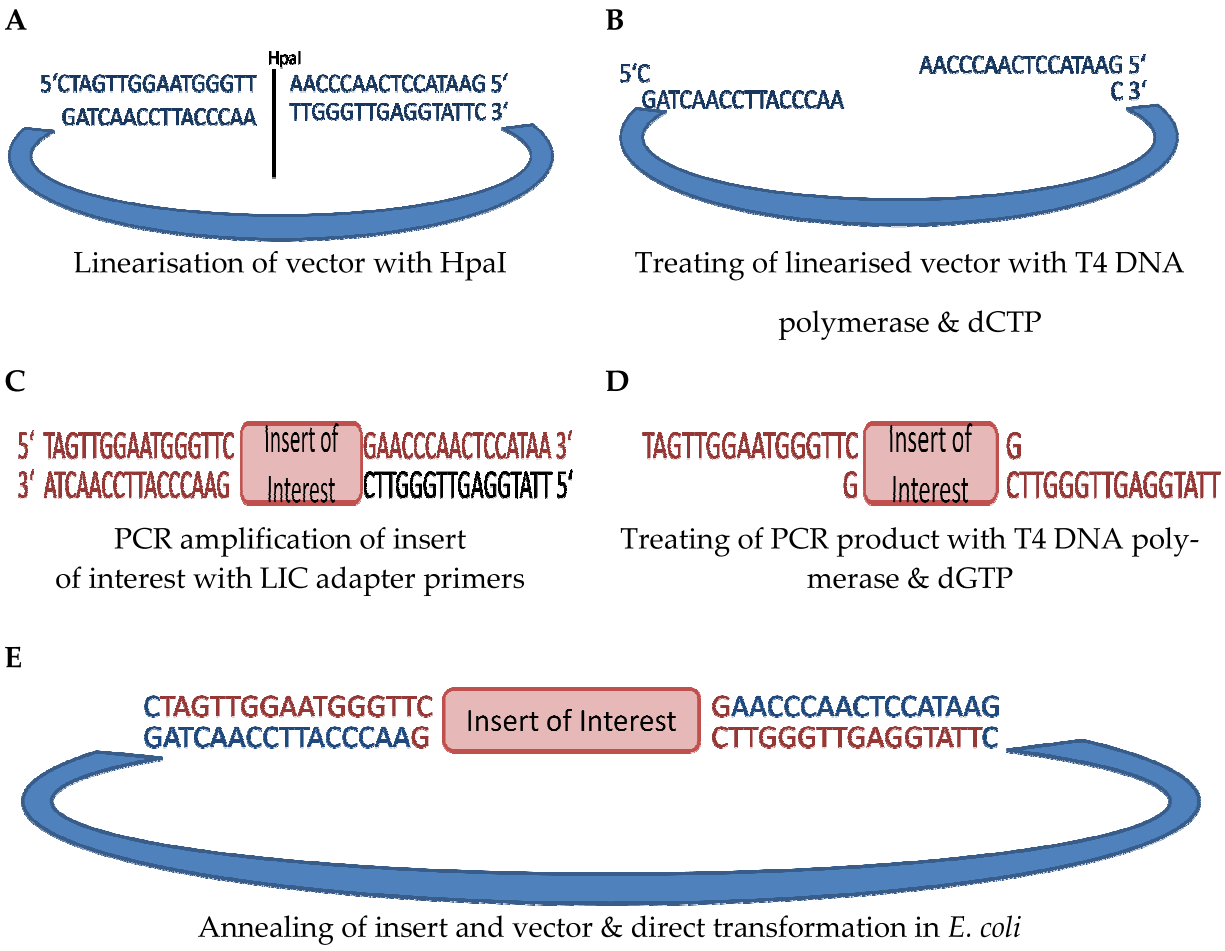

Figure 1: Schematic workflow of a ligation independent cloning reaction. The vector is depicted in blue, the insert of interest in red. A: The LIC site of the vector with an HpaI site in the middle for linearization. B: The vector was linearised using HpaI and then treated with T4 DNA polymerase and in the presence of dCTP. As a consequence, 15 bp long overhangs are generated. C: The insert of interest is PCR amplified using primers with special LIC adapters. D: The amplified insert of interest is treated with T4 DNA polymerase and in the presence of dGTP. As a consequence, 15 bp long overhangs are generated. E: Vector and insert of interest overhangs are annealed and then transformed into *E. coli*.

1.6 Promoter elements and transcriptional regulation

Gene expression is a tightly controlled process in eukaryotic cells. At any stage, several different factors contribute to regulation of genes. Genes are selectively expressed in stage, development or tissue-specific manner and by a manifold of environmental conditions. Genes can be regulated at the transcriptional, post-transcriptional, translational or post-translational level. Transcriptional regulation is carried out by promoter elements and their interacting proteins.

Promoters are regions upstream of genes on the DNA. Promoters harbour *cis*-acting DNA sequences responsible for the initiation with transcription factors and associated proteins. Nearly all promoter regions can be divided into proximal and distal elements in addition to the core promoter region, which alone is not sufficient for more than basal gene expression (Butler and Kadonaga 2002).

1.6.1 The core promoter

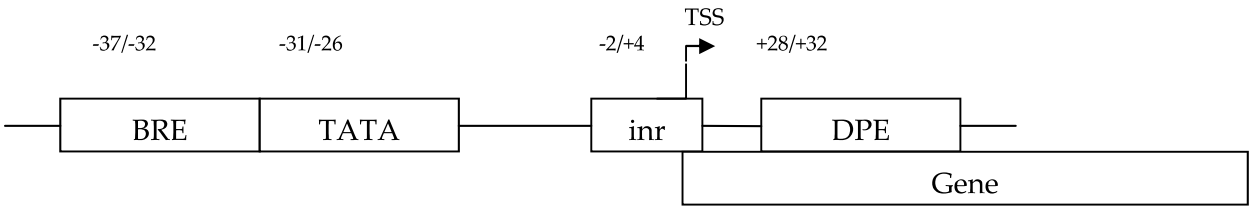

Figure 2: Core promoter elements. BRE: Transcription factor II B recognition element. TATA: Binding site for the TATA binding proteins. Inr: Initiator element. TSS: Transcriptional start site (+1). DPE: Downstream core promoter element.

The core promoter region is the binding site for the RNA polymerase II complex and thus the starting point for the transcription machinery. Usually, the core promoter only is about 40 nucleotides (nt) long and lies upstream of the transcriptional start site (+1). However, there are still a lot of open questions concerning the structure of core plant promoters, making *in silico* analyses difficult.

There are some common DNA elements in animal core promoters, e.g. the so called TATA-box, which is the binding site for the TATA binding proteins (TBPs). However, studies showed that only 20 – 30 % of predicted plant promoters contain a TATA-box (Molina and Grotewold 2005; Kumari and Ware 2013; Yamamoto et al. 2011). For *Populus trichocarpa*, Kumari and Ware 2013 estimate roughly 18 % of predicted promoter sequences to contain a TATA-box. Recent studies showed that TATA-boxes are more likely involved in the expression of regulated genes, whereas constitutive genes are controlled by CpG motif containing promoters (Melo et al. 2021; Müller and Tora 2014). CpG promoters contain GC rich regions and their activity depends on epigenetic methylation (Saxonov et al. 2006).

Another sequence motif of the core promoter is the initiator element (inr), which usually encompasses the transcriptional start site (The +1 site) (Butler and Kadonaga 2002). The transcription factor IID (TFIID), a multi subunit protein with associated proteins, binding to the

inr element is one of the first steps in the assembly of the preinitiation complex for transcription (Butler and Kadonaga 2002).

A downstream core promoter element (DPE) might be present in a core promoter. If present, DPE is found at the +28 to +32 position compared to the inr and disturbance in this distance between the DPE and the inr leads to several fold reduction of basal transcription activity due to incomplete binding of the TFIID element to the inr and the DPE (Kutach and Kadonaga 2000).

Immediately located upstream of the core promoter are the proximal promoter elements. The sites can be various and depending on composition and number of cis elements, influence the strength of gene expression. One frequently found proximal promoter element is the transcription factor II B recognition element (BRE), which usually lies directly upstream of the TATA-box if present (Butler and Kadonaga 2002). The BRE is the binding site for TFIIB, which is a single polypeptide interacting also with TBPs ((Butler and Kadonaga 2002).

Core promoters usually lead to low and basal expression of genes. For regulation of gene transcription, other elements play an important role.

1.6.2 *Cis* acting elements

Cis acting sequences are often located further upstream of the proximal promoter elements (-360) and can be located several kb away from the regulated gene (Zuo and Li 2011). Regulation of temporal and spatial expression of a gene is often mediated by elements called enhancers or silencers. Enhancer regions act as activators for gene expression, whereas silencer regions act as repressors (Porto et al. 2014).

Enhancers are often located far away (as in several kb) from the core promoter elements upstream or downstream of the regulated gene and enhance gene expression through interaction with different transcription factors, most possibly by altering DNA conformation (for reviews, see Porto et al. 2014; Biłas et al. 2016). They increase transcription by recruiting transcription factors and bringing them in contact with core promoter elements (Marand et al. 2017). Enhancer elements are generally more common than silencers (Biłas et al. 2016), however they are difficult to identify because their position in the genome is quite variable respective to the promoters they interact with

Silencers can be grouped into position-independent elements which lead to active repression mechanisms (silencers) and position-dependent elements that lead to a passive repression mechanism (negative regulatory elements, NREs) (for a review, see Ogbourne and Antalis 1998).

Enhancer and silencer elements do not necessary need to be located far away from the regulated gene, they can also be located within introns of genes (Porto et al. 2014).

1.6.3 Constitutive and inducible promoters

Promoters can be responsible for constitutive expression of genes, meaning the promoter is active under all circumstances and leads to at least basal expression of the controlled gene, mostly housekeeping genes (Porto et al. 2014) Constitutive promoters used in this study are the cauliflower mosaic virus 35S promoter (P_{35S}) and the *Arabidopsis thaliana* ubiquitin 10 promoter (P_{UBQ}).

In contrast, inducible promoters are activated by different chemical or physical stimuli. They can be dependent on activator recruitment, where next to the basic transcriptional machinery, further activator and co-activator proteins are necessary to start transcription. These promoters are called positive inducible (for a review, see Weake and Workman 2010). Furthermore, repressor proteins which block transcription can be liberated from the DNA by certain molecules, which in turn enables the transcription machinery to bind to the DNA. These promoters are called negative inducible (Gearing 2018).

In this work, the NOS promoter (P_{NOS}) of *Agrobacterium* was used. This is per se not a constitutively expressed promoter in plants, since it is organ specific (expressed in lower parts of plants) and dependent on developmental status of the plant (An et al. 1988). Furthermore, it is inducible by signals released upon wounding and activity of the NOS promoter is further enhanced by auxins in a concentration dependent manner (An et al. 1990).

1.7 Promoter analysis

Since a manifold of different promoter elements are known nowadays, promoter studies can start with an *in silico* analyses using different programs recognizing general promoter core motifs, e.g the Plant Promoter Analysis Navigator (PlantPAN, http://PlantPAN2.itps.

ncku.edu.tw) (Chow et al. 2016) or PlantCARE (plant *cis* acting regulatory elements) (Lescot 2002), which is a database for plant *cis* acting regulatory elements, enhancers and repressors.

However such databases do contain only known elements of very well investigated promoter regions and verification using laboratory techniques is mandatory. For models with only very limited data conventional analysis is still necessary. For experimental validation, stable or transient plant transformation is often carried out. The promoter of interest or fragments of the promoter of interest are fused to a reporter gene construct that gives detectable signals upon promoter activity. Enzymes and enzymatic reactions can be used as markers, as well as β-Glucuronidase or fluorescent proteins can be used. Fluorescent proteins as reporter system have the advantage of monitoring expression *in vivo*. Additionally, they do not need substrates or enzymes for activation.

In order to narrow down certain cis acting elements within a predicted promoter sequence, 5′ truncation experiments are often carried out.

1.8 Fluorescent reporter proteins

The most famous fluorescent protein, the green fluorescent protein (GFP) has been first described in 1962 as a bioluminescent protein from the jellyfish *Aequorea victoria* (Shimomura et al. 1962). In 1994, it has been used as fluorescent marker for the first time (Chalfie et al. 1994). Since then, many more fluorescent proteins have been found in different organisms. There is quite a natural diversity in fluorescent proteins already, in colour and in size (Chudakov et al. 2010). Genetic engineering led to variants with improved photostability for reduced photobleaching, increased brightness, shorter maturation time, higher quantum yield, higher or lower turnover rate and different excitation and extinction maxima for different purposes (Day and Davidson 2009). They are widely used to study gene expression and protein localisation. However, fluorescence is unstable under acidic conditions and therefore cannot be used in vacuoles (Berg and Beachy 2008).

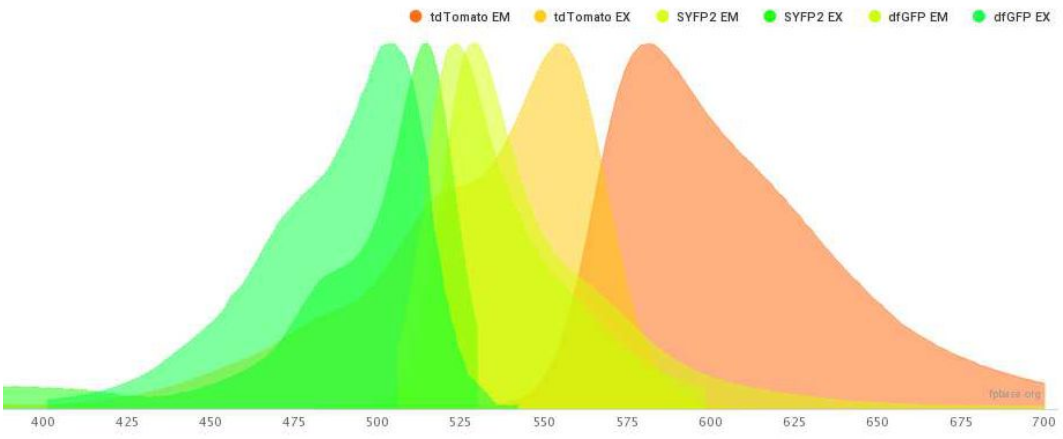

Figure 3: Excitation and emission spectra for different fluorescent proteins. Source: fpbase.org.

Proteins of the GFP family usually are about 25 kDa in size and fold into barrel like structures. The chromophore in the middle of the barrel is activated by posttranslational modification by incorporating an oxygen atom. Most GFP-like proteins associate *in vivo* and form oligomers (Chudakov et al. 2010). In contrast to other expression markers like β-Glucuronidase or Luciferase, GFP like proteins have the advantage of being visualised without the need for further substrates and without time delay (Voß et al. 2013). Their small size sometimes is a disadvantage as unwanted diffusion can take place. Therefore proteins have been engineered to become larger by fusing them (e.g. double GFP, dGFP), which also increases the brightness of the proteins.

Different fluorescent proteins with distinct excitation and emission maxima were developed and experiments therefore can be designed where two fluorescent proteins are used in parallel. This can be used for example to target different organelles within a cell, or localise different proteins simultaneously.

Using fluorescent proteins for *in planta* analysis is a reliable method for many purposes, but autofluorescence of plant tissues has to be taken into consideration (Voß et al. 2013). Chlorophyll emits light at around 680 nm, which interferes with the excitation ranges of red fluorescent proteins. GFP fluorescence however is difficult to detect in cells with lignified cell walls, since they show autofluorescence at 440 to 540 nm (Berg and Beachy 2008).

Fluorescent proteins can be used *in vivo* for protein labelling, localisation studies, analysis of promoter expression and protein-protein interaction using Förster resonance energy transfer (FRET) (Chudakov et al. 2010).

1.9 Promoters of interest in this study

1.9.1 Potrx6G1673

The function of Potrx6G1673 is not yet elucidated in Poplar, but alignments with *A. thaliana* showed homology to proteins related to oxysterol binding proteins (OSBPs). The *Arabidopsis* genome encodes for 12 different OSBPs and their expression has been shown to be under the control of different factors such as biotic stress, abiotic stress, temperature conditions and light intensity (Umate 2011). In plants, their function is largely unknown. However there is recent evidence that an OSBP from *Arabidopsis* is able to bind to sitosterol (Saravanan et al. 2009). Sitosterol has been shown to reduce water permeability in soybean phosphatidylcholine bilayers and thus seems to play an important role in membrane functionality (Schuler et al. 1991). In mammalian systems, they have been shown to be involved in the sterol and sphingomyelin metabolism, sterol transport, regulation of lipid metabolism and the regulation of signalling cascades (for a review, see (Yan and Olkkonen 2008)).

Quantitative PCR data of the working group (Nehls et al., unpublished) showed a strong upregulation of *Potrx6G1673* in mycorrhiza compared to non-infected fine roots. In leaves, stems and main roots, only very basal *Potrx6G1673* expression could be detected.

1.9.2 Potrx6G0093

Potrx6G0093 encodes for a protein with unknown function. Homology was found to a leucine zipper domain, which could hint for *Potrx6G0093* to be a transcription factor. Basic leucine zipper (bZIP) proteins all contain the conserved bZIP domain with a highly conserved core subdomain and a more diversified leucine zipper dimerisation subdomain. This subdomain contains leucines at every seventh position, which leads to the formation of an amphipathic helix (Landschulz et al. 1988). These leucine zipper regions are important for (hetero)dimer formation of bZIP proteins (O'Shea et al. 1991). For arbuscular mycorrhiza, studies showed more than twofold increase in transcripts of certain bZIP transcription factors hint-

ing to potential function of these proteins in the establishment and functionality of the symbiosis (Hohnjec et al. 2005; Handa et al. 2015). *Potrx6G0093* was found to be highly upregulated in mycorrhiza compared to fine roots by RNA sequencing supported by qPCR analysis (Nehls et al., unpublished).

1.10 Aim of the thesis

The research focus of this study is to analyse plant promoter (fragment) activity *in vivo* in composite poplar roots. For this purpose, a vector system with suitable properties needs to be established. Different fluorescence proteins will be tested in composite poplar for their suitability to visualise promoter (fragment) activity. These binary vector systems will be established with known plant promoters and functionality will be verified in *Nicotiana benthamiana* and composite poplar. Once the binary vector system is established, different plant promoter fragments of interest will be tested in composite poplar.

Previous RNA sequencing and qPCR data showed a strong upregulation of two poplar genes in mycorrhiza compared to non infected fine roots indicating mycorrhiza specific *cis* elements within the promoter regions. Promoter fragments will be amplified from genomic DNA and 5′ truncations will be generated. The promoter fragments of interest will be integrated into the previously established transformation vectors to analyse promoter expression *in vivo*. Plant experiments comprise the generation of composite poplar followed by mycorrhization.

2 Material and Methods

2.1 Materials

2.1.1 Chemicals and enzymes

All used chemicals had analytical quality or were supposed to be used for molecular biological purposes.

All media and cultures were maintained and propagated under sterile conditions. Media and solutions were prepared using double distilled water and autoclaved at 121 °C and 2 bar for 21 minutes. Not heat stable solutions or components were sterilised by filtering through cellulose acetate membranes with pore sizes of 0.2 µm (Carl Roth GmbH & Co. KG, Karlsruhe, Germany). Glass ware was either dry heat-sterilised (180 °C, 4 h) or autoclaved.

All enzymes used for this study were obtained from New England Biolabs (NEB, Massachusetts, USA) or Thermo Fisher Scientific (Waltham, Massachusetts, USA).

2.1.2 Media

For the preparation of solid media, the stated amount of agar was added to the liquid media before autoclaving.

Lyosgeny broth (LB) medium (Bertani 1951)

Peptone	10 g/L
Yeast extract	5 g/L
NaCl	5 g/L
Agar (Serva Kobe)	18 g/L

CPY medium

Peptone	5 g/L
Sucrose	5 g/L
Yeast extract	1 g/L
$MgSO_4 \times 7\ H_2O$	0.5 g/L
Agar (Serva Kobe)	15 g/L

MS6 medium (Murashige and Skoog 1962),
pH 5,6, adjusted with potassium hydroxide

MS6 salts (Duchefa Biochemie, Haarlem, Netherlands)	2.2 g/L
Sucrose	10 g/L
Plant agar (Duchefa)	6.8 g/L

MMN plates (Kottke et al. 1987)

NaCl	25 mg/L
KH_2PO_4	500 mg/L
For mycorrhization plates	845 mg/L
$(NH_4)_2HPO_4$	250 mg/L
For mycorrhization plates	50 mg/L
$CaCl_2$ x 2 H_2O	50 mg/L
$MgSO_4$ x 7 H_2O	150 mg/L
$FeCl_3$ x 6 H_2O	1 mg/L
KCl	12.28 mg/L
H_3BO_3	15.46 mg/L
$MnSO_4$ x H_2O	8.45 mg/L
$ZnSO_4$ x 7 H_2O	5.75 mg/L
$CuSO_4$ x 5 H_2O	1.25 mg/L
$(NH_4)_6Mo_7O_{24}$ x 4 H_2O	0.18 mg/L
Agar (Serva Kobe)	20 g/L
After autoclaving	
Thiaminhydrochloride (vitamin b1)	0.1 mg/L
Pyridoxinhydrochloride (vitamin b6)	1 mg/L
Nicotinic acid	1 mg/L
Myo-inositol	100 mg/L
Glucose	50 mM

2.1.3 Buffers and solutions

CTAB buffer (Doyle and Doyle 1987)

Hexadecyltrimethyl ammoniumbromide (CTAB)	2 %
NaCl	1.4 M
EDTA, pH 8	0.1 M
Tris-HCl, pH 8	0.1 M
β-mercaptoethanol	0.2 %

Wash buffer

Ethanol	76 %
Ammonium acetate	10 mM

TE buffer pH 7.4,
adjusted with hydrochloric acid

Tris-HCl	10 mM
EDTA, pH 8	1 mM
RNAse A	10 µg/ml

Solution I

Tris-HCl, pH 7.5	50 mM
EDTA, pH 8	10 mM
RNAse A	0.1 mg/ml

Solution II

NaOH	0.2 M
SDS	1 %

TAE buffer, pH 8, adjusted with glacial acetic acid

Tris	40 mM
Acetate	20 mM
EDTA, pH 8	1 mM

6 x loading dye

EDTA, pH 8	60 mM
Tris-HCl, pH 8	20 mM
SDS	0.1 %
Bromophenol blue	0.005 %
Xylene cyanol	0.005 %
Orange G	0.025 %

T4 DNA ligase buffer (New England Biolabs), pH 7.5

Tris-HCl	50 mM
$MgCl_2$	10 mM
ATP	1 mM
DTT	10 mM

NEB buffer 2.1 (New England Biolabs), pH 7.9

NaCl	50 mM
Tris-HCl	10 mM
$MgCl_2$	10 mM
BSA	100 µg/ml

Cutsmart® buffer (New England Biolabs), pH 7.9

Potassium acetate	50 mM
Tris-acetate	20 mM
Magnesium acetate	10 mM
BSA	100 µg/ml

RF1 solution,
pH 5.8, adjusted with acetic acid

KAc	30 mM
RbCl	10 mM
$CaCl_2$	10 mM
$MnCl_2$	50 mM
Glycerol	15 %

RF2 solution
pH 6.5, adjusted with potassium hydroxide

3-(N-Morpholino)propansulfonicacid (MOPS)	10 mM
$CaCl_2$	75 mM
RbCl	10 mM
Glycerol	15 %

KCM solution

KCl	100 mM
$CaCl_2$	30 mM
$MgCl_2$	50 mM

Activation buffer

MES/KOH, pH 5.6	10 mM
$MgCl_2$	10 mM
Acetosyringon	150 µM

2.1.4 Plasmids

Table 1: Original plasmids used in this study.

Plasmid	Description	Origin
pJET1.2/blunt	Entry vector for all cloning purposes	Thermo Fisher Scientific
pPLV04	LIC compatible binary plant transformation vector containing pGIIK-LIC-SV40-3xGFP-NOSt	(De Rybel et al. 2011) Nottingham Arabidopsis Stock Centre
pPLV06	LIC compatible binary plant transformation vector containing pGIIK-LIC-SV40-sYFP-NOSt	(De Rybel et al. 2011) Nottingham Arabidopsis Stock Centre
pSOUP	Helper plasmid for pPLV vectors containing pSa-*RepA*	(Hellens et al. 2000) Nottingham Arabidopsis Stock Centre
pCXUN-FLAG	Binary plant transformation vector derived from a pCAMBIA background	(Chen et al. 2009) Nottingham Arabidopsis Stock Centre
pBI121	Binary plant transformation vector derived from pBIN19 background	(Jefferson 1987) Nottingham Arabidopsis Stock Centre

2.1.5 Primers

Primers are oligonucleotides used for polymerase chain reactions (PCR) to bind specifically to a single stranded DNA for the amplification of specific sequences. These primers define the DNA region to be amplified. All of the oligonucleotides used in this work were ordered and synthesized by Eurofins Genomics Germany GmbH (Ebersberg, Germany).

Table 2: Overview of PCR primers used in this study. All primers were obtained from Eurofins Genomics (Ebersberg, Germany), solved in 5 mM Tris/HCl and stored at – 20 °C. Tm temperatures were calculated using the NEB Tm calculator (https://tmcalculator.neb.com/#!/main). F always refers to a forward primer while R always refers to a reverse primer. LIC adapter sequences are bold. Restriction endonuclease recognition sites are underlined.

Primer name	Sequence (5′-3′)	Description	Tm (°C)
sYFPforBamHI	GGATCCCATGACTAGTAAGG	F primer for sYFP wih BamHI site	61
sYFPrevPTS1BamHI	GGATCCTTAGAGGTTTGACTTGTACAGCTCGTCCATGC	R primer for sYFP with BamHI site and added SNL sequence (PTS1)	76
Potri6G1673ProF2	AGTGTCCTTTTCTAGTTAG	F primer promoter fragment 6G1673 gDNA	55
Potri6G1673ProR2	CATCATTAAGCTGTACTTA	R primer promoter fragment 6G1673 gDNA	53
Potri6G0093ProF1b	CCTTGGATTGTGACACTTGA	F primer promoter fragment 6G0093 gDNA	62
Potri6G0093ProF2	GACCTGTAGGGCTTCAATCT	F primer promoter fragment 6G0093 gDNA	64
Potri6G0093ProR2	AGGAGGTTAACTACAAGCTAGG	R primer promoter fragment 6G0093 gDNA	63
6G93ProF1bR2KpnF	TAGGTACCCCCTTGGATTGTGACACTTGA	F primer promoter fragment 6G0093 with KpnI site	74
6G93ProF2R2KpnF	TAGGTAC-CACCTGTAGGGCTTCAATCTT	F primer promoter fragment 6G0093 with KpnI site	70
6G93ProF1bR2SmaR	TACCCGGGGAGGAGGTTAACTA-CAAGCTAG	R primer promoter fragment 6G0093 with SmaI site	74
6G93ProF2R2SmaR	TACCCGGGAGGAGGTTAACTA-CAAG	R primer promoter fragment 6G0093 with SmaI site	70
pjetUnivLIC1_F1	**TAGTTGGAATGGGTT**CGAATGGCTCGAGTTTTTCAGC	Universal LIC primer for pJet1.2, left adapter	75
pjetUnivLIC1_R1	**TAGTTGGAATGGGTT**CGAATGA-GAATATTGTAGGAGATCTTCTAGA	Universal LIC primer for pJet1.2, left adapter	72
pjetUnivLIC1r_F1	**TTATGGAGTTGGGTT**CGAACTGGCTCGAGTTTTTCAGCA	Universal LIC primer for pJet1.2, right adapter	77
pjetUnivLIC1r_R1	**TTATGGAGTTGGGTT**CGAACTGAGAATATTGTAGGAGATCTTCTAGA	Universal LIC primer for pJet1.2, right adapter	73
P6G1673LIC_R	**TTATGGAGTTGGGTT**ATCAT-TAAGCTGTACTTATATA	LIC primer for a promoter fragment of 6G1673 in pJET1.2; right adapter	66

P6G1673LIC_F4	**TAGTTGGAATGGGTT**CCCAACTT AAATATATGAACATT	LIC primer for a promoter fragment of 6G1673 in pJET1.2; left adapter	68
P6G1673LIC_F3	**TAGTTGGAATGGGTT**TAAACAAT CTCATTGATATAATAATC	LIC primer for a promoter fragment of 6G1673 in pJET1.2; left adapter	66
P6G1673LIC_F2	**TAGTTGGAATGGGTT**CCATAACC TTAATTAAC	LIC primer for a promoter fragment of 6G1673 in pJET1.2; left adapter	66
P6G0093LIC_R	**TTATGGAGTTGGGTT**GAGGAGGT TAACTACAAGC	LIC primer for a promoter fragment of 6G0093 in pJET1.2; right adapter	72
P6G0093LIC_F1	**TAGTTGGAATGGGTT**ATAAGAGA CTAATTATTGTGAATGC	LIC primer for a promoter fragment of 6G0093 in pJET1.2; left adapter	68
P6G0093LIC_F2	**TAGTTGGAATGGGTT**TGTAAATTG CAAGGTCGCAAT	LIC primer for a promoter fragment of 6G0093 in pJET1.2; left adapter	73
P6G0093LIC_F3	**TAGTTGGAATGGGTT**CCATACTA GCTCAAACGTTTTAAGTT	LIC primer for a promoter fragment of 6G0093 in pJET1.2; left adapter	72

Table 3: Overview of sequencing primers used in this study. All primers were obtained from Eurofins Genomics (Ebersberg, Germany), solved in 5 mM Tris/HCl and stored at – 20 °C.

Primer	Sequence (5′-3′)	Target vector
pJET1.2 forward	CGACTCACTATAGGGAGAGCGGC	pJEt1.2
pJET1.2 reverse	AAGAACATCGATTTTCCATGGCAG	pJET1.2
M13-seq	GTAAAACGACGGCCAGTG	pPLV, pCXUN
M13 rev	GGAAACAGCTATGACCATG	pPLV, pCXUN

2.1.6 Kits

Table 4: Kits used in this study.

Kit	Purpose	Manufacturer
NucleoSpin® Gel and PCR Clean-up	Purification of DNA fragments from agarose gels or purification of PCR products	Macherey-Nagel (Düren, Germany)
CloneJET™ PCR Cloning Kit	Cloning of blunt end DNA fragments	Thermo Fisher Scientific
NucleoSpin® Plasmid	Isolation of plasmid DNA from *E. coli*	Macherey-Nagel

2.2 Cultivation of organisms

2.2.1 Bacteria

For all cloning purposes, *E. coli* strain TOP10 F' with the genotype F'{*lac*I^{q} Tn*10* (Tet^{R})} *mcr*A Δ(*mrr-hsd*RMS-*mcr*BC) Φ80*lac*ZΔM15 Δ*lac*X74 *rec*A1 *ara*D139 Δ(*ara-leu*)7697 *gal*U *gal*K *rps*L *end*A1 *nup*G was used (formerly Invitrogen, now Thermo Fisher Scientific, Waltham, Massachusetts, USA).

E. coli was routinely cultivated in Lysogeny Broth (LB) medium or on LB plates at 37 °C. Medium and plates were supplemented with different antibiotics (ampicillin 100 mg/L or kanamycin 50 mg/L) if required.

For all plant transformation events, *Agrobacterium rhizogenes* strain K599 (Savka et al. 1990) was used. For experiments on *Agrobacterium* transformation, *A. tumefaciens* GV3101(Van Larebeke et al. 1974; Koncz and Schell 1986) was used. The used GV3101 strain contained pSOUP and was kindly provided by AG Großhardt (University of Bremen, Germany).

Routinely, *Agrobacterium* was cultivated in CPY medium or on CPY plates at 28 °C. Medium and plates were supplemented with different antibiotics (kanamycin 50 mg/L or tetracycline 2.5 mg/L) if required.

For the long term storage of bacteria, glycerol cultures were generated. For this purpose, 600 µl of grown overnight culture were mixed with 600 µl of 98 % glycerol and deep-frozen in liquid nitrogen. The cultures were stored at – 80 °C and streaked out on appropriate media plates if needed.

2.2.2 Plants

Nicotiana benthamiana was used as a system for pre-screenings of different vector systems. The plants were grown from seeds in a 1 : 1 soil sand mixture in a phytotron with a long day cycle (15 h light, 74 µmol/m²s, 8 hours dark), 25 °C and 60 % humidity. For propagation purposes, seeds of some plants were kept and stored at 4 °C until needed.

For all other purposes, the poplar hybrids *Populus tremula x alba* (No. 7171-B4, Institut de la Recherche Agronomique, INRA) or *Populus tremula x tremuloides* (T89 (Tuominen et al. 1995))

were used. The plants were kept as axenic cultures in half strength MS6 medium pH 5.8 (Murashige and Skoog 1962) in climate chambers with a 16 h light/8 h dark cycle (80 µmol/m²s) at 18 ⁰C. Approximately every 4 weeks, the shoot tips of the plants (with one or two leaves) were cut under sterile conditions and either used for experiments or transferred to new medium for propagation of the plant cultures.

2.2.3 Fungi

All fungal cultures were maintained by Thea Fründ (University of Bremen, AG Nehls).

Amanita muscaria HB 2009 (sampled in Bremen in autumn of 2009 by Uwe Nehls) & *Pisolithus microcarpus* D2 (Maira Pereira, INRA Nancy, France) were used for the ectomycorrhization of poplar plants.

The fungal cultures were maintained on MMN plates (Kottke et al. 1987) The fungal plates were maintained at 18 °C. For propagation, parts of the fungal mycelia were cut out and set on fresh MMN plates.

2.3 Molecular biological methods

2.3.1 Bioinformatics & *in silico* analyses

All bioinformatics and *in silico* analyses conducted in this study were performed using the geneious software package version 6.1.8 (https://www.geneious.com).

2.3.2 Isolation of nucleic acids

2.3.2.1 Isolation of genomic DNA

Genomic DNA was isolated with a modified CTAB (hexadecyltrimethyl ammoniumbromide) method (Doyle and Doyle 1987). Therefore, 0.5 g of *P. tremula x tremuloides* leaf tissue either from plants grown in sterile culture or from wild grown plants were grounded under liquid nitrogen. 2.5 ml of preheated (60 °C) CTAB isolation buffer was carefully added to the powder. With a wide-bore pipette, the suspension was split into three

2.2 ml reaction tubes and then incubated for 30 min at 60 °C under gentle agitation. Afterwards, 600 µl of chloroform/isoamylalcohol (v/v 24/1) were added to the samples and the suspensions were shortly and carefully mixed. The samples were then centrifuged at room temperature for 10 min at 16 000 x g. The upper aqueous phase was then transferred to a new 1.5 ml reaction tube and 2/3 volumes of the aqueous phase of cold isopropanol were added. The procedure was followed by another centrifugation step at 4 °C and 16 000 x g. The supernatant was discarded and the pellet was incubated with 600 µl wash buffer (76 % ethanol, 10 mM ammonium acetate) for 20 min under gentle agitation. The suspension was then centrifuged for 5 min at 16 000 x g. The supernatant was again discarded and the pellet was air-dried for 5 min before resuspension in 150 µl TE buffer pH 7.4. The samples were first incubated for 5 min at room temperature, then 5 min at 50 °C, again 5 min at room temperature with flicking of the tube in between to resolve the pellet and finally the samples were incubated for 30 min at 37 °C. The DNA was then precipitated with 1/10 volume 4 M LiCl and 2 volumes cold 100 % ethanol followed by incubation at room temperature for 1 h. Afterwards, the samples were centrifuged at 16 000 x g. The supernatant was discarded and 500 µl 70 % (v/v) ethanol were added to the pellet. The samples were again centrifuged for 5 min at 16 000 x g and the supernatant was again discarded. The pellet was air dried at room temperature and resuspended in 50 µl TE buffer.

The isolated genomic DNA was stored at 4 °C until further use.

2.3.2.2 Isolation of plasmid DNA

Plasmid DNA for cloning purposes was isolated using commercially available kits.

For all others purposes, plasmid DNA was isolated according to the alkaline lysis protocol. 2 mL overnight culture of *E. coli* were harvested at 8 000 x g for 5 min. The supernatant was discarded and the pellet was thoroughly resuspended in 300 µl solution I. Subsequently, 300 µl of solution II were added and the samples were inverted 6 – 8 times and incubated for 5 min at room temperature. Then, 200 µl 1.5 M potassium acetate (pH 4.8) were added and the samples were incubated for 30 min on ice, followed by centrifugation for 20 min at 4 °C and 16 000 x g. The supernatant was transferred to a new 1.5 ml reaction tube and mixed with 500 µl isopropanol. After a 10 min incubation on ice, the samples were centrifuged for 30 min at room temperature and 16 000 x g. The supernatant was discarded and the pellet

was mixed with 500 µl 70 % (v/v) ethanol and again centrifuged at room temperature for 10 min and 16 000 x g. The pellet was subsequently air-dried and resuspended in 20 µl 5 mM Tris-HCl (pH 8).

Until further use, plasmid DNA was stored at – 20 °C.

2.3.3 Polymerase chain reaction (PCR) amplification of DNA fragments

Standard PCR reactions were performed using either the DreamTaq DNA polymerase (Thermofisher Scientific, 5 U/µl) or if a proof-reading function was required, the Q5® High-Fidelity DNA Polymerase (2 U/µl, New England Biolabs).

In brief, 1 x of appropriate buffer was mixed with 0.02 U/µl Q5® High-Fidelity DNA Polymerase or 0.5 U/µl DreamTaq DNA polymerase, 200 mM dNTPS, 0.5 µM specific primer mix (1:1 mixture of forward and reverse primer, each 100 pmol), variable amounts of DNA template (for standard reactions, approximately 20 ng) and ddH_2O to a total volume of 20 µl. Reactions were set up on ice, components were mixed carefully. Reactions were carried out in a gradient thermocycler maschine (Analytik Jena, Germany). PCR conditions varied depending on the used primers and the expected products. A standard protocol can be viewed in **Table 5**.The used annealing temperature depended on the primer combination and was calculated using the NEB Tm calculator (https://tmcalculator.neb.com/#!/main, standard settings). When establishing a PCR, an annealing gradient with ± 5 °C of the calculated annealing temperature was used. The extension time was always set to 30 sec per kb of the expected product.

Table 5: Standard PCR conditions.

Step	Time (sec)	Temperature (°C)	
Initial denaturation	30	98	
Denaturation	10	98	35 x
Annealing	30	variable	
Extension	variable	72	
Final extension	600	72	

2.3.4 Agarose gel electrophoresis

Depending on the length of expected DNA fragments, either 1 % /w/v) agarose or 2 % (w/v) agarose gels (for fragments shorter than 300 bp) were prepared in 0.5 x TAE buffer. The samples for gel electrophoresis were mixed with 6 x loading dye to a final concentration of 1 x and loaded into appropriately sized gel pockets. As a molecular size marker for DNA fragments, lambda DNA digested with Eco130I (StyI) (Bioron GmbH, Römerberg, Germany) or for shorter fragments, the GeneRuler™ 100 bp DNA ladder plus (Thermofisher Scientific) were used (see Figure 4).

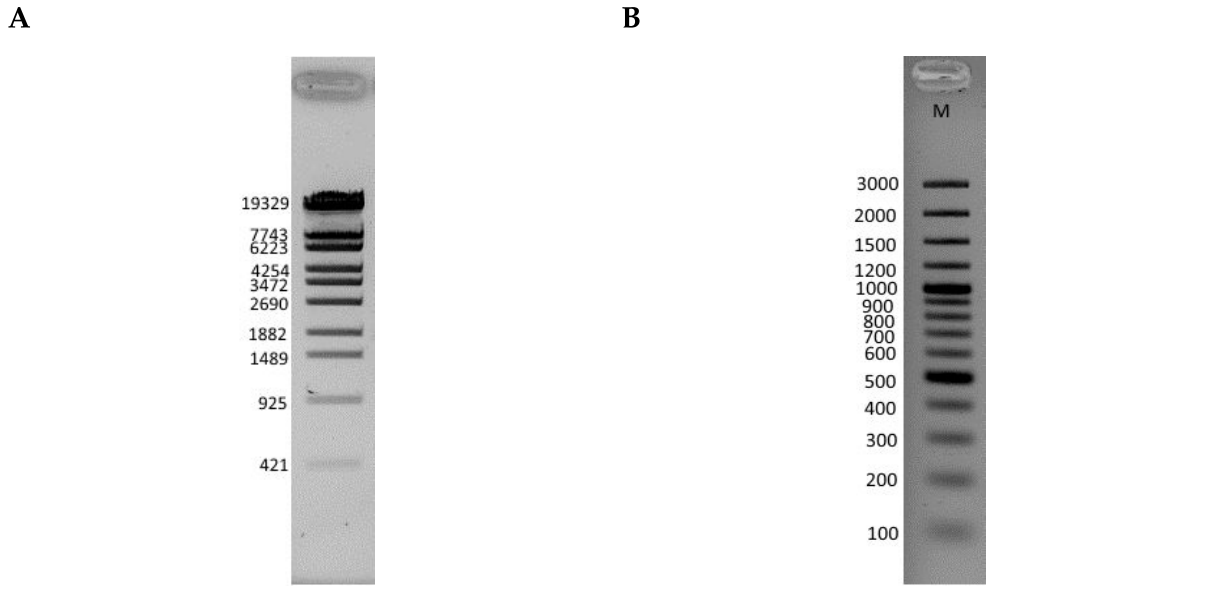

Figure 4: Molecular size markers used in the agarose gel electrophoresis. **A:** Lambda DNA digested with Eco130I (StyI), 2.5 µl on a 1 % agarose gel. **B:** GeneRuler™ 100 bp DNA ladder plus, 2.5 µl on a 2 % agarose gel.

The gels were placed in a gel chamber. An electric field was applied to the chamber leading the negatively charged DNA to migrate through the gel. The applied voltage was set between 70 and 90 V. Afterwards, the gels were incubated in ethidium bromide solution (0.167 ‰) and visualised under either UV-light (UV illuminator, Bachofer Laboratoriumsgeräte, Reutlingen, Germany) at 312 nm or under blue light (Blue/Green LED transilluminator XL, Nippon Genetics Europe, Düren, Germany) at 480 – 530 nm. Pictures were taken with a Doc Print II Hood camera (Vilber Lourmant, Eberhardzell, Germany) and digitally documented with a gel documentation system (ODC-PRINT II, PEQLAB Biotechnologie GmbH, Erlangen, Germany).

2.3.5 Cloning of DNA fragments

2.3.5.1 Use of restriction endonucleases

Restriction endonucleases were utilised to verify different constructs with specific expected band patterns on agarose gels and to isolate DNA fragments of interest from different vectors. If not indicated otherwise, restriction endonucleases were obtained from New England Biolabs and used according to the manufacturer's instructions. In general, 10 U of any enzyme were used for approximately 1 µg of DNA in a total volume of 20 µl.

2.3.5.2 Purification of DNA fragments

DNA fragments excised from agarose gels were purified using the Nucleospin® Gel and PCR Clean-up kit (Macherey-Nagel) according to the manufacturer's instructions. Integrity of the purified fragments was controlled on appropriate agarose gels. DNA concentrations were measured using the Nanodrop 1000 spectrophotometer (Peqlab GmbH, Erlangen, Germany) or by densitometric quantification

2.3.5.3 Ligation of DNA fragments and vectors

For cloning of DNA fragments into the entry vector pJET1.2, the CloneJET PCR cloning Kit (Thermofisher Scientific) was used according to the manufacturer's instructions.

DNA fragments and vector backbones other than pJET1.2 were mixed together in a molar ratio of 3:1 and incubated with 1 x T4 DNA ligase buffer (New England Biolabs), 4 U T4 DNA ligase (New England Biolabs) in a 20 µl reaction either overnight at 16 °C or for 2 hours at room temperature. The reaction was heat-inactivated at 65 °C for 10 minutes. Ligase reactions were used directly for the transformation of chemically competent *E. coli* TOP10 F'.

2.3.5.4 Ligation-independent cloning (LIC)

A ligase-free cloning technique was utilised whenever the use of restriction endonucleases was not possible. This was the case when the fragment of interest contained the cutting site needed for cloning or when the multiple cloning site of the vector did not contain a suitable site for cloning.

LIC compatible vectors (pPLV, pCXUN) contain a unique HpaI-site flanked by LIC-adapter sequences (left adapter sequence = left of the HpaI site; right adapter sequence = right of the

HpaI site). Fragments to be cloned were amplified using primers containing compatible LIC-adapter sequences at the 5′ end. For each PCR a primer containing a left adapter sequence (TAGTTGGAATGGGTT) was combined with a primer containing a right adapter sequence (TTATGGAGTTGGGTT). The fragments were gel purified. The vector was cut with HpaI and the excised fragment was purified to minimize contamination with uncut vector. The fragment of interest and the vector were then treated with T4 DNA polymerase (New England Biolabs) to generate specific 5′ end overhangs. Therefore, appropriate amount of vector (usually about 200 ng), respectively insert (usually about 100 ng) were mixed together with 2.5 mM dCTP (vector) or 2.5 mM dGTP (Insert), 5 mM DTT, 0.25 µg/µl BSA, 1 x NEB buffer 2.1 (50 mM NaCl, 10 mM Tris-HCl, 10 mM $MgCl_2$, 100 µg/ml BSA, pH 7.9) and 1.5 U T4 DNA polymerase in a 20 µl reaction. The reaction was incubated for 2 h at 22 °C and subsequently heat inactivated for 20 min at 75 °C. Afterwards, the vector and the insert of interest were mixed together in a 1:3 molar ratio and incubated for 2 h at 22 °C. The reaction was frozen at – 20 °C or directly used for transformation of chemically competent *E. coli* TOP10 F′.**Transformation of chemically competent *E. coli* TOP10 F′**

E. coli TOP10F′ were made competent by harvesting a culture of OD_{600} 0.2 to 0.4, which was centrifuged at 4 °C for 15 min at 2000 x g. The pellet was resuspended in 18 ml RF1 solution and incubated for 30 min on ice and subsequent centrifugation at 4 °C for 15 min at 2000 x g. The pellet was then resuspended in 4 ml RF2 solution and the suspension was frozen in aliquots of 100 µl in liquid nitrogen and stored at – 80 °C until further use.

For transformation of chemically competent *E. coli* TOP10F′, an aliquot of competent cells was thawed on ice, mixed with 5 – 20 µl of ligation reaction (5 µl in case of a pJET1.2 ligation, 20 µl in case of all other vector backbone ligation reactions), 20 µl KCM solution, filled up to 200 µl with ddH_2O and incubated on ice for 20 min. Afterwards, a heat shock was applied for 2 min at 42 °C, the samples were placed back on ice, 600 µl of LB medium were added and the samples were incubated for 45-60 min at 37 °C under shaking conditions. Afterwards, the samples were centrifuged for 5 min at 8000 x g, 700 µl of the supernatant were removed and the pellet was resupended in the rest of the supernatant. The suspension was then plated out on LB plates containing appropriate antibiotics and incubated overnight at 37 °C. For estimation of transformation efficiency, colonies formed on the plates were

counted the next day. Verification of correct plasmid transformation was carried out using the alkaline lysis plasmid preparation protocol (2.3.2.2).

2.3.7 Verification of plasmids

For verification of correctly ligated plasmids, *in silico* analysis with the geneious software package version 6.1.8 were paired together with the use of restriction endonucleases (2.3.5.1) and/or sequencing.

Sequencing reactions consisting of 500 ng plasmid DNA and 50 pmol appropriate sequencing primer in a total volume of 10 µl were sent to Macrogen Europe (Amsterdam, Netherlands).

2.3.8 Transformation of *Agrobacteria*

A chemical transformation method was used to transform *A. rhizogenes* K599 in this study. To prepare competent cells, an overnight culture from a freshly streaked out plate was inoculated the next day in 50 ml CPY-medium to an OD_{600} of 0.1. The culture was harvested when an OD_{600} of 0.5 was reached. The culture was cooled down on ice, centrifuged for 5 min at 3000 g at 4 °C and the pellet was resuspended in 1 ml 20 mM $CaCl_2$. Aliquots of 100 µl were frozen in liquid nitrogen and stored at – 80 °C until further use.

For transformation, aliquots of the bacteria were thawed on ice and inoculated with approximately 1µg plasmid DNA for 20 min on ice. Afterwards, the cells were frozen in liquid nitrogen for 5 min with subsequent incubation at 37 °C for 5 min. Then, 800 µl CPY were added to the cells and they were incubated for 3 – 4 hours at 28 °C and 130 rpm. Afterwards, the samples were centrifuged for 5 minutes at 8000 x g, 800 µl of the supernatant were removed and the pellet was resupended in the rest of the supernatant. The suspension was then streaked out on CPY plates containing appropriate antibiotics and incubated for two days at 28 °C. For estimation of transformation efficiency, colonies formed on the plates were counted.

2.4 Plant transformation

2.4.1 Transient transformation of *Nicotiana benthamiana*

Leaves of *Nicotiana benthamiana* were transiently transformed with *A. rhizogenes* K599 harbouring a binary vector system with the tDNA of interest. Therefore an overnight culture of

Agrobacteria with the plasmids of interest was inoculated in CPY-medium containing the appropriate antibiotics. The culture was centrifuged for 20 min at 4000 x g at room temperature. The pellet was resuspended in 2 ml activation buffer. The OD_{600} of the suspension was then adjusted to 0.3 and incubated for 2 h at 28 °C under shaking conditions. Afterwards, leaves of approximately 4 weeks old *N. benthamiana* plants were infiltrated with the suspension. Therefore, the suspension was filled into a 1 ml syringe without needle and pressed into the abaxial site of the leaves. The plants were incubated for two days in a phytotron with a long day cycle (15 h light, 74 µmol/m²s, 8 h dark), 25 °C and 60 % humidity. Transient expression was visualized using fluorescence microscopy.

2.4.2 Generation of composite poplar plants

Composite poplar plants are composed of an untransformed shoot and an at least partially transformed root system.

Cells of *A. rhizogenes* K599 containing a binary vector system with the tDNA of interest were streaked out on CPY agar plates containing 150 µM acetosyringon and incubated for 2 days at 28 °C. Tips of poplar shoots with 2 – 3 leaves were cut from axenic poplar cultures and the cutting site was dipped into the grown *Agrobacteria* on the plate. The shoots were then transferred to plates containing MS6-medium (one half of the agar was removed to accommodate the plant). Two dental rolls were placed at the bottom of the agar plate to absorb excess water. Additionally, the plates were sealed with a semi-transparent flexible film. After incubation for two days in the phytotron chamber (23 °C, 16 h light, upright position), the plants were transferred to new MS6 plates containing 1.18 mM carbenicillin and 0.52 mM cefotaxime to inhibit further growth of *Agrobacteria*. The plants were further incubated and after approximately 4 weeks, roots began to form. Evaluation of transgenic roots was performed using fluorescence microscopy.

2.4.3 Ectomycorrhization

Some composite poplar plants (2.4.2) and either *Amanita muscaria* or *Pisolithus microcarpus* were used for ectomycorrhization experiments.

Fungi cultures were set up at the time of composite poplar generation. Parts of either *A. muscaria* or *P. microcarpus* were transferred to mycorrhization plates (squared plates (12 cm x 12 cm x 1.7 cm). The agar was covered with autoclaved preservation foil which was

treated beforehand with 2 % $NaHCO_3$ and 1 mM EDTA (10 min incubation, subsequent washing in ddH_2O).

Half of the agar was removed (sterile) from the mycorrhization plates and the preservation foil with the grown fungus was applied to the agar. Up to four plants were then put on top of the foil in proximity to the fungal cultures. Then, a substrate mixture (1:1:1(v/v/v) vermiculite/clay/coconut husk. vermiculite and clay were autoclaved, the coconut husk substrate was washed extensively in ddH_2O, autoclaved, moisturised with MMN medium without glucose, left for one week at 30 °C and autoclaved again). The substrate mixture was spread over the plant roots and the fungi. Dental rolls were applied to the top of the agar to absorb excess water. The plates were then sealed with PVC-insulating tape. The plates were incubated in climate chambers with a 16 h light/8 h dark cycle (80 µmol/m²s) at 18 ^{0}C with the substrate side facing upwards. After one week, the plates were turned and further incubated. After approximately 3 – 4 months, formed ectomycorrhiza could be investigated using fluorescence microscopy.

2.5 Fluorescence microscopy

2.5.1 Fluorescence stereo microscope

Transformed tobacco leaves or transgenic roots were evaluated using a stereo microscope (Mz10F, Leica Microsystems, Wetzlar, Germany) with an 80-fold magnification maximum. Filter sets for the different fluorescent signals are shown in **Table 6**. As a light source, a Leica EL6000 (Leica Microsystems) was used.

Table 6: Filter sets used with the fluorescence stereo microscope.

Detected fluorescence protein	Excitation (nm)	Emission (nm)
dGFP	450 - 490	500 – 550
sYFP	500 - 520	540 – 580
tdtomato	510 - 560	590 – 650

Pictures were taken using a Leica DFC425C camera and the LAS 2.0 Software (Leica Application Suite version 3.5.0).

2.5.2 Fluorescence microscopy

For further analysis, cuttings of transformed tobacco leaves or transgenic roots were analysed using a Leica DMRB microscope (Leica Micvrosystems). The different filter sets are shown in **Table 7**. As a light source, a Leica EL6000 (Leica Microsystems) was used.

Table 7: Filter sets used with the fluorescence microscope.

Detected fluorescence protein	Excitation (nm)	Emission (nm)	Filter
dGFP	450 - 490	500 - 550	495 LP
sYFP	490 - 510	520 - 550	515 LP
tdtomato	540 - 580	595 - 635	585 LP

Pictures were taken using a Leica DFC425C camera and the LAS 2.0 Software (Leica Application Suite version 3.5.0).

2.5.3 Confocal laser scanning microscopy (cLSM)

Either fine root or ectomycorrhiza samples were investigated using the cLSM 880 (Zeiss, Obekochen, Germany). For the excitation of GFP, an argon laser (488 nm) and for the excitation of tdtomato a helium laser (542 nm) was used. An integrated beam splitter deterred detection of light between 540 and 548 nm. A photomultiplier tube (PMT) detector was used for detection of the signals. Laser intensities and objectives varied depending on the samples. All cLSM pictures were taken by Professor Dr. Uwe Nehls.

3 Results

For *in planta* analysis of promoter activity, fluorescent proteins were chosen as visual markers. Therefore, transformation of respective constructs is necessary. However, since transformation efficiency can vary a lot, identification of transgenic organisms, organs and/or cells prior to analysis of promoter activity is an issue. For that reason, vectors containing a second fluorescence cassette driven by a constitutive promoter were designed to easily screen for transformed poplar roots in this work. The constitutively expressed marker cassette was constructed by Jana Schnakenberg (Schnakenberg 2020) and consists of a td-tomato gene driven by the NOS promoter.

In this thesis, experiments were conducted to develop a suitable fluorescence marker cassette for *in planta* analysis of promoter activity.

As generation of fully transgenic poplar plants is rather time consuming and takes about a year, only composite poplar plants were generated in this work, consisting of non-transgenic shoots and transgenic roots (Neb et al. 2017). The *Agrobacterium rhizogenes* strain K599 was chosen for all plant transformation experiments, since previous studies showed successful transformation capability (Neb et al. 2017). The vector backbone pPLV as plant transformation vector was chosen because of its small size in combination with a high copy number in *E. coli* (Hellens et al. 2000). Proof of concept experiments were carried out using the constitutively expressed 35S promoter, since previous studies showed strong expression ability in poplar roots (Neb et al. 2017).

3.1 Transformation of *A. rhizogenes* K599 with pPLV vector backbone constructs

In a first experiment to monitor the *in planta* promoter activity, the construct pPLV_**P$_{35S}$**_**sYFP**_T$_{OCS}$ (Schnakenberg 2020), containing a non targeted sYFP under the control of the 35S promoter was chosen.

However, this pPLV construct (pGreen vector backbone) repeatedly failed to transform competent *A. rhizogenes* K599 cells efficiently. After a period of seven days, very few colonies appeared on the selection agar plates that did not grow further after transfer to liquid growth medium. Freshly prepared chemically competent *A. rhizogenes* K599 also did not yield more colonies on transformation plates. The same was true for electrical competent *A. rhizogenes* cells transformed with the pPLV construct via electroporation. Experiments were performed in parallel with another *Agrobacterium* strain, *Agrobacterium tumefaciens* GV3101, which yielded many colonies on transformation plates, regardless of the transformation protocol (**Table 8**). This indicated that the used K599 strain cannot be transformed with pPLV vector backbones.

Table 8: Colony forming units monitored over a time span of seven days for different transformation methods and Agrobacteria. *A. tumefaciens* GV3101 and *A. rhizogenes* K599 were transformed with the same pPLV construct, either chemically or via electroporation.

Strain	Day 1	Day 2	Day 3	Day 4	Day 5	Day 6	Day 7
K599 chemical competent batch 1	0	0	0	0	0	0	**4**
K599 chemical competent batch 2	0	0	0	0	0	0	0
K599 electrical competent	0	0	0	0	0	0	1
GV3101 chemical competent	0	**17**					
GV3101 electrical competent	0	**18**					

In a second experiment, a different vector backbone (pCAMBIA backbone, pCXUN (Chen et al. 2009)) was used to transform cells of the same batch of competent K599 yielding approximately 100 colonies on transformation plates already after two days. This indicated principal problems when using pPLV as vector backbone in combination with *A. rhizogenes* K599. In literature, it was stated that pPLV vectors need a helper plasmid (e.g. pSOUP) in order to become replicated in an agrobacterial host as pSOUP provides the *repA* gene in trans necessary for plasmid replication (Hellens et al. 2000). *A. tumefaciens* strain GV3101 already contained pSOUP, enabling pGreen plasmid replication, as indicated from the above experiments. *A. rhizogenes* K599 is reported in literature to contain a compatible *repA*, which would omit the need for pSOUP (Cevallos et al. 2008). However, after transformation of *A.*

rhizogenes K599 with pSOUP prior to pPLV vector transformation (Immoor 2021) pPLV revealed transgenic *A. rhizogenes* K599 colonies, indicating the demand of pSOUP by the K599 strain used in the laboratory (**Table 9**).

Table 9: Colony forming units obtained after transformation after two days using different combinations of *Agrobacterium* strains and different vector backgrounds, pPLV and pCAMBIA.

Strain	Vector background	CFU after two days
K599	pPLV	0
K599	pCAMBIA	83
K599 pSOUP	pPLV	165
K599 pSOUP	pCAMBIA	170

The helper plasmid pSOUP also had a positive effect on the transformation efficiency when using a pCAMBIA vector background.

3.2 sYFP as a visual marker for *in planta* promoter activity

3.2.1 sYFP expression in *N. benthamiana* leaves

As proof of concept, the construct pPLV**_P$_{35S}$_sYFP**_T$_{OCS}$ (Schnakenberg 2020), containing a non targeted sYFP expressed under the control of the strong, constitutive 35S promoter was chosen for agroinfiltration of *N. benthamiana* leaves to see if sYFP fluorescence could be detected *in planta* (**Figure 5**).

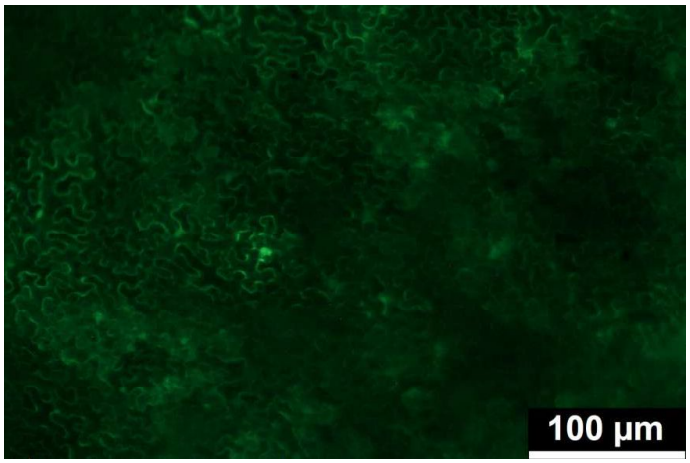

Figure 5: pPLV_P35S_sYFP_TOCS expressed in leaves of *N. benthamiana*. Tobacco leaves were infiltrated with *A. rhizogenes* K599 pSOUP harbouring pPLV_P_{35S}_sYFP-T_{OCS}. Fluorescence in the YFP channel was observed three days after infiltration. Exposure time: 4 sec.

YFP fluorescence was detected in the cytoplasm and nuclei of transgenic tobacco leaf epidermal cells. Since tobacco leaf epidermal cells contain a voluminous central vacuole, YFP fluorescence was located mainly in a thin cytoplasmic layer next to the cell wall. Since sYFP is a relatively small protein (27 kDa), it can diffuse through nuclear pores explaining why sYFP was also found inside the nucleus. Due to the strong autofluorescence in the cell walls and cytoplasmic layers of poplar root cells (Voß et al. 2013) and the resulting expected interference with the construct, no poplar plant experiments were carried out.

3.2.2 Targeted sYFP as a visual marker for *in planta* analysis in poplar roots

Two constructs targeting sYFP to different organelles, the nucleus (sYFP-NLS) and peroxisomes (sYFP-SNL) were chosen to identify suitable compartments for *in planta* analysis.

3.2.3 Construction of sYFP-SNL and sYFP-NLS expression cassettes

A sYFP-SNL coding sequence was PCR amplified from a previous construct (Neb 2017) containing a non-localised sYFP with primers adding BamHI restriction sites to the 5′ ends of the sYFPs. The reverse primer additionally contained a peroxisomal localisation sequence (PTS), consisting of the amino acids serine, asparagine and leucine (SNL). The PCR product was subcloned into pJET1.2 and the orientation was determined using restriction analysis.

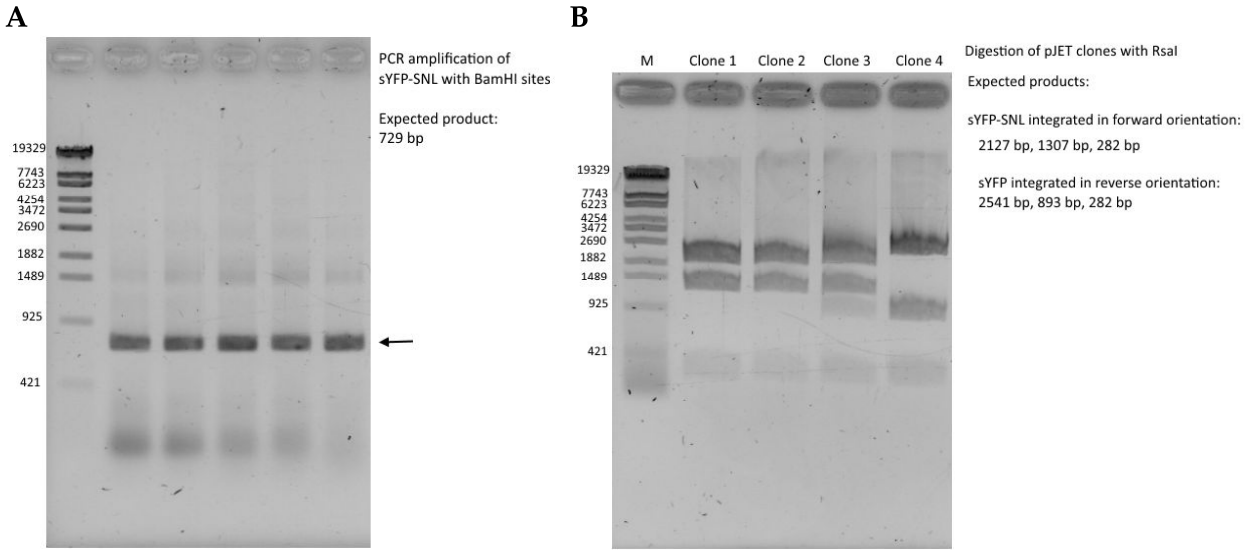

Figure 6: Amplification of a sYFP-SNL cassette and verification of the products in the entry vector pJET. A: PCR amplification of a 729 bp sYFP-SNL fragment with additional BamHI sites at both ends. **B:** Restriction analysis of four pJET1.2 clones containing the amplified sYFP-SNL fragment. Clone 1 & 2 showed forward orientation, clone 3 showed an unexpected pattern and clone 4 showed the reverse orientation.

The orientation of the amplified construct was important for the further cloning purpose because a restriction site of the multiple cloning site in the target vector would be used for directional cloning. Clone 1 (**Figure 6**B) showed the requested orientation of the sYFP-SNL in restriction analysis and thus was partially sequenced to prove the expected orientation of the sYFP-SNL fragment (supplemented data, **Figure 36**). Further vector construction was carried out using this clone.

A sYFP cassette with nuclear localisation signal (NLS) was released by BamHI restriction- from the plasmid pPLV06 (Hellens et al. 2000) (data not shown).

Both BamHI released sYFP-SNL and sYFP-NLS cassettes were cloned into the BamHI digested and dephosphorylated plant transformation vector pPLV_P35S_TOCS (Schnakenberg 2020). In the final vectors, pPLV_**P$_{35S}$_sYFP-SNL**_T$_{OCS}$ and pPLV_**P$_{35S}$_sYFP-NLS**_T$_{OCS}$, the respective sYFP constructs expressed under the control of a 35S promoter. Successful integration and correct 5′-3′ orientation of the respective sYFP cassettes were analysed via restriction endonucleases (**Figure 7**). Selected clones showing the requested orientation of the cassettes according to restriction analysis were partially sequenced. For the sYFP-SNL cassette

clone 3 and for the sYFP-NLS cassette clone 4 were chosen. Sequencing results confirmed the expected integration of the respective sYFPs (supplemented data, **Figure 37**).

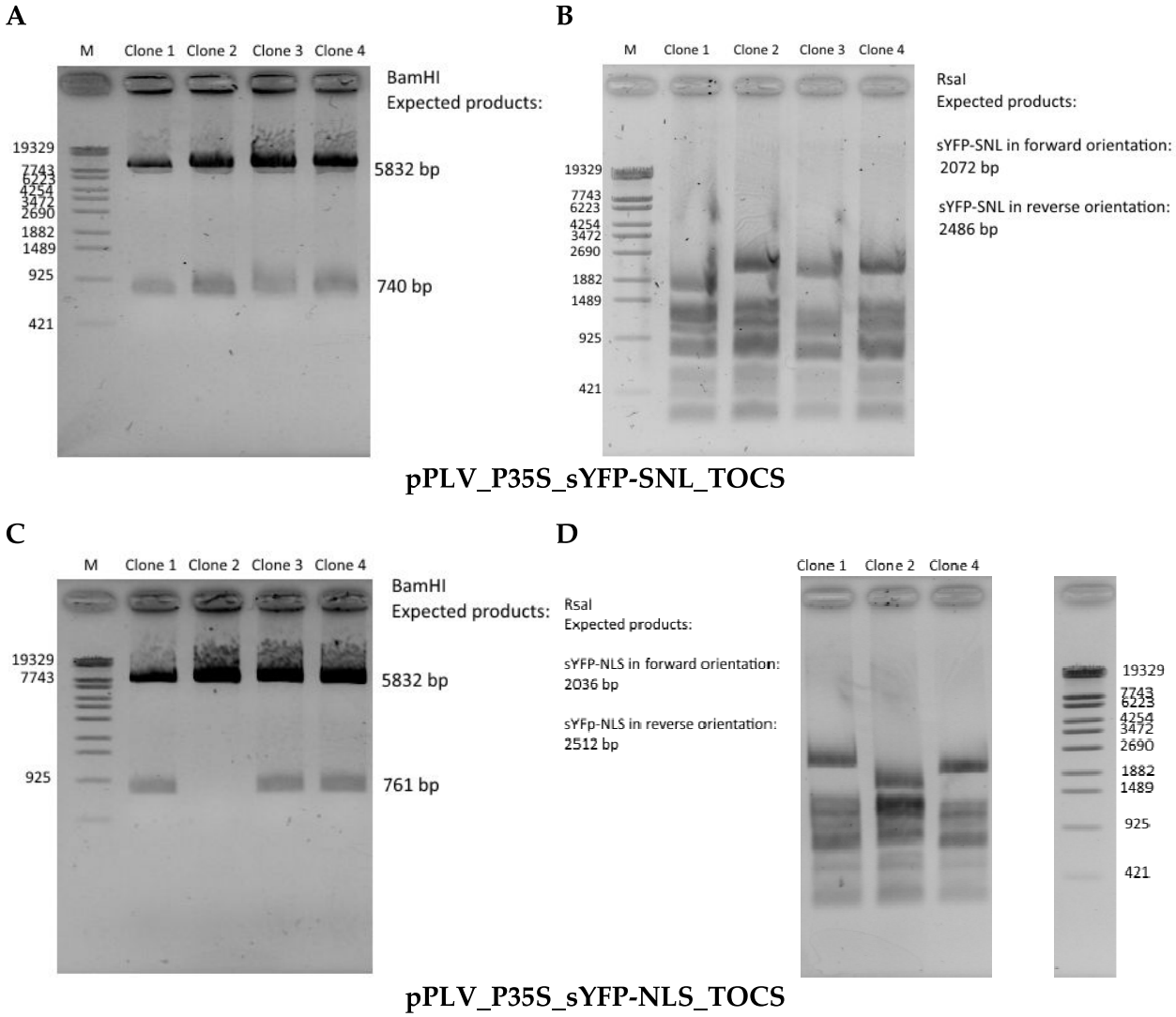

Figure 7: Restriction analysis of pPLV_P35S_sYFP-SNL_TOCS and pPLV_P35S_sYFP-NLS_TOCS constructs. **A:** Restriction analysis with BamHI, confirming the successful integration of sYFP-SNL into the vector backbone. Shown are four independent transformants. **B:** Analysis of the orientation of the fragment. Indicated is only the expected size of relevant DNA bands. Clones 2 and 4 showed reverse orientation of the sYFP-SNL cassette while clone 3 showed forward orientation. **C:** Restriction analysis with BamHI, confirming the successful integration of sYFP-NLS in the vector backbone. Clone 2 does not contain the insert. **D:** Analysis of the orientation of the fragment. Indicated is only the expected size of relevant DNA bands. Clone 1 showed reverse orientation while clone 4 showed forward orientation, and clone 2 could not be clearly identified.

3.2.4 Transient expression of constructs in tobacco leaves

Both constructs, pPLV_**P35S_sYFP-SNL**_Tocs and pPLV_**P35S_sYFP-NLS**_Tocs were transformed into *A. rhizogenes* K599 containing the helper plasmid pSOUP and used for agroinfiltration of *N. benthamiana* leaves. YFP fluorescence was observed three days after agroinfiltration using a fluorescence microscope.

A pPLV_P35S_sYFP-SNL_Tocs **B pPLV_P35S_sYFP-NLS_Tocs**

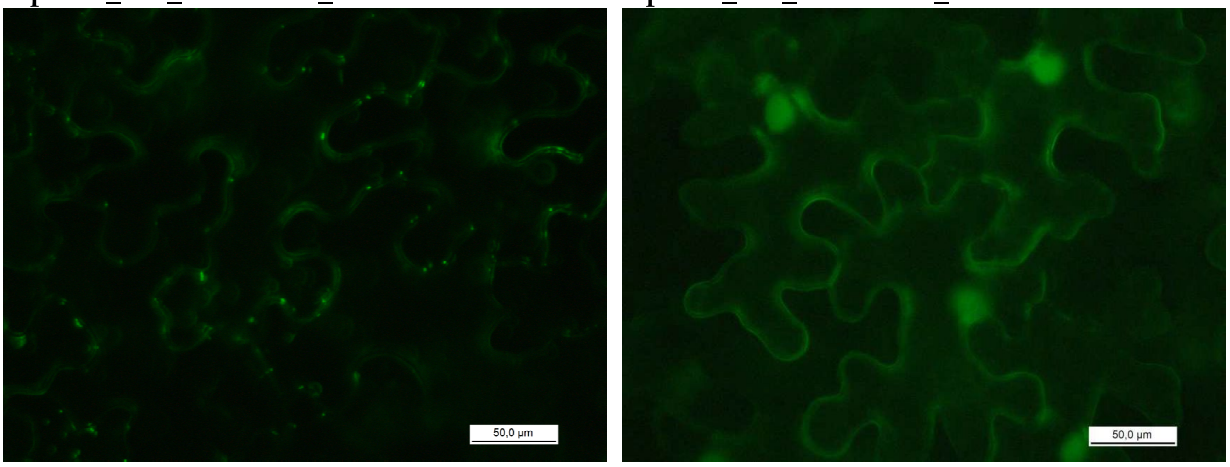

Figure 8: Localisation of sYFP in tobacco leaf cells. *T*he constructs pPLV_P35S_sYFP-SNL_Tocs (**A**) and pPLV_P35S_sYFP-NLS_Tocs (**B**) were transiently expressed in *N. benthamiana* leaf cells. Fluorescence was observed three days after incubation under a fluorescence microscope using the GFP filter. **A:** 2 sec exposure time. **B:** 4 sec exposure time.

For the construct pPLV_P35S_sYFP-SNL_Tocs, YFP fluorescence signals were observed in the cytoplasm and cell compartments which are in the size range of peroxisomes (0.5 µm) as expected due to the peroxisomal targeting sequence of this sYFP (**Figure 8**A). The strong 35S promoter in combination with a strong fluorescent gene expression caused by multiple tDNA transfer after agroinfiltration explains the cytoplasmic localisation of the fluorescence signal. Since the 35S promoter was chosen for establishment of the system, it can be expected that the signal intensities will become weaker when using weaker promoters.

The construct harbouring a nuclear import signal revealed fluorescent nuclei as well as a cytoplasmic signal (**Figure 8**B).

3.2.5 Generation of composite poplars with the sYFP constructs

Both pPLV_**P35S_sYFP-SNL**_Tocs and pPLV_**P35S_sYFP-NLS**_Tocs were used for subsequent generation of composite poplars. However, in two independent plant batches, only few fluo-

rescent roots could be detected two months after transformation. The transformation efficiency was calculated as the percentage of fluorescent roots. These results obtained (Table 10) were even lower than results from Jana Schnakenberg (Schnakenberg 2020) and Anneke Immoor (Immoor 2021) who described transformation efficiencies around 30 % for different pPLV vector backbones in composite poplars.

Table 10: Poplar transformation efficiencies of pPLV_P35S_sYFP-SNL_Tocs and pPLV_P35S_sYFP-NLS_Tocs. The transformation efficiencies were calculated as the percentage of fluorescent roots. If independent plant batches were used for the calculation, standard deviation is given.

Construct	Transformation efficiency	Batches
pPLV_P35S_sYFP-SNL_Tocs	15% ± 6%	70/81/52 roots, 15/12/4 fluorescent
pPLV_P35S_sYFP-NLS_Tocs	15 %	60 roots, 9 fluorescent

As higher transformation efficiencies were described for other vector backbones, e.g. pBI121 (Neb et al. 2017), the fluorescent cassettes were integrated into this backbone.

3.2.6 Cloning of sYFP constructs into the binary vector pBI121

From pPLV_**P35S_sYFP-SNL**_Tocs and pPLV_**P35S_sYFP-NLS**_Tocs the sYFP cassettes were excised using the restriction endonucleases KpnI and SacI and integrated into pBI121_LIC_sYFP_td1 (Schnakenberg 2020) leading to pBI121_P35S_sYFP-SNL_Tocs and pBI121_P35S_sYFP-NLS_Tocs (**Figure 9**).

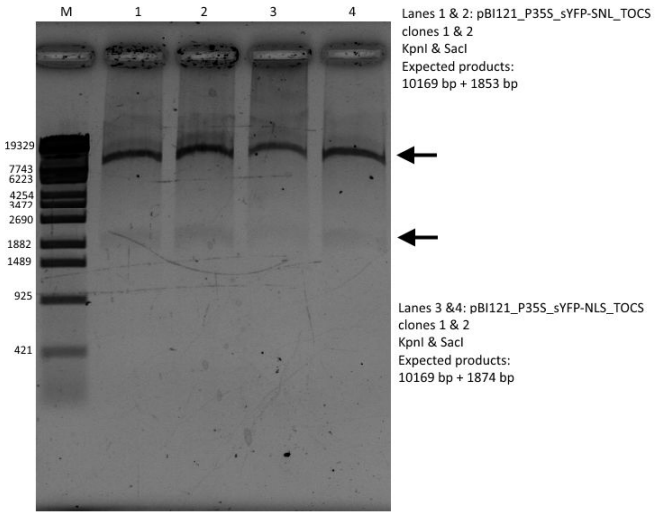

Figure 9: Restriction analysis of pBI121 sYFP constructs. pBI121_P35S_sYFP-SNL_TOCS and pBI121_P35S_sYFP-NLS_TOCS using KpnI and SacI. Lanes 1 & 2: pBI121_ P35S_sYFP-SNL_TOCS. Expected products around 10169 bp & 1853 bp. Lanes 3 & 4: pBI121_P35S_sYFP-NLS_TOCS expected products at 10169 bp & 1874 bp.

3.2.7 Tobacco leaf infiltration with pBI121 sYFP constructs

To prove the constructs, the novel pBI121 constructs targeting sYFP either to peroxisomes or to the nucleus were transiently transformed into *N. benthamiana* leaves and analysed by epifluorescence microscopy (**Figure 10**).

A: pBI121_P35S_sYFP-SNL_TOCS **B: pBI121_P35S_sYFP-NLS_TOCS**

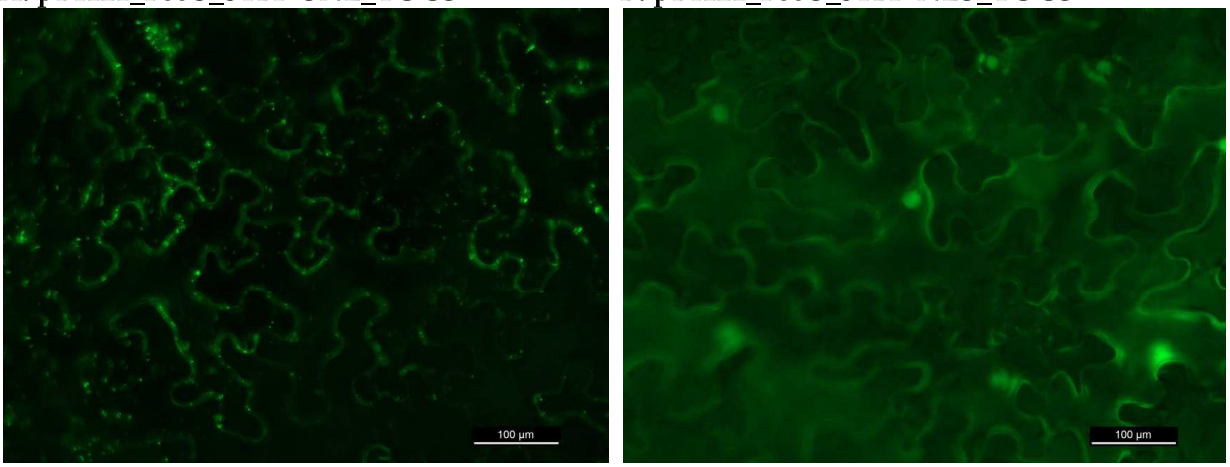

Figure 10: Analysis of pBI121 sYFP constructs in tobacco leaf cells. *A. rhizogenes* K599 harbouring the constructs pBI121_P35S_sYFP-SNL_TOCS or pBI121_P35S_sYFP-NLS_TOCS were used for agroinfiltration of *N. benthamiana* leaves. Fluorescence was observed after three days by epifluorescence microscopy using the YFP-filter set and an exposure time of. **A:** 1 sec and **B:** 1 sec.

The expected peroxisomal or nuclear localisation of sYFP fluorescence was observed. As for previous constructs also a cytoplasmic fluorescence was detected for both constructs.

3.2.8 Generation of transgenic poplar plants using pBI121 sYFP constructs

Similar to the pPLV-sYFP constructs, transformation efficiency was again rather low in composite poplars. For pBI121_**P35S_sYFP-SNL**_TOCS transformation an efficiency of 30 % (59 roots, 18 fluorescent) and for pBI121_**P35S_sYFP-NLS**_TOCS a transformation efficiency of 23 % (26 roots, 6 fluorescent) was obtained. Similar results were obtained for pBI121 derivates by J. Schnakenberg (Schnakenberg 2020). In contrast, when transformation experiments were performed with a pCAMBIA background (pCXUN), transformation efficiencies were much higher (80 % (Immoor 2021)), leading to the decision to focus further efforts on this vector.

Additionally, in all previous studies a monomeric sYFP was used. It was assumed that the strong cytoplasmic fluorescence which was observed for both peroxisomal and nuclear targets was due to the small size of the monomeric sYFP leading to the leakage out of the targeted compartments. Therefore, it was decided to exchange the fluorescence cassette for a double GFP. Due to the larger size of the GFP, leakage problems should be reduced. Furthermore, GFP fluorescence is generally stronger than that of YFP.

3.3 Construction of a promoter analysis vector with a double GFP (dGFP) as visual marker

To investigate whether non transformed poplar roots show autofluorescence in one of the channels of interest (dsred, GFP), a non transformed poplar root in the composite poplar system was investigated using the stereomicroscope. No fluorescence could be detected in the channels of interest.

The vectors pCXUN_**PUBQ_dGFP-NLS**_TNOS and pCXUN_**PUBQ_dGFP-NLS_TNOS_PNOS_tdtomato-NLS**_TOCS were constructed. For proof of concept, two different promoters, the *A. thaliana* ubiquitin promoter PUBQ as well as the 35S promoter were used to control expression of a nuclear targeted double GFP (dGFP-NLS). As a control, a promoterless construct containing dGFP was generated as well. The dGFP-NLS should later be expressed under the control of a promoter fragment of interest.

3.3.1 The double GFP cassette

pPLV04 (De Rybel et al. 2011) was obtained from the Nottingham Arabidopsis Stock Centre where it is annotated as pGIIK- LIC-SV40-3GFP-tNOS, containing a triple GFP with a SV-40 nuclear localisation signal and a NOS terminator. However, routine verification of the vector with endonucleases showed differences to the fragments as expected by *in silico* analysis of the vector.

Table 11: Restriction analysis of pPLV04. Shown in bold are different fragment sizes for triple or double GFP.

	pPLV04 triple GFP expected	pPLV04 double GFP expected	Fragment sizes obtained
BamHI & XbaI	4818 bp	4818 bp	4800 bp
	2459 bp	**1472 bp**	1400 bp
			6000 bp
PvuI	2888 bp	2888 bp	2600 bp
	2450 bp	**1733 bp**	1900 bp
	1937 bp	1937 bp	1700 bp
			400 bp
PvuII	3605 bp	3605 bp	3600 bp
	2907 bp	**2190 bp**	2100 bp
	757 bp	757 bp	700 bp

The sizes of the DNA fragments obtained with NcoI digestion corresponded to the expected in silico sizes. However, it is difficult to distinguish if there are two bands (754 bp and 727 bp respectively) as expected for a triple GFP or a single 700 bp band as expected for a double GFP **(**supplemented data, Figure 38A, lane 1). When using the endonucleases BamHI & XbaI, the lower band was clearly approximately 800 bp too small (supplemented data, Figure 38A, lane 2; **Table 11**). Assuming a double instead of triple GFP, the band size pattern corresponded perfectly to the observed result (**Table 11**). An analysis of the vector with PvuI led to no clear result regarding the status of the GFP (supplemented data, Figure 38B, lane 1; **Table 11**), since the expected band at 2888 bp corresponding to the vector backbone could not be detected and an additional very faint band at 400 bp appeared. Another analysis per-

formed by using PvuII (supplemented data, Figure 38B lane 2) indicated a DNA fragment of 2000 bp instead of 2900 bp indicating a double GFP (**Table 11**). Sequencing was performed, but a double GFP sequence is too large to be completely sequenced (data not shown). Internal sequencing primers can also not be designed, since no unique binding sites are present.

All in all, restriction analysis of pPLV04 gave strong hints for a double instead of a triple GFP sequence. Thus, the GFP will be further termed dGFP in this work.

3.3.2 Construction of dGFP cassettes

pPLV04 (De Rybel et al. 2011), containing a dGFP with an SV40 nuclear localisation signal was linearised by double digestion with the endonucleases EcoRI and XhoI. Both sites are located in front of the GFP start codon. The respective promoters P_{UBQ} (pPLV06_P_{UBQ}) and P_{35S} (pPLV11_P_{35S}_sYFP-SNL_T_{OCS}) were excised by digestion of the respective vectors with EcoRI and XhoI and integrated into the linearised pPLV04 to obtain the constructs pPLV04_P_{UBQ} and pPLV04_P_{35S} (**Figure 11**).

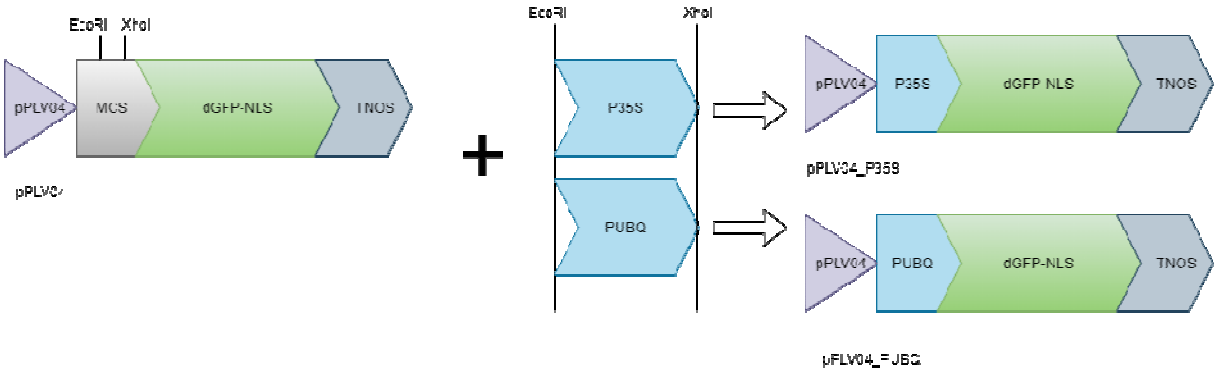

Figure 11: Insertion of selected promoters to in front of a dGFP-NLS expression cassette in pPLV04. Two different promoters, P_{35S} and P_{UBQ} were cloned in a directed manner in front of the dGFP-NLS in pPLV04.

Both constructs were transformed into *A. rhizogenes* K599 pSOUP and tested for functionality in composite poplar plants. Both constructs showed the expected fluorescence in the nuclei. However dGFP fluorescence seemed to be stronger when expressed under control of the 35S promoter (**Figure 12**, A & C). It was thus decided to continue with the P_{UBQ}_dGFP-NLS construct to minimise artefacts due to a too strong GFP expression.

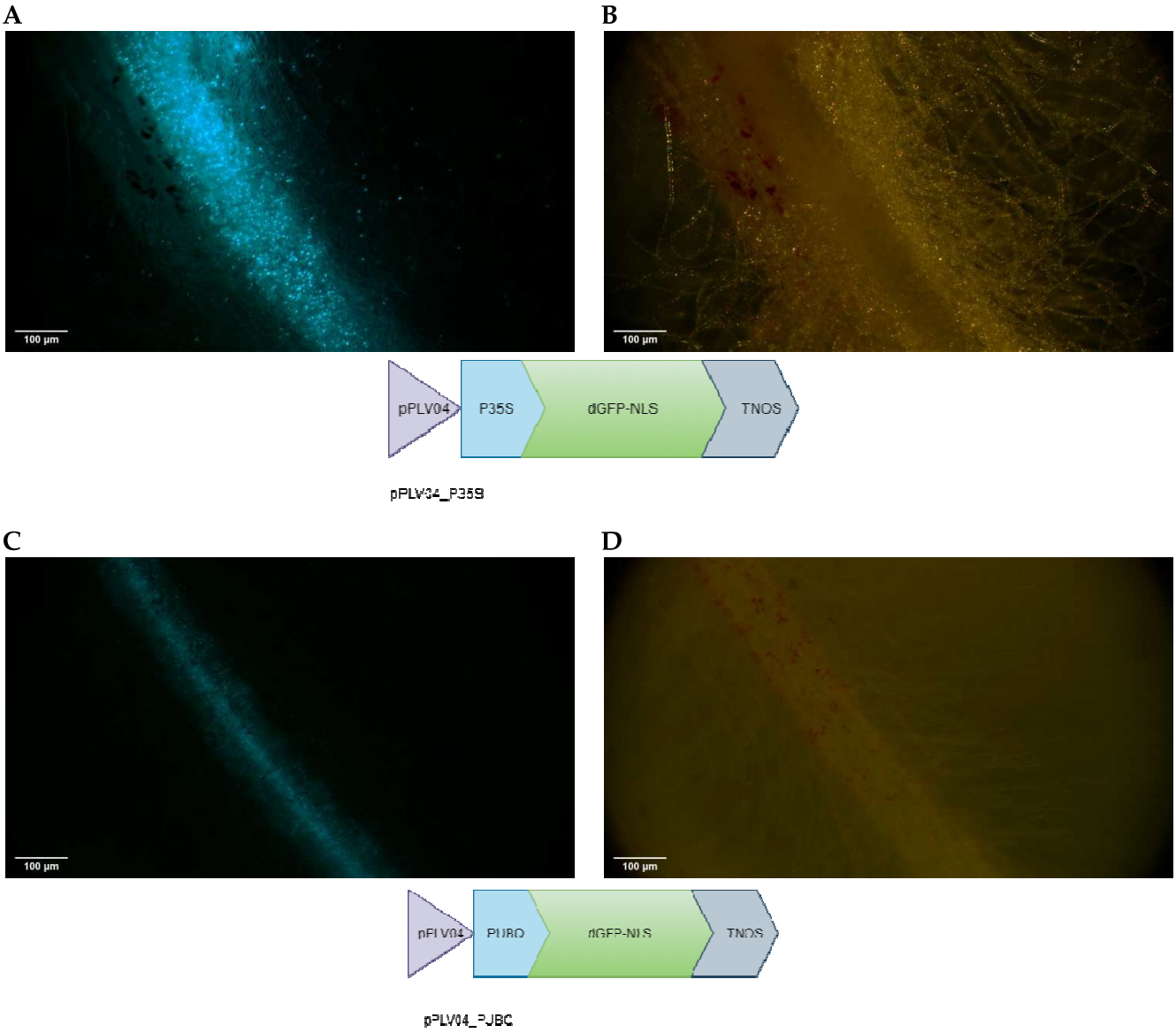

Figure 12: Images of transgenic *P. tremula x alba* roots harbouring promoter_dGFP-NLS constructs. The images were taken 4 weeks after infection of poplar plants with *A. rhizogenes* K599 pSOUP strain containing the plasmid of interest. **A:** pPLV04_P35S, GFP channel, 200 msec exposure time. **B:** transmission light channel, 200 msec exposure time. **C:** pPLV04_PUBQ, GFP channel, 250 msec exposure time. **D:** transmission light channel, 100 msec exposure time.

3.3.3 Constitutively expressed red fluorescence marker cassette

The final aim was the development of a plant transformation vector containing two fluorescent protein marker cassettes: one expressing a nuclear localised GFP under the control of a promoter of interest and a nuclear localised td-tomato under the control of a constitutive promoter. For a proof of concept, P_{UBQ} was used as a "variable" promoter while P_{NOS} was chosen for the constitutively expressed cassette.

From a pJET1.2 construct, the second marker cassette PNOS_**tdtomato-NLS**_TOCS (Schnakenberg 2021) was excised with the endonucleases NotI-HF and SacI-HF. The vector pPLV04_PUBQ' was linearised with the same enzyme combination and the second marker cassette was integrated into the vector to obtain pPLV04_PUBQ_**P**NOS_**tdtomato-NLS**_TOCS. The same procedure was performed in parallel with pPLV04 to obtain pPLV04_**P**NOS_**tdtomato-NLS**_TOCS (**Figure 13**).

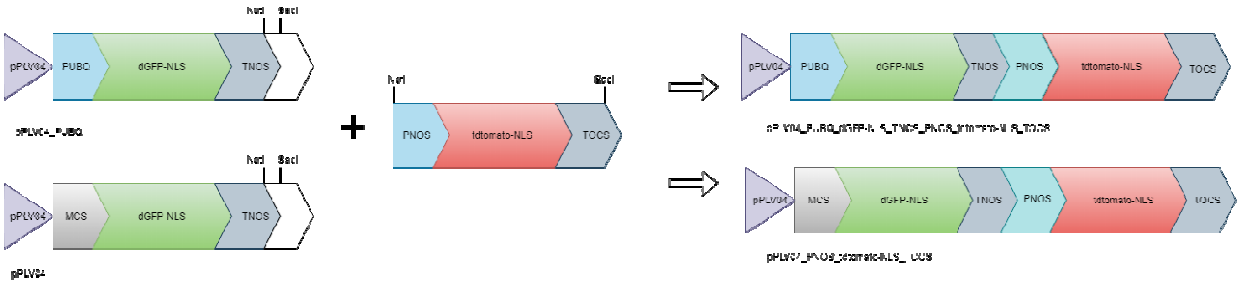

Figure 13: Insertion of the td-tomato-NLS fluorescence cassette into different pPLV constructs. The tdtomato cassette was cloned in tandem behind the dGFP cassettes of the vectors pPLV04_PUBQ and pPLV04.

pCXUN06 (Schnakenberg 2020), a derivative of pCXUN-FLAG (Chen et al. 2009) was digested with KpnI and SacI and the vector backbone was gel purified. The vectors pPLV04_PUBQ_PNOS_tdtomato-NLS_TOCS, pPLV04_PNOS_tdtomato-NLS_TOCS and pPLV04_PUBQ were also digested with KpnI and SacI and the cassettes were gel purified. Both inserts were then integrated into the linearised pCXUN vector backbone to generate the vectors pCXUN_**P**UBQ_**dGFP-NLS**_**T**NOS_**P**NOS_**tdtomato-NLS**_TOCS, pCXUN_**dGFP_NLS**_**T**NOS_**P**NOS_**tdtomato-NLS**_TOCS (vector map: supplemented data, **Figure 42**) and pCXUN_**P**UBQ_**dGFP-NLS**_TNOS **Figure 14**, **Figure 15**).

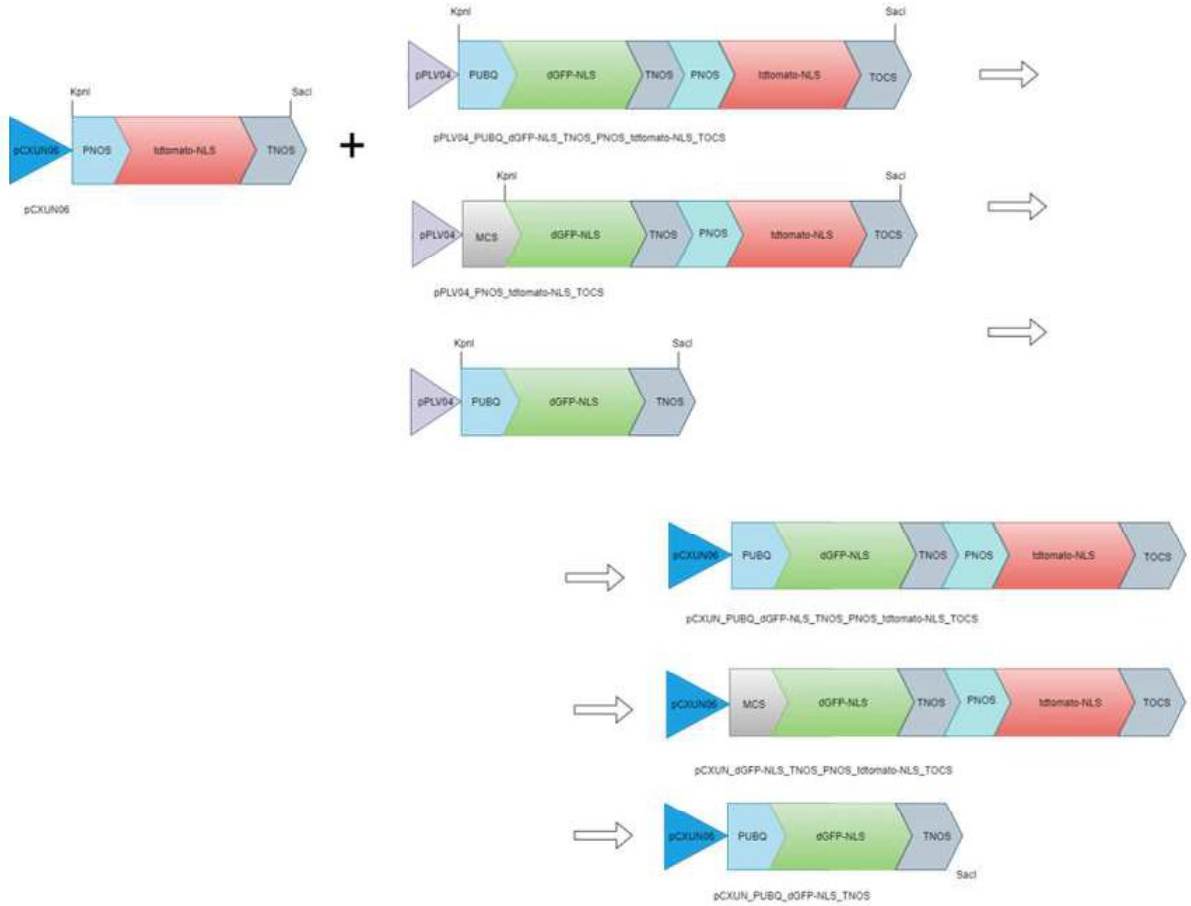

Figure 14: Insertion of the double marker cassettes and the single dGFP cassette into pCXUN. The directed integration of the cassettes were enabled by KpnI and SacI. The cassettes were cut out from the pPLV04 vector background and inserted into the pCXUN backbone.

A: pCXUN_PUBQ_dGFP-NLS_PNOS-tdtomato-NLS

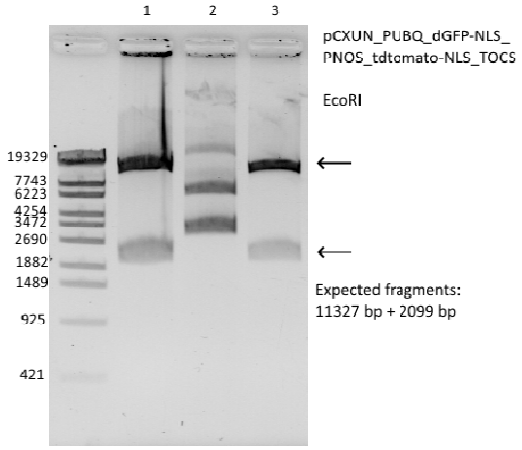

B: pCXUN_dGFP-NLS_PNOS-tdtomato-NLS

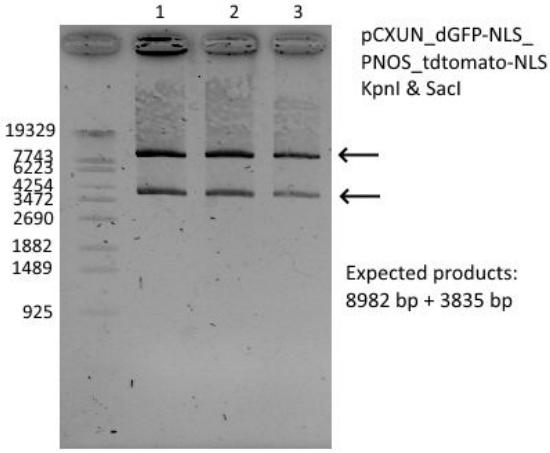

C: pCXUN_PUBQ_dGFP-NLS

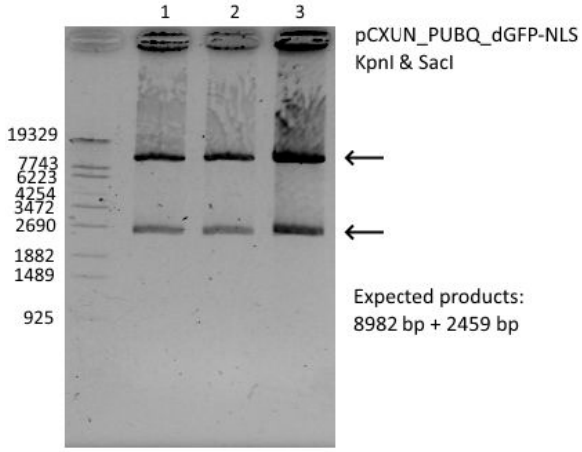

Figure 15: Restriction analysis of pCXUN-dGFP constructs. **A**: pCXUN_PUBQ_dGFP-NLS_PNOS_tdtomato-NLS digested with EcoRI; expected fragments: 11327 bp & 2099 bp. **B**: pCXUN_dGFP-NLS_PNOS_tdtomato-NLS digested with KpnI & SacI; expected fragments: 8982 bp & 2835 bp. **C**: pCXUN_PUBQ_dGFP-NLS digested with KpnI & SacI; Expected fragments: 8982 bp & 2459 bp.All constructs were transformed into *A. rhizogenes* K599 and used for transient expression in tobacco leaf cells and for the generation of composite poplars.

3.3.4 Functional analysis of marker cassettes in *N. benthamiana* leaves & composite poplar plants

The construct pCXUN06_**PUBQ_dGFP-NLS**_TNOS was tested for its functionality by leaf infiltration in *N. benthamiana* (**Figure 16**) as well as in roots of composite poplar plants (**Figure 17**). In both experimental setups the GFP fluorescence was detected in the nuclei. Slight background fluorescence was observed in the red channel in leaves.

The vector control containing a promoterless dGFP cassette and a tdtomato cassette under the control of the NOS promoter revealed only red nuclei in epifluorescence stereo micros-

copy in *N. benthamiana* leaves (**Figure 18**) and poplar roots (**Figure 19**) and unspecific GFP background fluorescence.

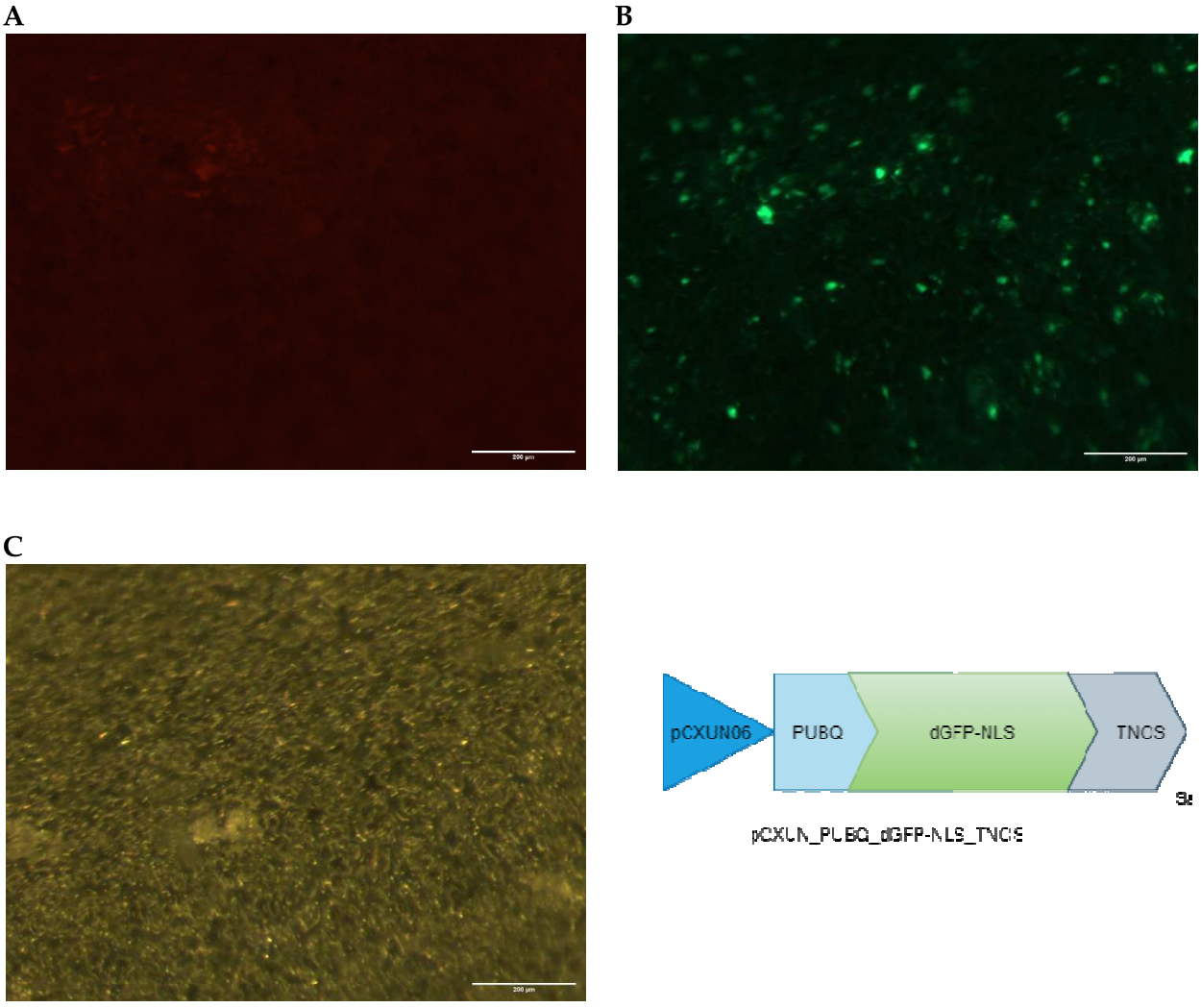

Figure 16: Images of the construct pCXUN06_P$_{UBQ}$_dGFP-NLS_T$_{NOS}$ transiently expressed in leaves of *N. benthamiana*. The construct contained a nuclear targeted dGFP under the control of the UBQ promoter. The pictures were taken two days after infiltration of the leaves with *A. rhizogenes* K599. **A:** red channel, 5 sec exposure time. **B:** GFP channel, 1 sec exposure time. **C:** transmission light channel, 90 msec exposure time. Scale bar = 200 μm.

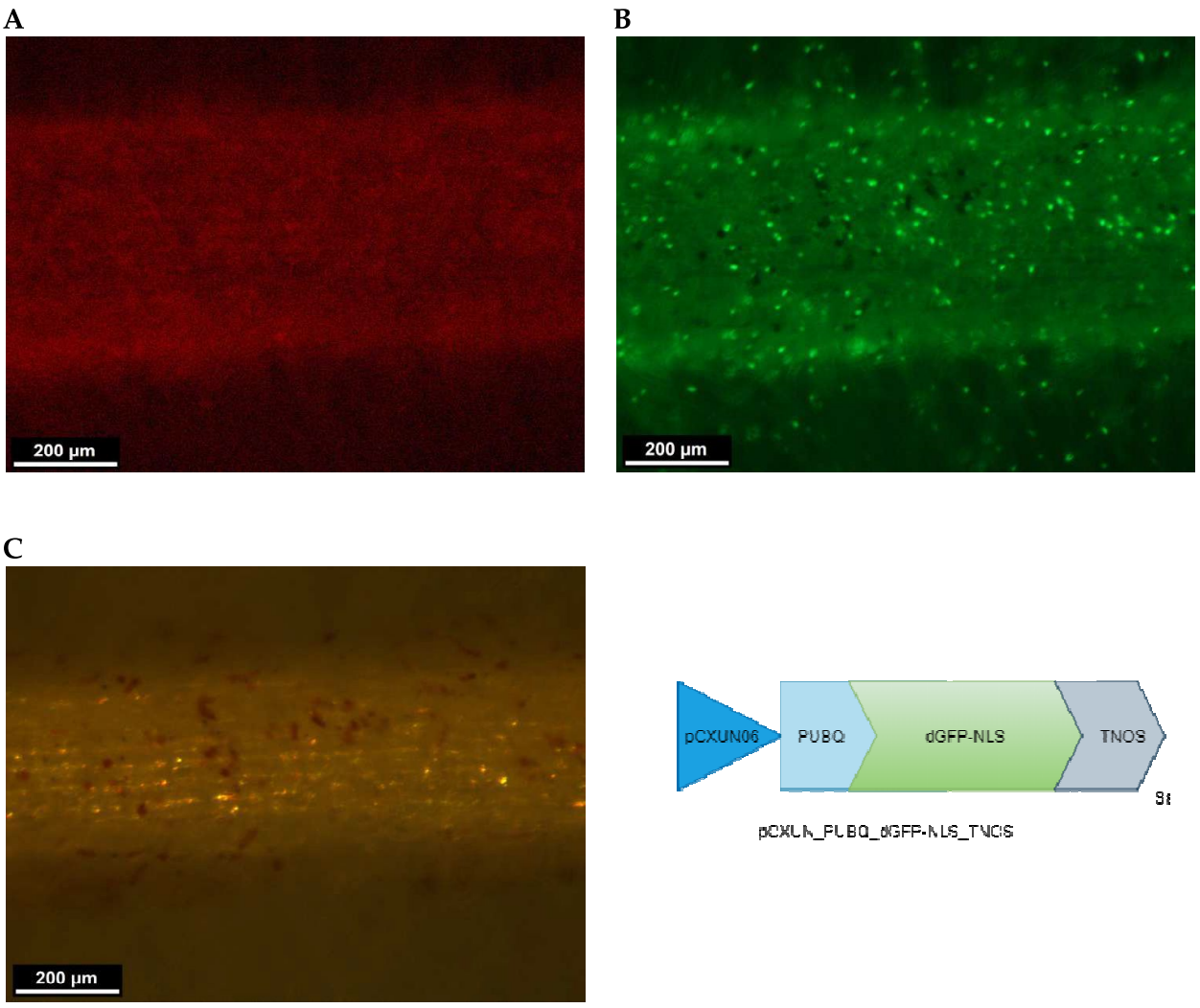

Figure 17: Images of *P. tremula x alba* roots transformed with *A. rhizogenes* harbouring the construct pCXUN06_PUBQ_dGFP-NLS_TNOS. Pictures were taken 4 weeks after the generation of composite poplars. **A:** red channel, 2 sec exposure time. **B:** GFP channel, 2 sec exposure time. **C:** transmission light channel, 130 msec exposure time.

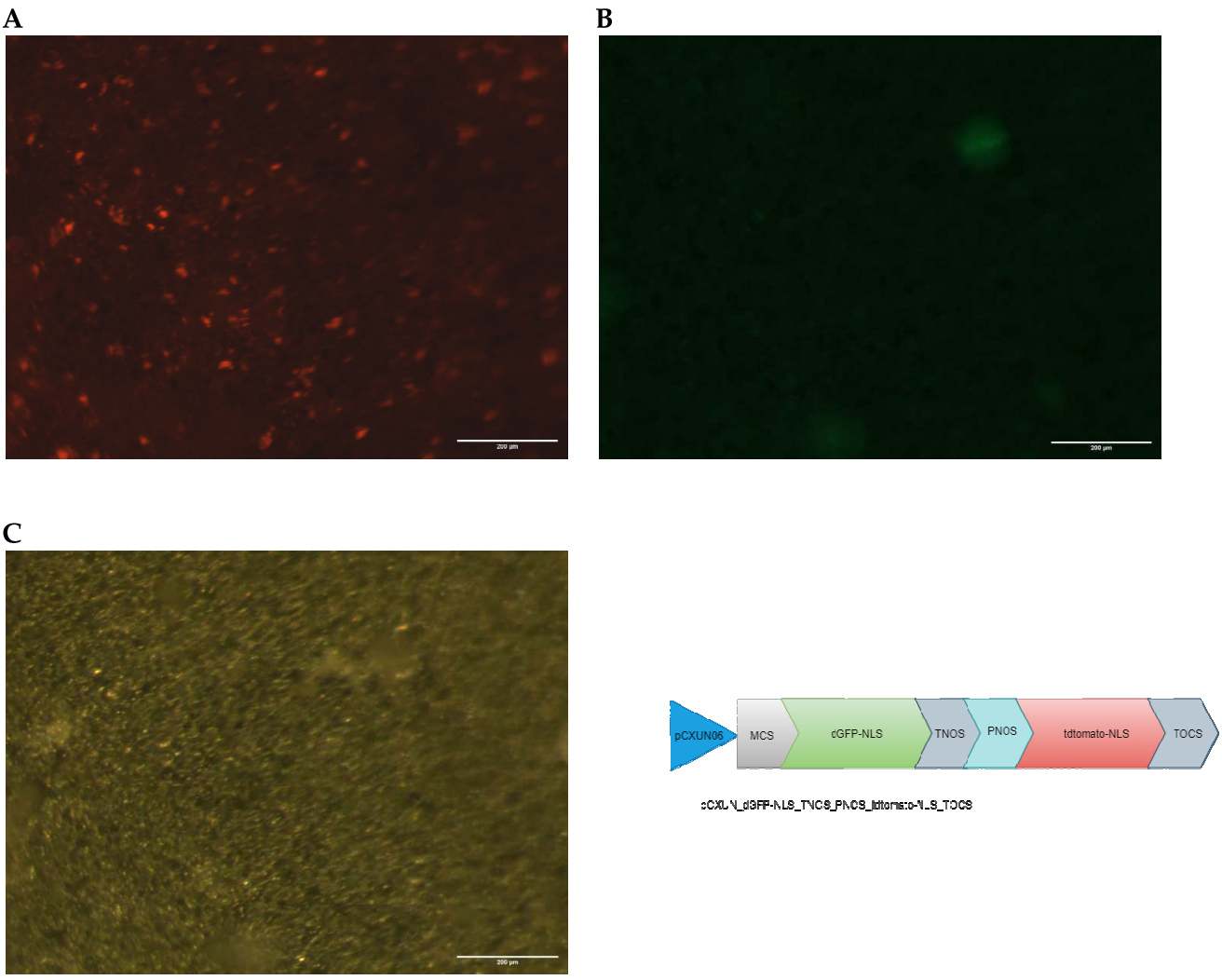

Figure 18: Images of the construct pCXUN06_dGFP-NLS_T$_{NOS}$_P$_{NOS}$_tdtomato-NLS_T$_{OCS}$ transiently expressed in leaves of *N. benthamiana*. The construct contained a promoter less nuclear targeted dGFP cassette and a nuclear targeted tdtomato cassette driven by a NOS promoter. The pictures were taken two days after infiltration of the leaves with *A. rhizogenes* K599. **A:** red channel, 1 sec exposure time. **B:** GFP channel, 5 sec exposure time. **C:** transmission light channel, 90 msec exposure time. Scale bar: 100 µm.

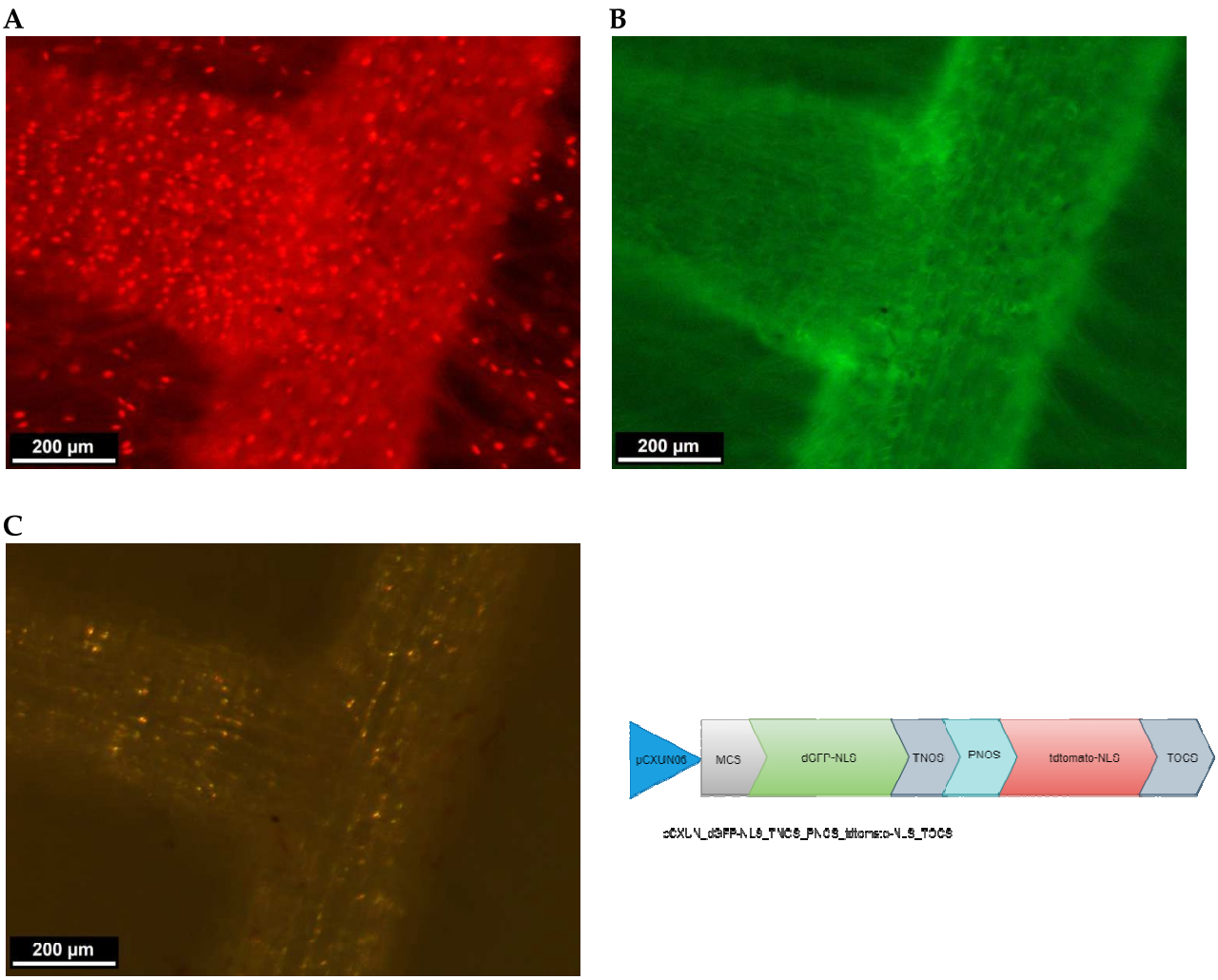

Figure 19: Images of *P. tremula x alba* roots transformed with *A. rhizogenes* harbouring pCXUN06_dGFP-NLS_T$_{NOS}$_P$_{NOS}$_tdtomato-NLS_T$_{ocs}$. Pictures were taken 4 weeks after inoculation of plant cuttings. **A:** red channel, 1 sec exposure time. **B:** GFP channel, 2 sec exposure time. **C:** transmission light channel, 100 msec exposure time.

For the construct pCXUN06_P$_{UBQ}$_**dGFP-NLS**_T$_{NOS}$_P$_{NOS}$_**tdtomato-NLS**_T$_{ocs}$ detection of nuclei in the red channel was difficult, whereas GFP fluorescence was detected in many nuclei of *N. benthamiana* leaves (**Figure 20**). However, in poplar roots, both tdtomato and GFP signals were detected in nuclei (**Figure 21**).

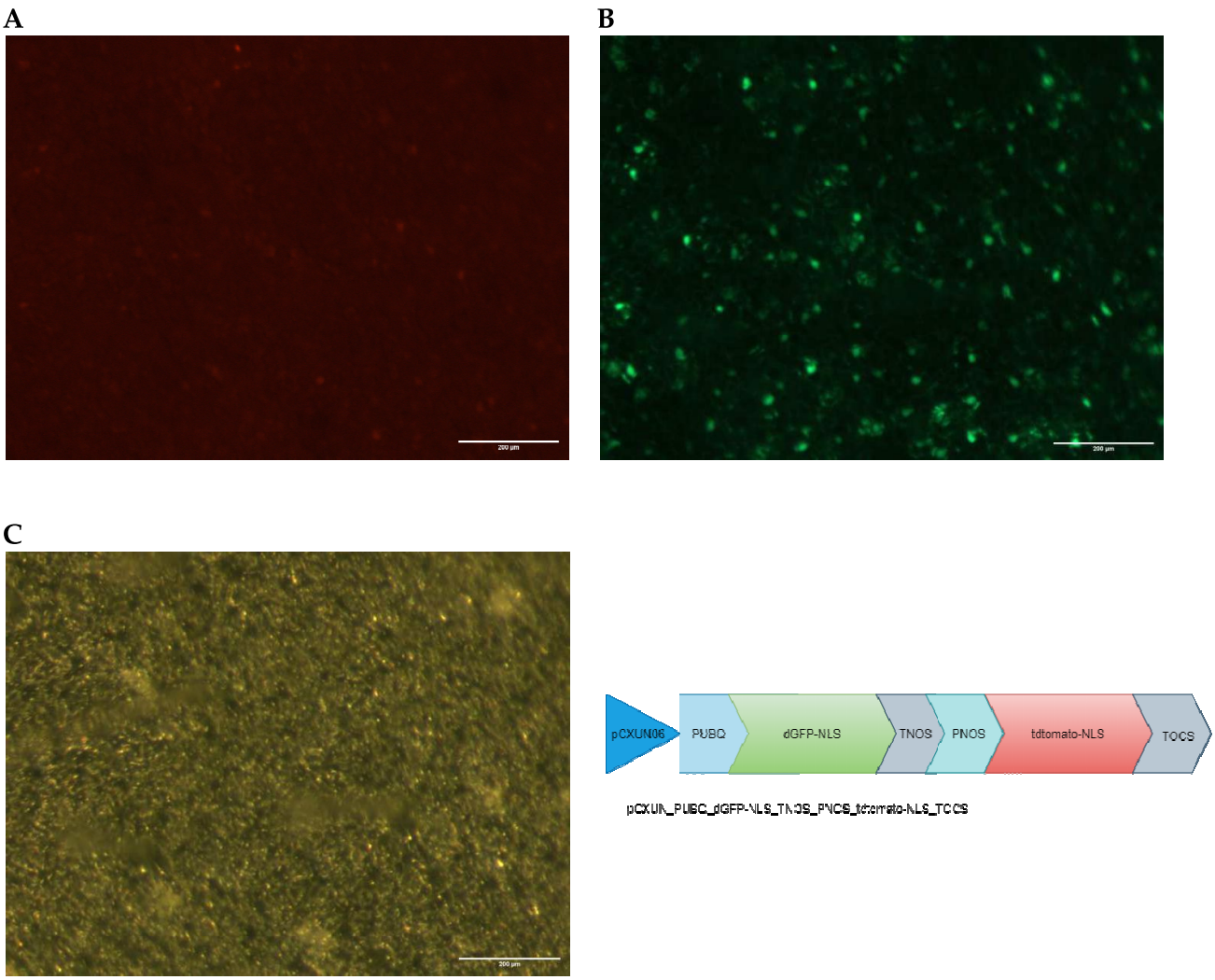

Figure 20: Images of the construct pCXUN06_P$_{UBQ}$_dGFP-NLS_T$_{NOS}$_P$_{NOS}$_tdtomato-NLS_T$_{OCS}$ transiently expressed in leaves of *N. benthamiana*. The construct contains a nuclear targeted dGFP under the control of the Ubiquitin promoter and a nuclear targeted tdtomato under the control of the NOS promoter. The pictures were taken two days after infiltration of the leaves with *A. rhizogenes* K599. **A:** red channel, 5 sec exposure time. **B:** GFP channel, 1 sec exposure time. **C:** transmission light channel, 90 msec exposure time. Scale bar = 200 µm.

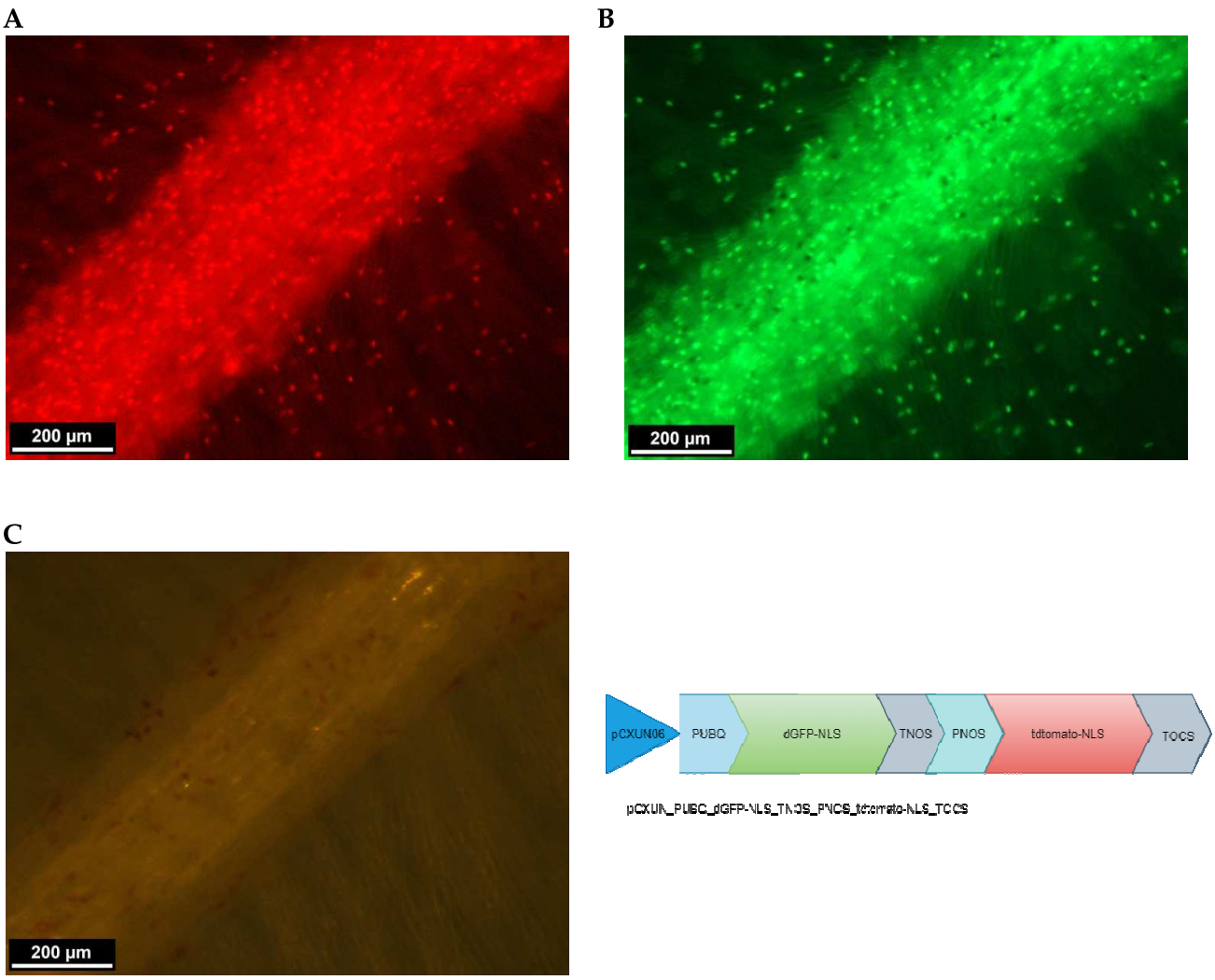

Figure 21: Stereo microscopic images of *P. tremula x alba* roots transformed with *A. rhizogenes* harbouring pCXUN06_P$_{UBQ}$_dGFP-NLS_T$_{NOS}$_P$_{NOS}$_tdtomato-NLS_T$_{OCS}$. Pictures were taken 4 weeks after inoculation of plant cuttings. **A:** red channel, 4 sec exposure time. **B:** GFP channel, 2 sec exposure time. **C:** transmission light channel, 130 msec exposure time.

To conclude, it was possible to obtain fluorescence signals in nucleus from two different marker proteins in composite poplar roots. The tdtomato is suitable as a marker for successfully transformed roots, as the constitutively expressed cassette could be detected in transformed poplar roots in all cases.

3.4 Amplification of promoter fragments from selected poplar genes and subcloning into pJET1.2

Promoter fragments for genes of interest were first PCR amplified using a proof reading Taq polymerase and gene specific primers from genomic DNA of *P. tremula x tremuloides* (T89). For *Potrx6G1673*, a 2.2 kb fragment and for *Potrx6G0093*, two fragments of 3.5 2.6 kb respectively were amplified by PCR (**Figure 22**).

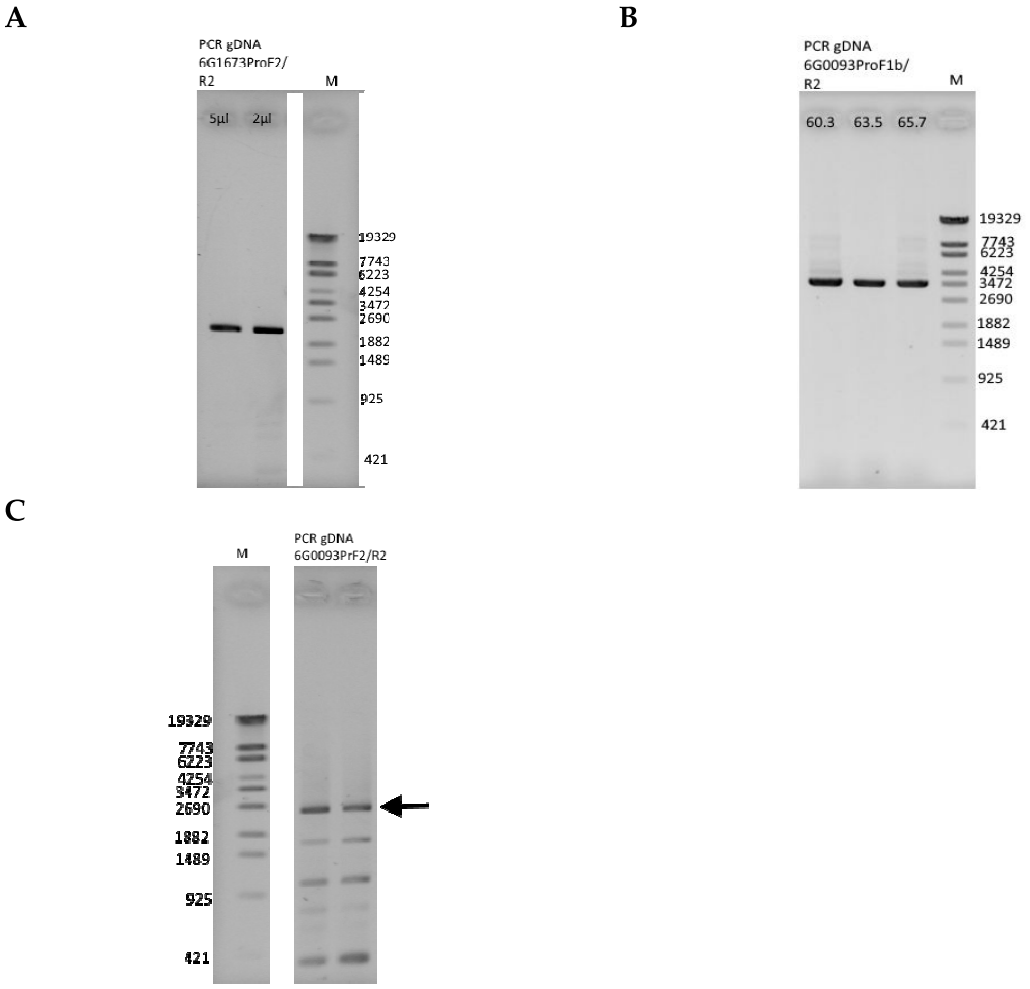

Figure 22: PCR amplification of selected promoter fragments from *P. tremula x tremuloides* genomic DNA. 2 µl of PCR product were loaded on to a 1 % agarose gel. Lambda DNA StyI digested was used as a molecular size marker. **A:** Amplification of a 2230 bp promoter fragment of 6G1673 using the primers P6G1673ProF2/6G1673ProR2. 5 µl and 2 µl template gDNA (1:10 diluted) were used. The annealing temperature was set to 47 °C and elongation was set to 90 sec. **B:** Amplification of a 3520 bp promoter fragment of 6G0093 using the primers P6G0093ProF1b/P6G0093R2. 2 µl template gDNA were used for the reaction, for annealing, a temperature gradient was used and elongation was set to 90 sec. **C:** Amplification of a 2651 bp promoter fragment of 6G0093 using the primers P6G0093F2/P6G0093R2. 2 µl template gDNA were used and amplification was performed with a temperature gradient at annealing, for annealing and elongation time was set to 90 sec.

For all promoter fragments, amplification was successful (**Figure 23**). The respective DNA bands were excised from the gels, purified and initially cloned into pJET1.2. Positive clones were determined using restriction analysis (**Figure 23**) and sequencing (supplemented data, **Figure 39**).

A **B**

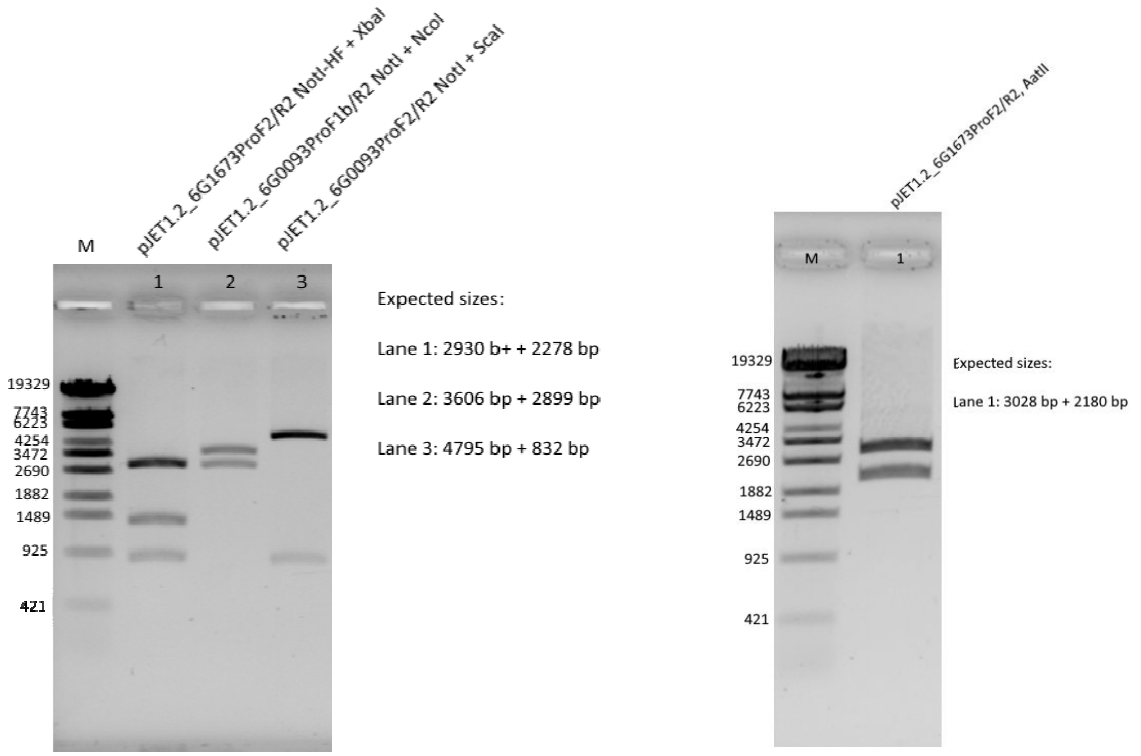

Figure 23: Restriction analysis of pJET1.2 promoter constructs. . **A:** Restriction analysis of the three promoter fragments 6G1673ProF2/R2, 6G0093ProF1b/R2, 6G0093ProF2/R2 in pJET1.2 with different enzymes. **B:** Additional digestion of pJET1.2_6G1673ProF2/R2 with AatII.

Restriction analysis of the pJET1.2 constructs showed the fragments of expected size, except for pJET1.2_6G1673ProF2/R2 (**Figure 23**A, lane 1). Here, two bands at approximately 1400 bp and 920 bp were detected, instead of one band at 2278 bp. As these bands add up to roughly 2300 bp, it was concluded, that the promoter fragment 6G1673ProF2/R2 contains an additional recognition site for one of the used enzymes. In a second approach, a different endonuclease was used for the analysis (**Figure 23**B, lane 1) resulting in the expected band sizes.

The pJET1.2 constructs were further used as template for promoter truncations and subsequent cloning into suitable plant transformation vectors.

3.5 *Potrx6G1673* promoter truncations

3.5.1 Cloning of the obtained promoter fragment and its 5′ truncations into the plant transformation vector pCXUN

pJET1.2_6G1673ProF2/R2 specific LIC primers were used to amplify the promoter fragment and selected 5′ truncations.

Table 12: Primer combinations and sizes of the promoter fragment and 5′truncations with LIC primers. Shown are primer combinations and the length of the expected product by using pJET1.2_6G1673ProF2/R2 as a template.

Primer pair	Product	Product length
Univ LICr_F1/univ LICR1	6G1673_2.2kb	2260 bp
P6G1673LICR/P6G1673LIC_F4	6G1673_1kb	1092 bp
P6G1673LICR/P6G1673LIC_F3	6G1673_500bp	569 bp
P6G1673LICR/P6G1673LIC_F2	6G1673_250bp	268 bp

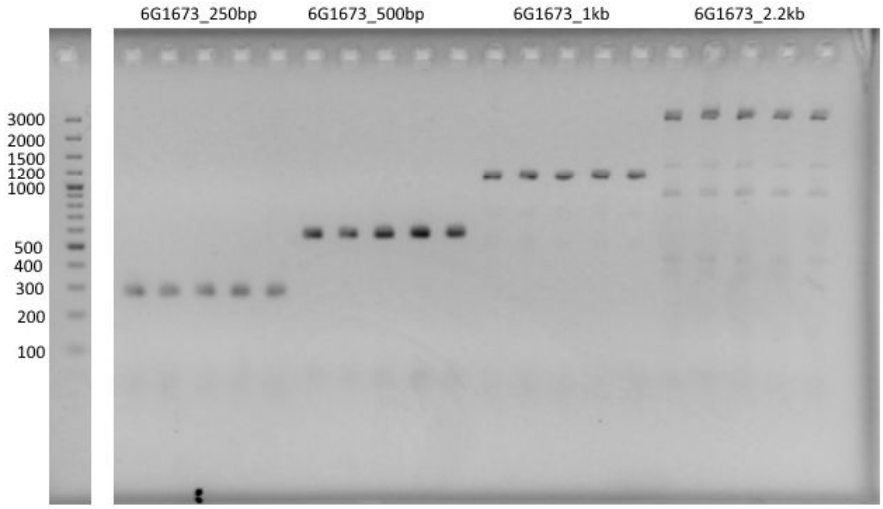

Figure 24: LIC PCR fragments of 6G1673. By using different primer combinations, the promoter fragment and the 5′ truncations were amplified with LIC adapters from the template pJET1.2_6G1673ProF2/R2. The GeneRuler™ 100 bp DNA ladder plus was used as a size marker. Lanes 1-5: Replicates of 6G1673_250bp (expected product length: 268 bp). Lanes 6-10: Replicates of 6G1673_500bp (expected product length: 569 bp). Lanes 11-15: Replicates of 6G1673_1kb (expected product length: 1092 bp). Lanes 16-20: Replicates of 6G1673_2.2kb (expected product length 2260 bp).

For all desired fragments, PCR amplification with LIC adapter sequences was successful. All fragments were then cloned into the vector pCXUN06_dGFP-NLS_T_{NOS}_P_{NOS}_tdtomato-NLS_T_{OCS} using the strategy LIC.

A: pCXUN_6G1673_2.2 kb

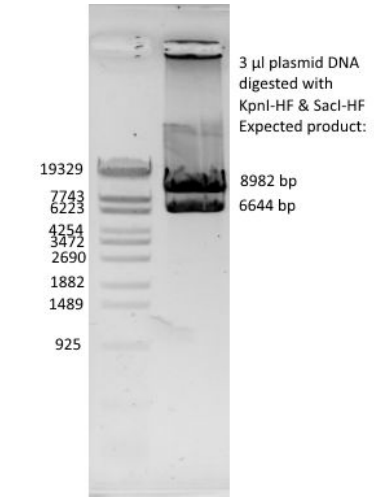

B: pCXUN_6G1673_1kb

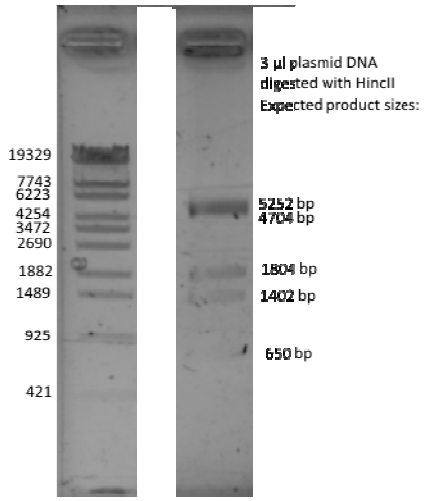

C: pCXUN_6G1673_500bp

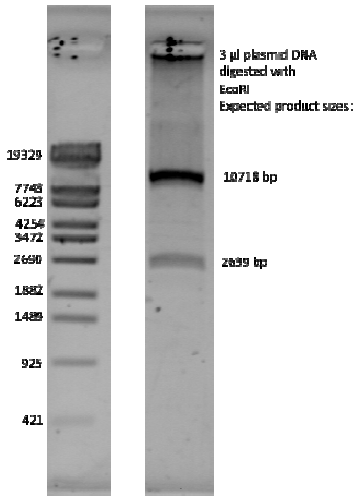

D: pCXUN6G1673_250bp

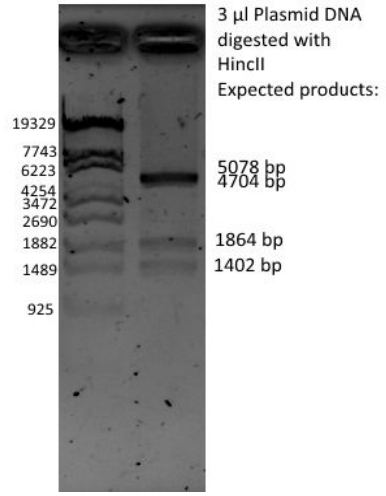

Figure 25: Restriction analysis of pCXUN_6G1673 promoter constructs. Lambda DNA digested with StyI was used as a molecular size marker on 1 % agarose gels. **A:** pCXUN_6G1673_2.2kb digested with KpnI-HF and SacI-HF. Expected product sizes: 8982 bp, 6644 bp. **B:** pCXUN_6G1673_1kb digested with HincII. Expected product sizes: 5252 bp, 4704 bp, 1804 bp, 1402 bp, 650 bp. **C:** pCXUN_6G1673_500bp digested with EcoRI. Expected product sizes: 10718 bp, 2639 bp. **D:** pCXUN_6G1673_250bp digested with HincII. Expected sizes: 5078 bp, 4704 bp, 1536 bp, 1402 bp.

Figure 26: Scheme of 6G1673 5`promoter truncations.

All plasmids were transformed into *Agrobacterium rhizogenes* K599. To test for the functionality and the integrity of the plasmid and the tDNA, all constructs were first tested in *N. benthamiana* leaves.

3.5.2 Agroinfiltration into *N. benthamiana* leaves with fragments of the *6G1673* promoter

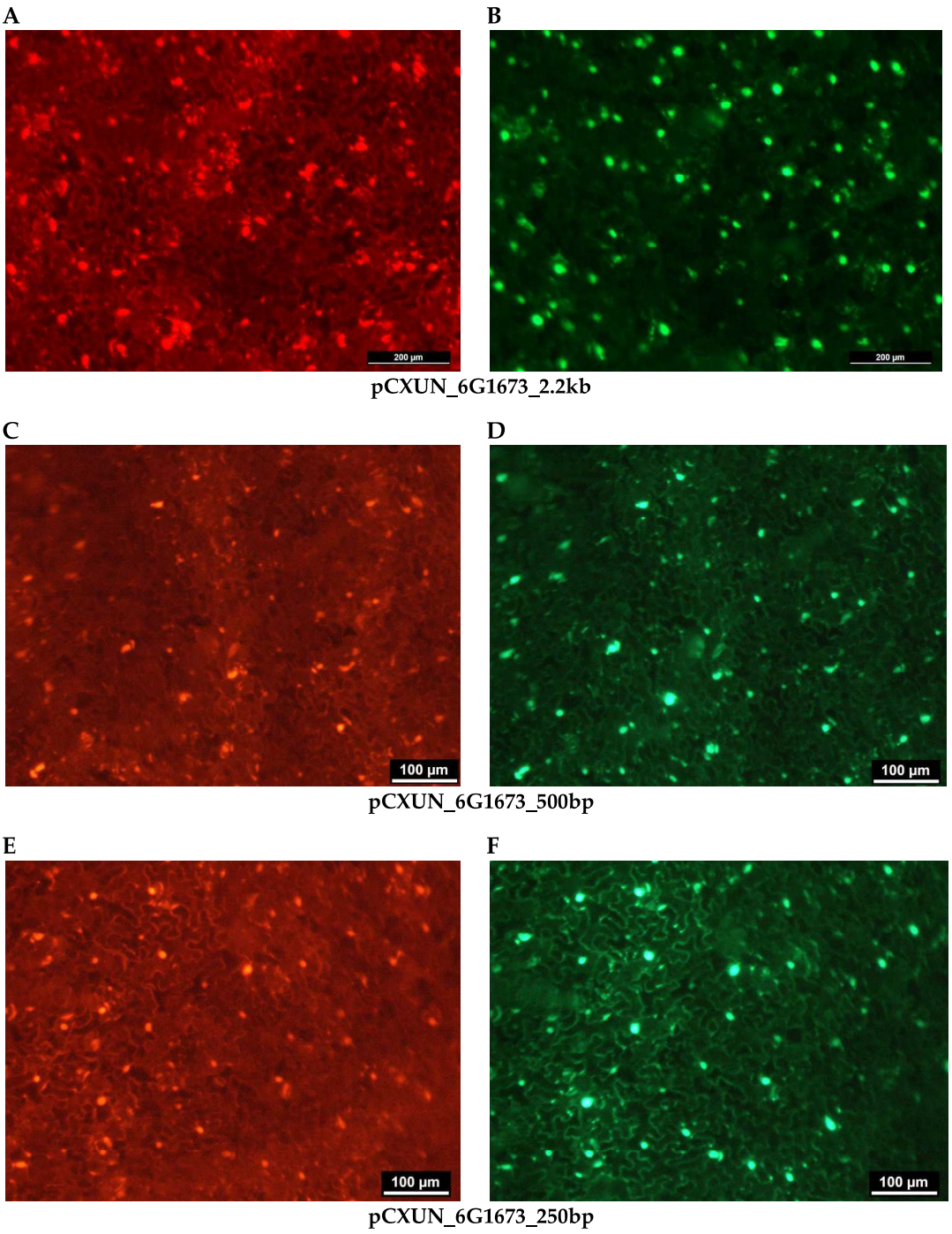

Figure 27: Epifluorescence microscopy of pCXUN_6G1673 constructs transiently expressed in leaves of *N. benthamiana*. Both fluorescence markers were targeted to the nucleus. The pictures were taken two days after infiltration of the leaves with *A. rhizogenes* K599. **A/B:** pCXUN_6G1673_2,2kb with A: red channel, 2 sec exposure time and B: GFP channel, 2 sec exposure time. **C/D:** pCXUN_6G1673_500bp with E: red channel, 2 sec exposure time and F: GFP channel, 1 sec exposure time. **E/F:** pCXUN_6G1673_250bp with G: red channel, 2 sec exposure time and H: GFP channel, 1 sec exposure time.

The constitutively expressed tdtomato was detected regardless of the second fluorescence cassette containing the dGFP.

The dGFP was under the control of different 6G1673 promoter truncations ranging from 2.2 kb to 250 bp. In all truncations investigated, dGFP fluorescence targeted to the nucleus was observed. All promoter truncations therefore exhibited sufficient promoter activity to drive expression of dGFP in leaves of *N. benthamiana*.

3.5.3 Expression of the promoter fragments of *6G1673* in poplar roots

Previous qPCR results revealed a strong induction in the expression of 6G1673 in mycorrhizas formed by *P. tremula x alba* and *P. tremula x tremuloides* compared to non infected fine roots (Nehls, unpublished). Therefore, selected promoter truncations were tested in addition to the longest fragment with *P. tremula x alba* & *P. tremula x tremuloides*.

A B

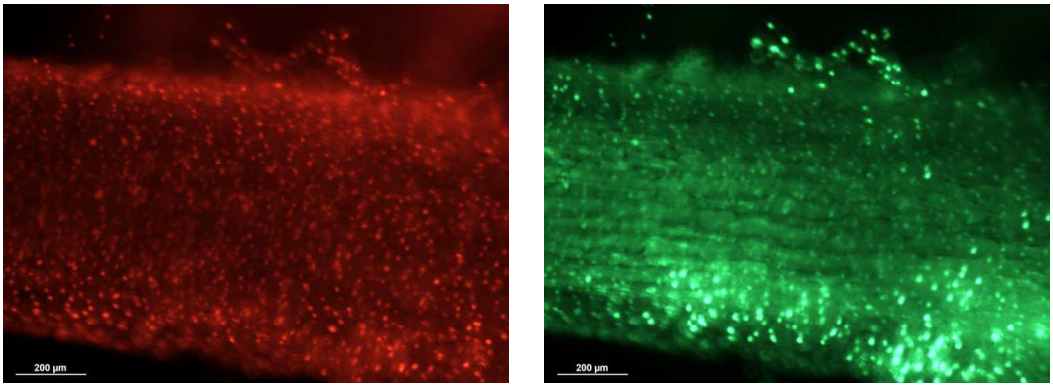

pCXUN_6G1673_2.2kb in *P. tremula x alba*

C D

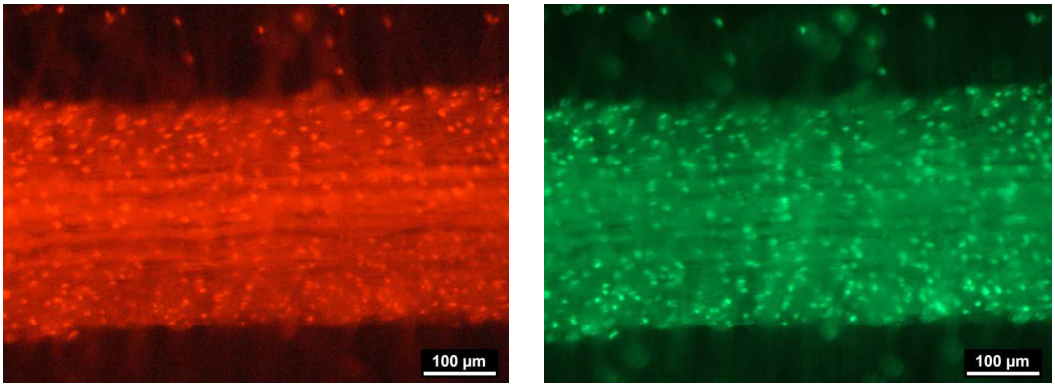

pCXUN_6G1673_1kb in *P. tremula x alba*

E F

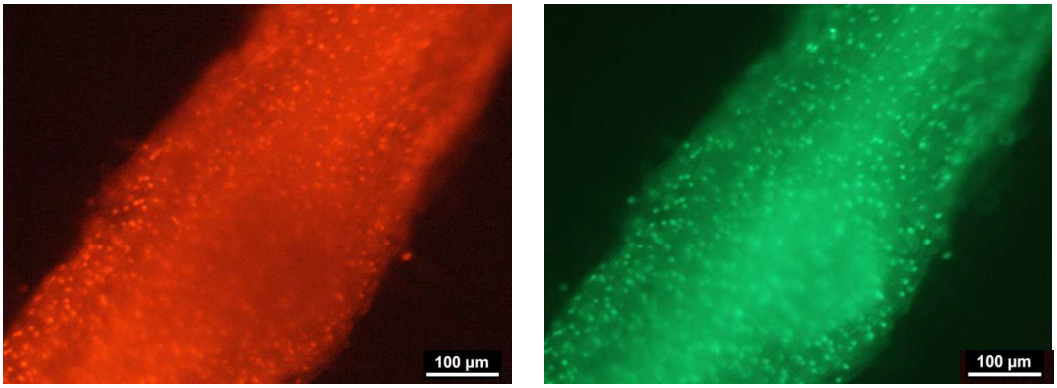

pCXUN_6G1673_500bp in *P. tremula x alba*

G H

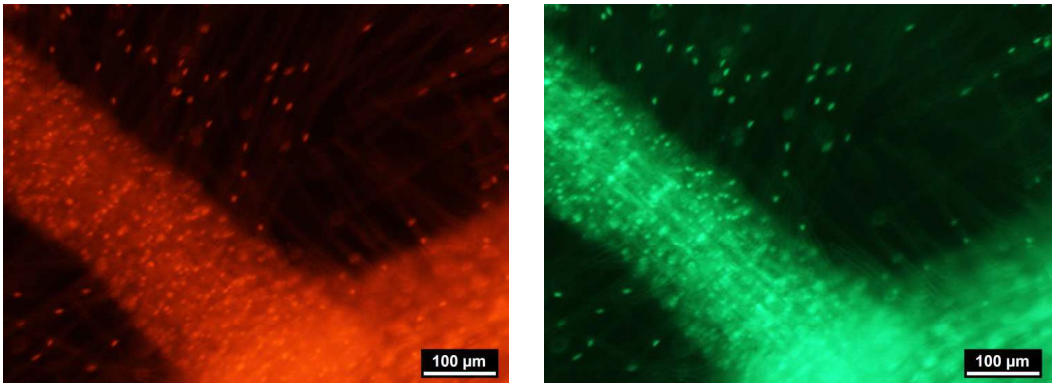

pCXUN_6G1673_250bp in *P. tremula x alba*

Figure 28: Fluorescence microscopy of *P. tremula x alba* roots transformed with different promoter fragments of pCXUN_6G1673. Both fluorescence markers were targeted to the nucleus. The pictures were taken 4 weeks after transforming the roots with *A. rhizogenes K599*. **A/B:** pCXUN_6G1673_2.2kb. A: red channel, 4 sec exposure time. B: GFP channel, 2 sec exposure time. **C/D:** pCXUN_6G1673_1kb. C: red channel, 2 sec exposure time and D GFP channel with 1 sec exposure time. **E/F:** pCXUN_6G1673_500bp. E: red channel with 2 sec exposure time and F: GFP channel with 2 sec exposure time. **G/H:** pCXUN_6G1673_250bp. G: red channel with 3 sec exposure time and H: GFP channel with 3 sec exposure time.

Regardless of whether *P. tremula x alba* or *P. tremula x tremuloides* were used for the composite poplar experiments, all tested promoter fragments of 6G1673 revealed promoter activity as seen from nuclear targeted dGFP signals (**Figure 28**, supplemented data, **Figure 40**).

Noticeably, shorter promoter truncations needed longer exposure times to detect clear signals.

Experiments set up with *A. muscaria* did not lead to mycorrhiza formation. Experiments conducted with *P. microcarpus* yielded some mycorrhiza after 3 months incubation time. However, no transgenic mycorrhiza could be detected and therefore no results concerning the activity of 6G1673 promoter fragments in mycorrhiza were obtained.

3.6 *Potrx6G0093* promoter truncations

3.6.1 Cloning of promoter truncations into the plant transformation vector pCXUN

The longest promoter fragment was used as a PCR template for the amplification of all promoter truncations. Specific 3′ LIC primers were used together with a universal 5′ primer (P6G0093LICR) to amplify promoter fragments.

Table 13: Promoter truncations with LIC primers. Shown is the length of the expected product when pJET1.2_6G1673ProF2/R2 is used as a template.

Specific primer	Product	Product length
P6G0093LICF3	6G0093_1kb	1040 bp
P6G0093LICF2	6G0093_500bp	537 bp
P6G0093LICF1	6G003_250bp	286 bp

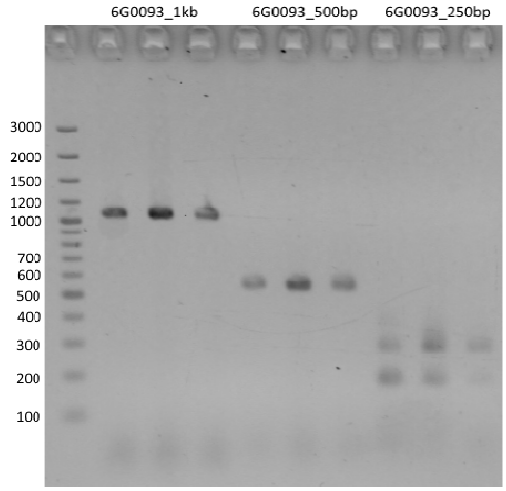

Figure 29: LIC PCR fragments of 6G0093. Using the primers mentioned above, 3 5' truncated promoter fragments harbouring LIC adapters were amplified from the template pJET1.2_6G0093ProF1b/R2 and 1 µl was visualised on a 2 % agarose gel. The GeneRuler™ 100 bp DNA ladder plus was used as a size marker. Lanes 1-53: Replicates of 6G0093_1kb, expected product length: 1040 bp. Lanes 4-6: Replicates of 6G0093_500bp, expected product length: 537 bp. Lanes 7-9: Replicates of 6G0093_250bp, expected product length: 286 bp.

For all desired fragments, PCR amplification with LIC adapter sequences was successful. All fragments were then cloned into a plant transformation vector containing a promoterless dGFP and a tdtomato under the control of the NOS promoter, both with nuclear localisation signal (pCXUN06_dGFP-NLS_T$_{NOS}$_P$_{NOS}$_tdtomato-NLS_T$_{OCS}$) using LIC.

To generate the constructs pCXUN_6G0093_3.6kb and pCXUN_6G0093_2.6kb PCR amplification was performed with primers containing KpnI and SmaI sites and were again subcloned into pJET1.2 (supplemented data, **Figure 41**). The fragments were then excised from the pJET1.2 constructs, using KpnI and SmaI. pCXUN06_P$_{UBQ}$_dGFP-NLS_T$_{OCS}$_P$_{NOS}$_tdtomato-NLS_T$_{OCS}$ was opened up with KpnI and HpaI, which eliminated the ubiqutin promoter in front of the dGFP. The fragments and the vector backbone were gel purified and subsequently ligated.

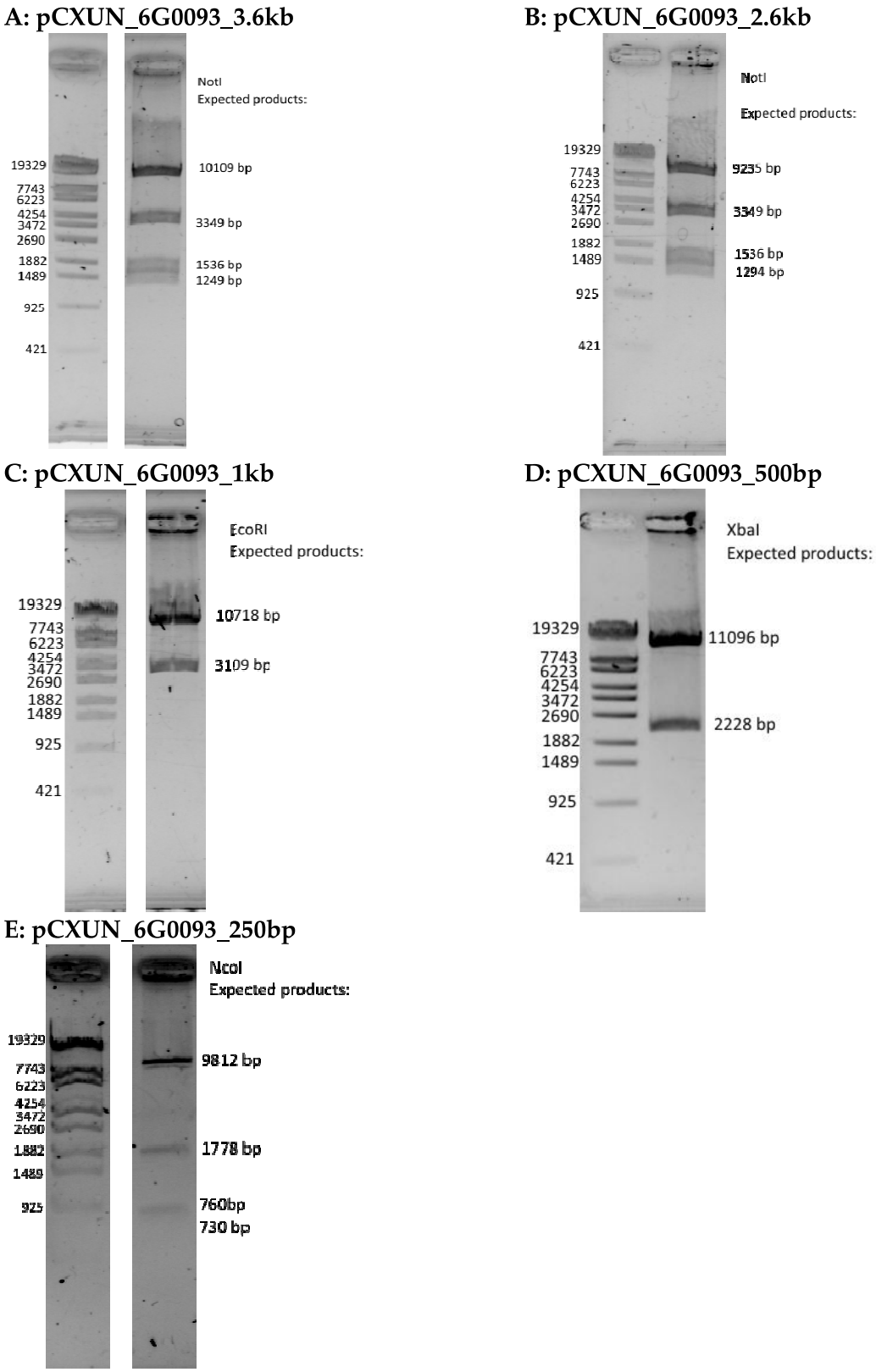

Figure 30: Verification of pCXUN constructs containing different promoter truncations of 6G0093 using restriction analysis. **A:** pCXUN_6G0093_3.6kb digested with NotI. **B:** pCXUN_6G0093_2.6kb digested with Not: **C:** pCXUN_6G0093_1kb digested with EcoRI. **D:** pCXUN_6G0093_500bp digested with XbaI. **E:** pCXUN_6G0093_250bp digested with NcoI.

All promoter constructs were successfully integrated into the plant transformation vector pCXUN upstream of the dGFP cassette.

Figure 31: Scheme of 6G0093 5′ promoter truncations.

All promoter constructs were then used to transform *Agrobacterium rhizogenes* K599 and used for the infiltration of *N. benthamiana* leaves.

3.6.2 Agroinfiltration of *N. benthamiana* leaves with *6G0093* promoter truncation constructs

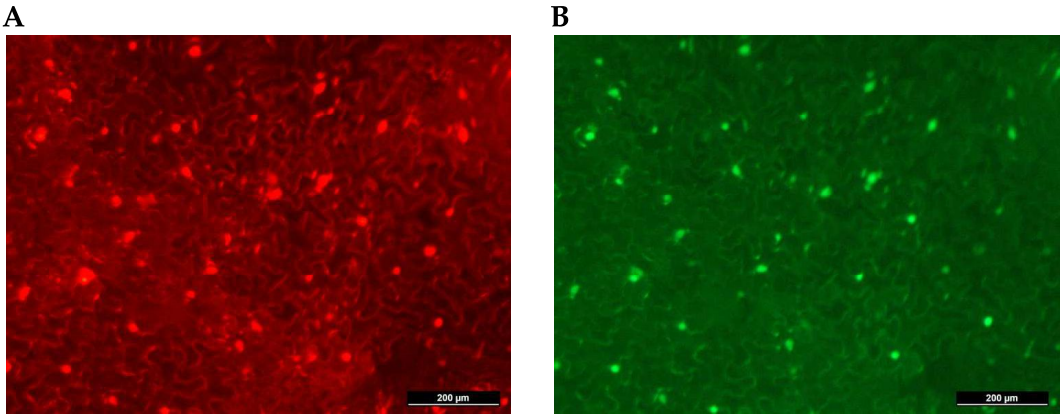

pCXUN_6G0093_3.6kb

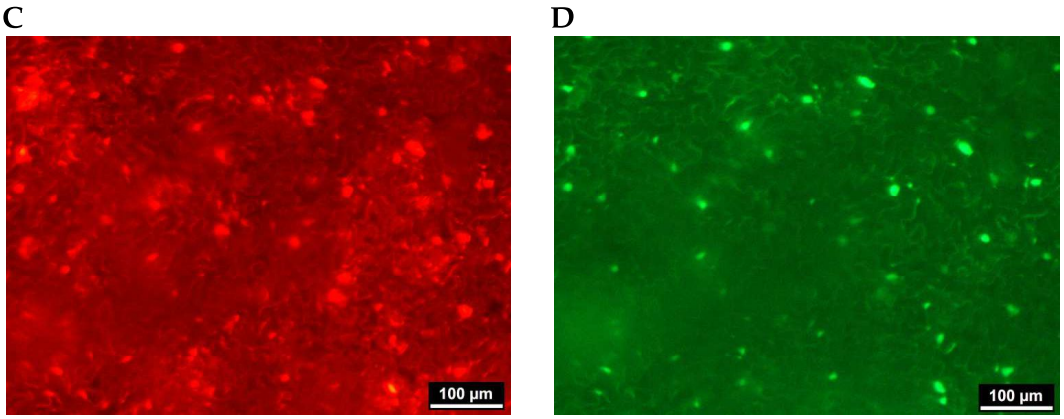

pCXUN_6G0093_2.6kb

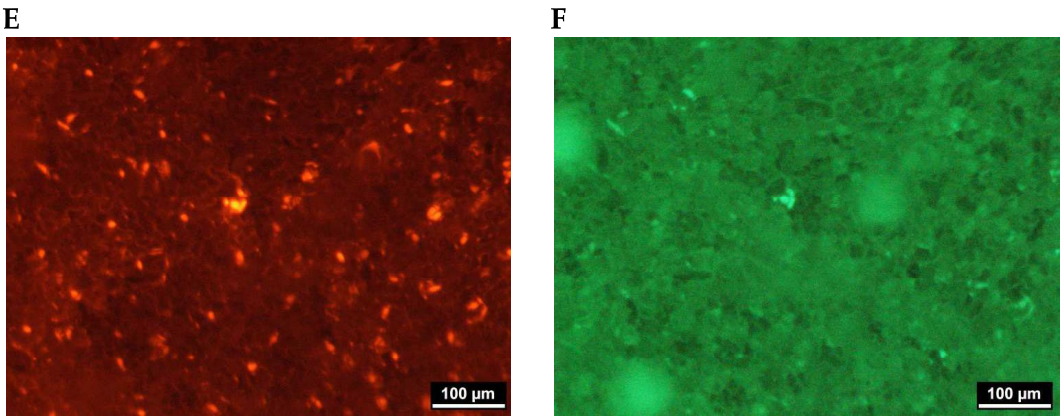

pCXUN_6G0093_500bp

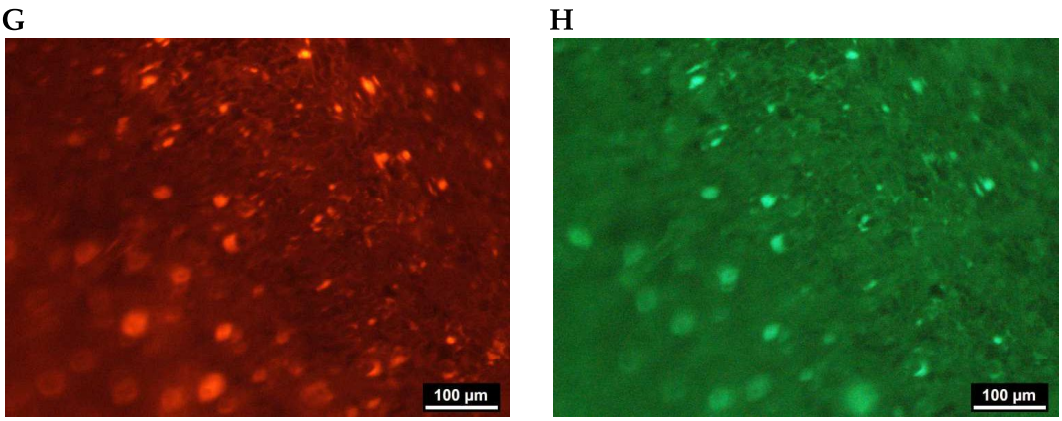

Figure 32: Epifluorescence images of pCXUN_6G0093 constructs transiently expressed in leaves of *N. benthamiana*. Both fluorescence markers were targeted to the nucleus. The pictures were taken two days after infiltration of the leaves with *A. rhizogenes* K599. **A/B:** pCXUN_6G0093_3.6kb with A: red channel, 1 sec exposure time and B: GFP channel, 3 sec exposure time. **C/D:** pCXUN_6G0093_2.6kb with C: red channel, 1 sec exposure time and D: GFP channel, 3 sec exposure time. **E/F:** pCXUN_6G0093_500bp with E: red channel, 1 sec exposure time and F: GFP channel, 5 sec exposure time. **G/H:** pCXUN_6G0093_250bp with G: red channel, 1 sec exposure time and H: GFP channel with 3 sec exposure time.

The tdtomato was detected in all infiltrated tobacco leaves after an exposure time of 1 second. GFP fluorescence was much weaker, but detectable in all cases after 3 seconds exposure time except for the construct pCXUN_6G0093_500bp, where only few fluorescent nuclei could be seen after 5 seconds exposure time.

Except for the 500 bp truncation, expression levels did not seem to differ with the length of promoter truncation.

3.6.3 Composite poplar experiments with *6G0093* promoter truncation constructs

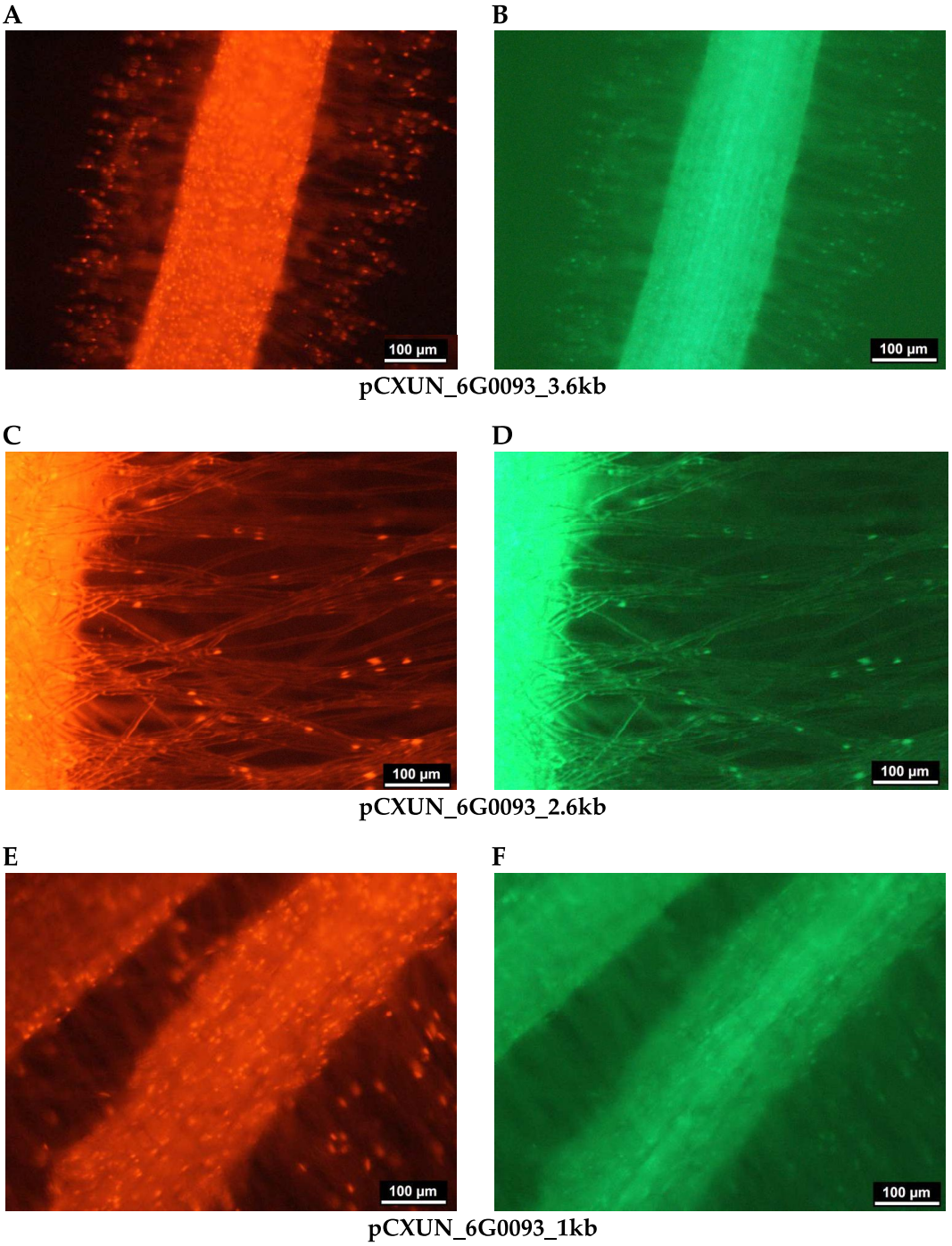

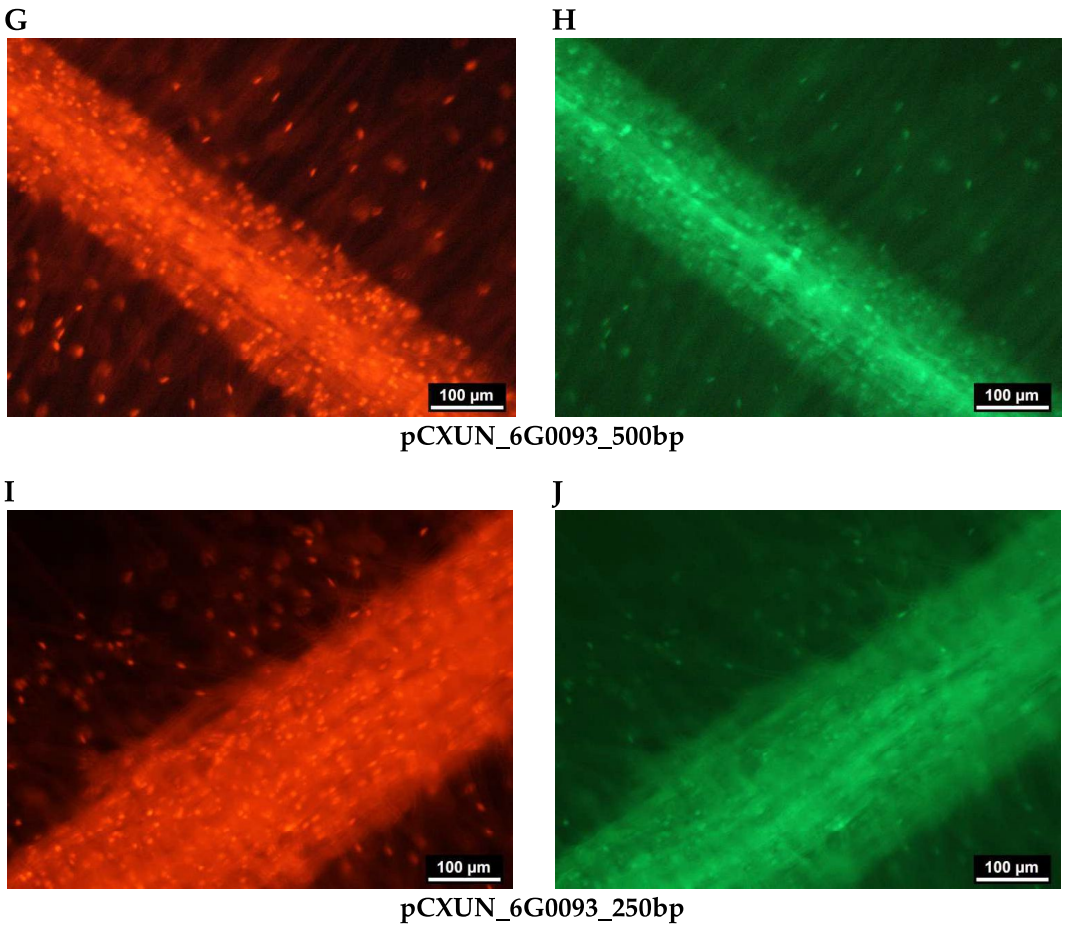

Figure 33: Epifluorescence images of *P. tremula x alba* roots transformed with promoter truncation constructs of pCXUN_6G0093. Both fluorescence markers were targeted to the nucleus. The pictures were taken 4 weeks after transforming the roots with A. rhizogenes K599. **A/B:** pCXUN_6G0093_3.6kb with A: red channel, 2 sec exposure time. B: GFP channel, 2 sec exposure time. **C/D:** pCXUN_6G0093_2.6kb with C: red channel, 1 sec exposure time and D GFP channel, 3 sec exposure time. **E/F:** pCXUN_6G0093_1kb with E: red channel, 1 sec exposure time and F: GFP channel, 3 sec exposure time. **G/H:** pCXUN_6G0093_500bp with G: red channel, 2 sec exposure time and H: GFP channel, 2 sec exposure time. **I/J:** pCXUN_6G0093_500 bp with I: red channel, 1 sec exposure time and J: GFP channel, 3 sec exposure time.

A tdtomato signal was detected in the nuclei of roots of all composite plants indicating that the tDNA of interest was integrated into the plant genome. The expression of dGFP was only faintly detectable in few cases and was mostly only visible in nuclei of root hairs. In contrast to tdtomato expression, longer exposure times were needed to visualise dGFP. The length of the truncated promoter did not seem to influence dGFP expression greatly except for the 1 kb fragment.

For better estimation of fluorescence intensity difference between the constructs, increasing exposure times were tested for selected promoter truncations.

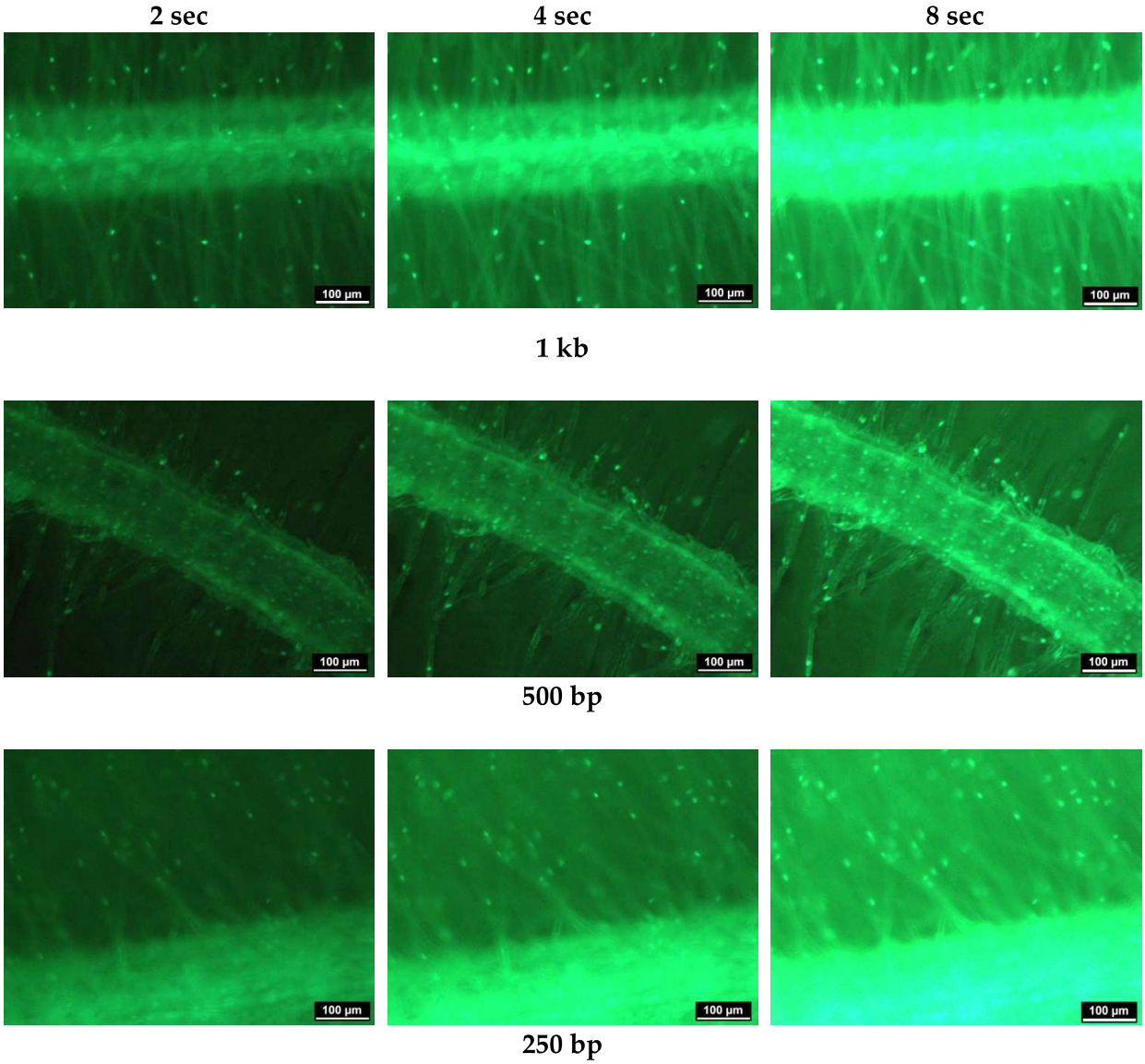

Figure 34: Increasing exposure times for selected promoter truncations of 6G0093.The 1 kb, 500 bp and 250 bp promoter truncations in pCXUN were evaluated and dGFP was detected with 2 sec, 4 sec and 8 sec exposure time under the stereo microscope respectively. Pictures were taken 4 weeks after composite poplar formation.

Even after 8 sec exposure time, GFP signals were still very weak. For the shortest tested promoter fragment, dGFP seemed slightly weaker than for the longer promoter fragments. This indicated further that all tested promoter truncations induced only basal expression of dGFP under the tested conditions.

3.6.4 Mycorrhiza of *6G0093* promoter truncations

No mycorrhiza could be obtained with *A. muscaria*. Mycorrhization with *P. microcarpus* was successful for some roots. These roots were analysed using the cLSM and compared to non mycorrhized fine roots.

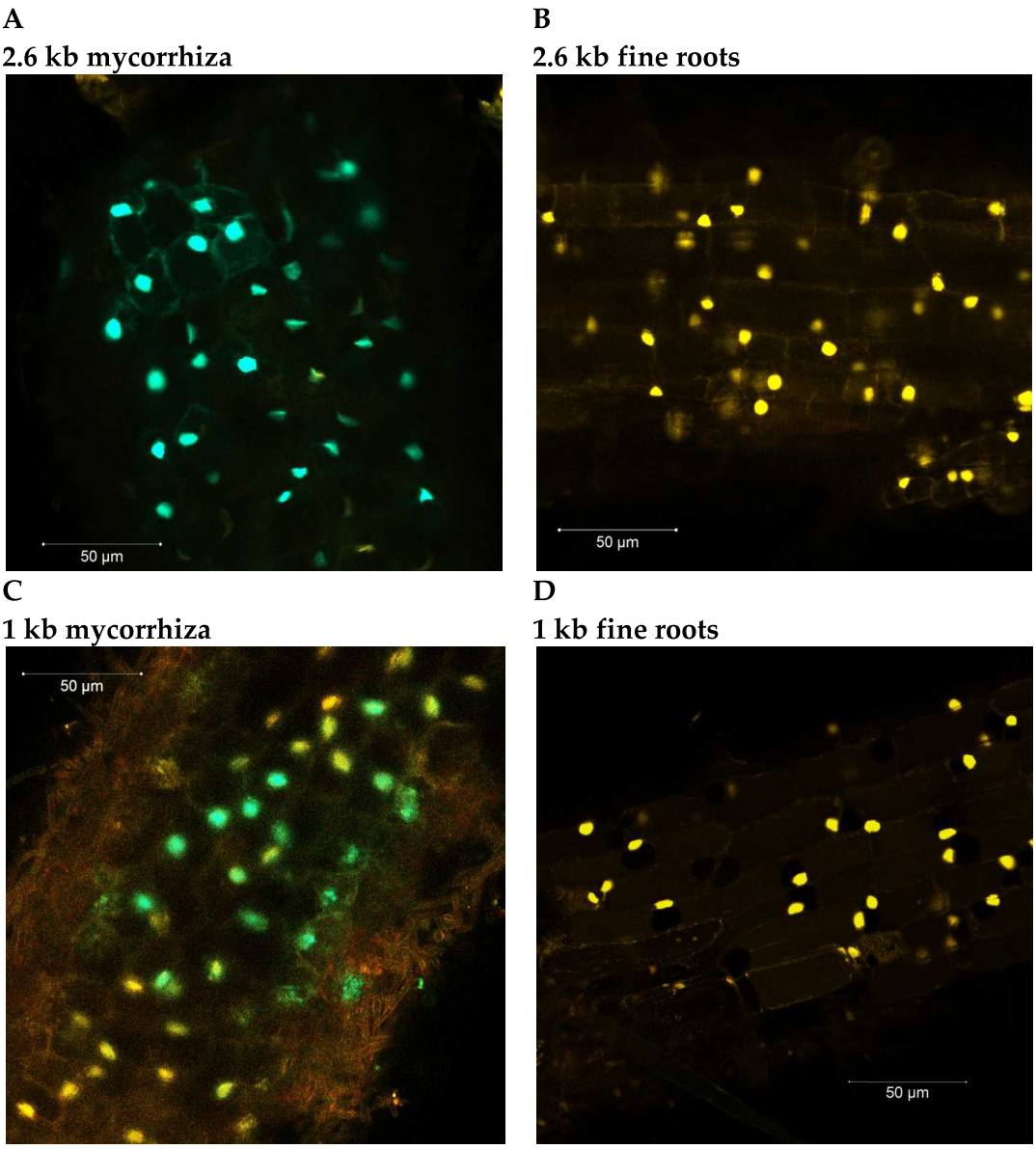

Figure 35: Analysis of 6G0093 promoter truncation activity in mycorrhiza and fine roots using the cLSM. Shown are different mycorrhiza and fine roots samples with dGFP-NLS under the control of the different 6G0093 promoter truncations and tdtomato-NLS under the control of a NOS promoter. A shift towards the red spectrum indicated higher tdtomato-NLS fluorescence in the nucleus, a shift towards the green spectrum indicated higher dGFP-NLS fluorescence. **A:** 6G0093_2.6 kb mycorrhiza. **B:** 6G0093_2.6 kb fine roots. **C:** 6G0093_1kb mycorrhiza. **D:** 6G0093_1kb fine roots. All pictures were taken by Uwe Nehls.

Using the cLSM, the intensities of dGFP and tdtomato were compared within different root samples. A shift towards the red spectrum (depicted in yellow) indicated higher tdtomato fluorescence, a shift towards the green spectrum indicated higher dGFP fluorescence.

In all tested mycorrhiza, green fluorescent nuclei could be observed within the root cortex cells. For all fine root samples, only yellow depicted tdtomato fluorescent nuclei were observed. This indicated that in fine root samples, tdtomato was expressed in higher concentrations than dGFP, whereas in mycorrhiza, dGFP was expressed in higher concentrations since more green signal was observed. Therefore, higher activity of the tested promoter truncations was observed in mycorrhiza samples compared to fine root samples. The 1kb fragment showed a shift towards yellow depicted tdtomato fluorescence in mycorrhiza samples, indicating lesser activity of this truncation compared to the bigger fragments in mycorrhiza (**Figure 35**C). Transgenic roots with shorter truncations unfortunately did not form mycorrhiza, therefore it remained unclear if these shorter truncations would show similar results or if activity induction under mycorrhiza formation would decrease.

4 Discussion

4.1 *A. rhizogenes* and pPLV vector backbones

The pPLV vectors were constructed by (De Rybel et al. 2011) to generate binary vector systems for fast and easy plant transformation using *Agrobacteria*. All pPLV vectors constructed by De Rybel et al. 2011 based on the vector backbone pGreen (Hellens et al. 2000). The pGreen/pPLV vector background is much smaller compared to other standard binary vector systems, because the small *pSa* replication locus has been divided, the *pSA ori* is found on pGreen/pPLV and the *pSa replicase* gene (*repA*) is resident on pSOUP, a helper plasmid to pGreen/pPLV. The pSOUP vector therefore is needed to provide *in trans* the replication function for pGreen/pPLV in *Agrobacterium*. Studies showed that some *Agrobacterium* strains like K599 already contain *repA* (Cevallos et al. 2008) which could omit the need for pSOUP. Interestingly, there is one study showing that *A. tumefaciens* LBA4404 can replicate a pGreen derivative without pSOUP and an intrinsic *repA* (Zangi et al. 2019). The mechanism as to how this is working is not yet known but raises the question if pSOUP is needed for pGreen replication in every *Agrobacterium* strain. Not needing pSOUP would be of advantage, since then the need for co-transformation or the maintenance of *Agrobacterium*/pSOUP cultures would be avoided and therefore the use for two different antibiotics in the bacterial culture (kanamycin for pGreen and tetracycline for pSOUP). However, in this study, it was shown that the intrinsic *repA* is not sufficient for the replication of pGreen/pPLV vectors in *Agrobacterium rhizogenes* K599.

Concerning pGreen, colonies of K599 could only be obtained when the bacteria where co-transformed with pSOUP. Surprisingly, co-transformation of pCAMBIA and pSOUP seemed to also have an effect on the number of K599 colonies (**Table 9**) since the number of colonies clearly was increased with co-transformation. Therefore the *repA* present on pSOUP seems to be able to interact with the *pSV1 ori* of pCAMBIA vectors as well.

4.2 Poplar root transformation efficiencies with different vector backbones

It was found in this work and in parallel works of members of the working group (Schnakenberg 2020, Immoor 2021) that only around 30 % of shoot derived roots contained the tDNA of interest when using pPLV or pBI vector backbones. Alpizar et al. 2006 obtained similar transformation efficiencies when using a pBI backround vector and *Agrobacterium* mediated transformation of coffee plants. In contrast, when using pCXUN (a pCAMBIA vector background), roughly 80 % of roots contained the tDNA of interest. As transformation efficiencies of 30 % are not sufficient for downstream mycorrhization experiments, the pCAMBIA derived vector was much better suited to the experimental demand of mycorrhiza research and was thus chosen for further experiments, although the bigger size of the vector and only medium copy numbers in *E. coli* are of disadvantage.

Agrobacterium mediated transformation is a complex process comprising of many different steps (see 1.4.1). The tDNA is transferred mediated by different proteins into the nucleus of the host cell and there integrated into the genome. The border sequences are the target sequences for the *Agrobacterium*'s endonucleases VIRD1 and VIRD2, which then release the tDNA by cutting of the DNA upon specific signals (Tzfira and Citovsky 2008). VIRD2 covalently attaches to the 5′ end of the tDNA, mediating transport into the plant cell nucleus and protecting it from nucleases (Permyakova et al. 2009).

Comparing the tDNA left and right border sequences of the three used vector backbones delivers a possible explanation why pPLV and pBI vector backbones show low and pCXUN vector backbones show high transformation efficiency.

Table 14: tDNA right and left border sequences of different vector backbones.

Vector backbone	Right border	Left border
pPLV	TGACAGGATATATTGGCGGGTAAAC-TAAGTCGCTGTATGTGTTTGTTTG	TGGCAGGATATATTGTGGTGTAACGTT
pBI	TGACAGGATATATTGGCGGGTAAAC-TAAGTCGCTGTATGTGTTTGTTTG	TGGCAGGATATATTGTGGTGTAACGTT
pCXUN	GGTAAACCTAAGAGAAAAGAGCGTTT	GTGGCAGGATATATTGTGGTGTAAAC

The pPLV and pBI vector backbones share the same right and left border sequences, whereas the pCXUN vector backbone has different sequences, indicating that the pPLV and pBI sequences might be problematic due to two reasons: a.) pPLV and pBI border sequences may not be optimal for the liberation of the tDNA, because the sequences are not compatible to the *A. rhizogenes* K599 VIRD1 and VIRD2 endonucleases. This would lead to inefficient excision of tDNA from the binary vector. b.) It may also be that VIRD2 is not well attached to the 5′ end of the released tDNA and thus, transport of the tDNA into the host cell is either impaired or the tDNA is not well protected from plant nucleases. In either case, less tDNA copies would be the result leading to lower integration into the host's genome and thus reduced transformation efficiency. This problem does not occur in tobacco leaves, since transient transformation leads to a much higher copy number of tDNA transcripts (Krenek et al. 2015).

Since composite poplar formation depends on the generation of transgenic roots, it is dependent on the use of an *A. rhizogenes* strain. So far, *A. rhizogenes* K599 to be most suitable strain in the formation of transgenic poplar roots with a tDNA of interest (Neb et al. 2017).

To test this working hypothesis, the tDNA border sequences of pPLV could be exchanged with those of pCXUN to see if the effect can be reversed. If so, pPLV vector backbones would again be the vector backbone of choice, since they are easier to handle and to manipulate than the pCXUN vector background.

4.3 Fluorescent markers for *in planta* promoter expression studies

4.3.1 sYFP

In contrast to other markers, like β-Glucuronidase (GUS), fluorescent proteins can be studied *in vivo*. In this work, it was necessary to have a visual marker for transgenic poplar roots before mycorrhization in order to prove successful transformation Otherwise, no visual signals in mycorrhiza experiments could also be attributed to unsuccessful plant transformation. For this purpose, a constitutively expressed fluorescent protein was established as a marker for transgenic roots containing the tDNA of interest (Schnakenberg, 2020). This marker cassette consists of a nopaline synthase promoter from *Agrobacterium* enabling the expression of a tdtomato with nuclear localisation signal. For promoter analysis, a second fluorescent

marker cassette needed to be established to visualise promoter activity *in vivo*. Both fluorescent proteins should be expressed and detected within the same cell, because only then promoter analysis results in subsequent mycorrhiza experiments are trustworthy. Since the promoters of interest are mycorrhiza induced, they should only induce visual signals in mycorrhiza, but a missing signal could also be attributed to a root that is non-transgenic. A signal of both the constitutive marker and the fluorescent protein under the control of the tested promoter within the same cell show a clear result. Therefore, both fluorescent proteins should show emission maxima that can be separated by filter sets such that no overlap of the fluorescent signals is detected.

In this study, sYFP and dGFP were tested as candidates for promoter expression analysis, since their emission maxima (YFP: 524 nm, GFP: 509 nm) differ enough from that of tdtomato (581 nm) to be suitable for simultaneous detection.

YFP is a monomeric fluorescent protein with a size of 27 kDa. Thus, it is small enough to freely diffuse through nuclear pores. As a consequence, sYFP fluorescence could be detected in the cytoplasm and the nucleus (**Figure 5**). Since the overall fluorescence signals were rather weak even when using a 35S promoter, it was to be expected that the signal would be under the detection limit if weaker promoters would be used. To concentrate the fluorescence signal, nuclear or peroxisomal targeting was tested. However, a nuclear target was not retained in the nucleus as expected. Due to the small size of the protein, free diffusion out of the nucleus was supposed leading to only weak accumulation in the nucleus. The NLS-based nuclear import signal was not efficient enough to decrease sYFP signal in the cytoplasm. The peroxisomal targeted sYFP accumulated in peroxisomes and since they are comparatively smaller than the nucleus (0.1 – 1 µm compared to approximately 10 µm), the brightness seemed to be increased compared to sYFP-NLS (**Figure 8**). However, since peroxisomal transport is post translational and it can be assumed that import mechanisms are not fast enough to remove all sYFP from the cytoplasm, strong sYFP fluorescence was detected in the cytoplasm,. An alternative explanation would be that if the capacity of peroxisomes is reached, additional sYFP will remain in the cytoplasm.

All in all, due to the relatively weak fluorescence signal, sYFP was found not to be the ideally suited for promoter analysis.

4.3.2 GFP

GFP was tested as a second candidate for the promoter expression analysis cassette. In contrast to the single YFP, a tripleGFP with a nuclear target sequence was tested (De Rybel et al. 2011). Tests showed, however, that the annotated tripleGFP of the pPLV vector contained only a doubleGFP and was therefore termed dGFP. The size of the fluorescent protein by approximately 30 kDa was supposed to be big enough to be retained in the nucleus. De Rybel et al. 2011 modified their pPLV04 vector containing tripleGFP from a vector previously described in (Takada and Jürgens 2007), where one GFP-NLS, GFP and GFP-stop were amplified via PCR and fused together to generate *NLS:3xEGFP::nost.* However, no cloning results are shown in (Takada and Jürgens 2007), so it remains speculative if the original vector contained 3 GFP sequences or if in later cloning steps, one GFP was lost. Since the used GFP clearly showed nuclear localisation and no problems where observed in translation indicating that the stop codon is functional, the middle GFP might have been lost in cloning processes. This is difficult to prove by restriction analysis or sequencing, since standard sequencing reactions cover only about 1000 bp, and one monomeric GFP is already about 800 bp. Internal sequencing primers will also be difficult to design, since the sequences of the used GFP should be identical, except that the middle GFP does not contain a start and a stop codon. However, since functionality of the used GFP was shown in this work, further investigations were not performed.

The dGFP-NLS cassette was tested with two different constitutively expressed promoters. Both the 35S promoter and the *Arabidopsis* ubiquitin promoter showed bright signals with only 200 respectively 250 msec exposure times in composite poplar roots. In contrast, 1 sec exposure times needed to detect sYFP signals even in tobacco leaves, which generally show much higher fluorescence signals due to transient expression.

Autofluorescence of *N. benthamiana* leaves was never a problem when working with dGFP or tdtomato and the stereomicroscope. The quality of the filter sets was enough to avoid most of the autofluorescence of the chloroplasts.

When using the stereo microscope also no strong autofluorescence interfering with the tdtomato or GFP signals was observed when signals were targeted to organelles. Therefore, dGFP was found to be suitable as a fluorescent marker for the focus of this work.

4.4 Challenges in promoter expression analysis

4.4.1 Transcriptional interference

The final binary vectors contained two fluorescent marker cassettes within the tDNA: A constitutively expressed cassette expressing a tdtomato-NLS under the control of the constitutive promoter PNOS and a dGFP-NLS driven by a promoter that should be analysed. As proof of concept, P_{35S} and P_{UBQ} promoters controlling dGFP-NLS were used. Both cassettes were cloned in tandem orientation. The simultaneous presence of a constitutively expressed tdtomato and a GFP revealing variable signal which is depending on the strength of the respective promoter would allow a normalisation when comparing different promoters. Furthermore, different fluorescence intensities of individual transgenic roots due to a different number in tDNA copies that were integrated into the genome could be normalised, too.

However with this setup, transcriptional interference can be a problem. Bhullar et al. 2009 carried out experiments with test and reference promoters controlling the reporter genes *β-glucuronidase* (*gus*) and *chloramphenicol acetyl transferase* (*cat*). They found that the activity of the reference promoter can be influenced by the activity of the test promoter especially when common *cis* elements are similar. In their case, the interaction was positive, meaning a weakened activity for one of the promoters led to enhanced activity of the second promoter. But effects can also occur when obviously no *cis* elements are shared, as shown by Eszterhas et al. 2002, who found that transcriptional interference strongly suppressed gene expression in their testing system depending on how both cassettes are oriented to each other. Tandem repeat orientation (→→) gave strongest suppression in the second gene. They also found that overall expression of the two genes in tandem was reduced compared to when they were integrated alone. However, the exact mechanisms on how the two cassettes influence each other still remain unknown.

Transcriptional interference is one explanation as to why only weak tdtomato signals could be detected in tobacco leaves when the P_{UBQ}_dGFP-NLS_T_{NOS}_P_{NOS}_tdtomato-NLS_T_{NOS} construct was used (**Figure 20**). The transient transformation of tobacco leaves leads to high copy numbers of tDNA within the cell, thus it might be possible that *trans* acting elements are not sufficient within the cell to express all proteins (Eszterhas et al. 2002)

For future double marker cassettes, a novel approach with the two marker cassettes not in tandem, but in head to head orientation (←→) could be established, since at least Padidam and Cao 2001 showed, that this might reduce transcriptional interference. Similar, Jiang et al. 2017 as well as Chen et al. 2010 found that head to head orientation led to more correlated changes in transcription levels compared to other orientations.

4.4.2 Integration of tDNA into the plant genome

Stable root transformation depends on the integration of the tDNA of interest into the host plant's genome. However, the mechanism of tDNA integration into the host's genome is not yet fully elucidated. Integration seems to be random, but chromatin modulating proteins might play a role in the integration process (Mysore et al. 2000). Every root generated in composite poplars is an independent transformation event and position of genome integration and copy number of the integrated tDNA will differ. Studies showed that depending on the integration site, even promoterless genes can exhibit gene expression when integrated into actively transcribed regions (Koncz and Schell 1986).

4.4.3 Ectomycorrhization

With *A. muscaria*, no mycorrhiza formation was observed for the constructs in any circumstances. This might be due to the fact that the used strain was propagated for over 10 years in the working group and fresher material should be used for future research. Older cultures seem to lose the ability for efficient mycorrhization (Nehls, personal communication). An explanation might be gene shifts or mutations slowly accumulating over the years.

P. microcarpus formed few ectomycorrhizas under the tested conditions. The number of mycorrhizas was however very low compared to previous experiments. All mycorrhization experiments in this study were set up in late autumn/winter. Temperature and light conditions do not change within the experiments, as they are carried out in growing chambers. One possible reason for low mycorrhiza formation might be changes in water content in the mycorrhization plates, especially since they were overlayed with a substrate mixture (1:1:1(v/v/v) vermiculite/clay/coconut husk). Buée et al. 2005 found that changes in Ectomy-

corrhiza dynamics in a mature beech forest depend on the season, temperature and soil moisture.

Additionally, evaluation of mycorrhiza is challenging in some aspects. A lot of plant material is needed to make reliable statements concerning the different tested constructs since every transgenic root is a single transformation event and positional and copy number effects could distort results on a single root level. Also, the harvesting time point of mycorrhiza is crucial for the evaluation, since mycorrhiza are highly dynamic and depending on the stadium of mycorrhization, different expression patterns of transcription factors can be observed (Daguerre et al. 2017). Transcription rates are generally lower in already fully developed than in developing tissues. Therefore expression of the promoter fragments of interest might be underestimated in older tissues.

Additionally, it might be worthwhile to test different experimental setups for mycorrhization. Plants grown *in vitro* have different physiological characteristics than plants grown *ex vitro*. In vitro grown plants show altered photosynthesis due to the presence of sugar in the propagation medium and the microenvironment of the culture vessels is different with higher relative humidity content, lower CO_2 concentration and higher ethylene concentration (Xiao et al. 2011). The plates used in the mycorrhization system have even less air volume than the propagation vessels, which might negatively influence the photosynthetic capacities of the plants and therefore reducing mycorrhization since not enough sugar is produced to offer to the fungal partner. Either another *in vitro* mycorrhization system or *ex vitro* mycorrhization might reflect natural circumstances better. For example, Oliveira et al. 2003 used a mycorrhization system for *Pinus* where they cultured the plants on Woody Plant Medium (WPM), adapted the fungal partner to this medium as well and then used a bilayer of WPM medium without sucrose overlayed with a small layer of WPM containing 2 % sucrose. After an incubation time of 2 to 4 weeks, they transferred the plants and fungi to a system with sterile vermiculite which they soaked with quarter strength WPM without sucrose. This system could be tested as well. However, it has to be stated that the compositions of WPM and MS medium are quite different and therefore, the system would need to be adapted.

Also, since mycorrhiza are a symbiotic interaction to improve the nutrient status of both partners (Smith and Read 2008) one might speculate that leaving plants on nutrient deprived

medium for some weeks before starting mycorrhiza experiments, more efficient mycorrhiza formation could be achieved since the plants would be more dependent on nutrients delivered by the fungal partner.

4.5 *Potrx6G1673*

The gene function is not yet elucidated in poplar, however homology analysis suggests possible involvement of the protein in oxysterol binding. RNA sequencing and qPCR results show a strong upregulation of Potrx6G1673 in mycorrhized root tips (Nehls, unpublished data). Since there is evidence that oxysterols play a role in membrane fluidity, permeability and membrane associated processes (for a review, see Lindsey et al. 2003), one might speculate that upon initiation of mycorrhiza formation, Potrx6G1673 is involved in rearrangement processes for the accommodation of mycorrhiza and the initialisation of the Hartig net.

In contrast to RNAseq and qPCR analysis, all tested promoter truncations of *Potrx6G1673* showed expression in non mycorrhized poplar roots and *N. benthamiana* leaves. Expression was evenly distributed along poplar roots. However, expression profiles also were dependent on the poplar species, since *P. tremula x alba* generally showed higher fluorescence than *P. tremula x tremuloides* for all tested constructs.

Unfortunately, the longest promoter fragment that could be obtained was only about 2.2 kb in size. It may be that longer promoter fragments are needed to better reflect the situation *in planta* and to find specific mycorrhiza induced *cis* elements, since possible enhancer and silencer elements can be located far away from the core promoter(for reviews, see Porto et al. 2014; Biłas et al. 2016). Also, qPCR analysis of *Potrx6G1673* revealed strong expression only in mycorrhized root tips, not in whole roots (Nehls, unpublished). However, when dGFP-NLS expression was triggered by the longest promoter fragment, fluorescent signals were observed all along the roots and not only concentrated in the tips. This makes it rather likely, that specific *cis* acting elements are needed to allow only root tip specific gene expression and that these elements are missing from the tested promoter fragments This would indicate the presence of enhancer or silencer elements either further upstream of the tested sequences

or within introns of *Potrx6G1673*. Silencing would then inhibit expression of *Potrx6G1673* until specific signals from the fungal partner terminate silencing mechanisms.

4.6 *Potrx6G0093*

Nothing is known about the gene function of *Potrx6G0093*, however sequence analysis shows homology to a leucine zipper domain, *Potrx6G0093* might function as a transcription factor. This would be of interest, since transcription factors might help elucidating ectomycorrhiza dependent reprogramming of the plant's transcriptome.

In contrast to *Potrx6G1673, Potrx6G0093* truncations showed basal levels of expression in *N. benthamiana* leaves and non mycorrhized poplar roots. In mycorrhized samples however, an increase of dGFP fluorescence could be observed for the 3.6, 2.6 and 1 kb promoter truncations compared to tdtomato fluorescence (**Figure 35**). The 3.6 (data not shown) and 2.6 kb promoter truncations showed clear overabundance of dGFP, in case of the 1 kb promoter fragment, some tdtomato fluorescence could be observed in the mycorrhized samples. This strongly indicates the presence of a mycorrhiza dependent element within the sequence around the 2.6 and 1 kb promoter truncation. Unfortunately, the shorter promoter truncations did not produce mycorrhiza so no results are available on these fragments. If shorter promoter truncations show a shift towards tdtomato fluorescence in cLSM analysis, this would further hint to mycorrhiza regulatory elements located within the 2 to 1 kb region of the promoter. Further focus should be on the evaluation of the shorter fragments to obtain an answer to this question.

5 Conclusion and Outlook

The establishment of a functional reporter cassette for promoter activity in poplar fine roots and mycorrhiza was successful. Nuclear targeted GFP can be used as functional marker for promoter truncations together with a transformation control cassette of nuclear targeted tdtomato. In cLSM analysis, analysis of fluorescence ratios between dGFP and tdtomato can be used to determine which of the proteins is dominantly expressed. A shift from the constitutively expressed tdtomato to dGFP under control of the promoter of interest can then give insights into mycorrhiza dependent expression. Comparison of expression levels of dGFP and tdtomato in fine roots and mycorrhiza then gives first insights into different activity levels of mycorrhiza induced promoter elements.

However, in this study, no quantitative analysis is possible. For future research, it would be highly relevant to compare different signal intensities obtained with the cLSM to gain more insights into the induction of promoter activity under different conditions. Therefore, in a next step, calibration of the signal intensities should be performed with different known promoters to allow normalisation of the obtained signal intensities. Then, it would be possible to specify the strength of different promoter elements under different conditions.

Mycorrhiza formation proved to be difficult depending on the season and more experiments should be conducted to gain routinely more mycorrhiza. Then, the shorter promoter fragments of *6G0093* should be tested again to see if the shift from dGFP to tdtomato fluorescence holds true for fragments under 2.6 kb.

For *6G1673*, mycorrhiza experiments should be repeated to learn the expression status of the promoter fragments in mycorrhiza. Also, efforts should focus on generating longer promoter fragments of *6G1673* from genomic DNA to evaluate the presence of possible cis acting elements further upstream of the amplified promoter fragment.

6 List of figures

7 List of tables

8 References

Alpizar, E., Dechamp, E., Espeout, S., Royer, M., Lecouls, A. C., Nicole, M., Bertrand, B., Lashermes, P., and Etienne, H. 2006. Efficient production of Agrobacterium rhizogenes-transformed roots and composite plants for studying gene expression in coffee roots. Plant Cell Rep. 25:959–967

Alves, L., Oliveira, V. L., and Filho, G. N. S. 2010. Utilization of rocks and ectomycorrhizal fungi to promote growth of eucalypt. Brazilian J. Microbiol. 41:676–684

An, G., Costa, M. A., and Ha, S. B. 1990. Nopaline synthase promoter is wound inducible and auxin inducible. Plant Cell. 2:225–233

An, G., Costa, M. A., Mitra, A., Ha, S.-B., and Márton, L. 1988. Organ-Specific and Developmental Regulation of the Nopaline Synthase Promoter in Transgenic Tobacco Plants. Plant Physiol. 88:547–552

Aslanidis, C., and de Jong, P. J. 1990. Ligation-independent cloning of PCR products (LIC-PCR). Nucleic Acids Res. 18:6069–6074

Bahramnejad, B., Naji, M., Bose, R., and Jha, S. 2019. A critical review on use of Agrobacterium rhizogenes and their associated binary vectors for plant transformation. Biotechnol. Adv. 37:107405

Bakker, P. A. H. M., Berendsen, R. L., Doornbos, R. F., Wintermans, P. C. A., and Pieterse, C. M. J. 2013. The rhizosphere revisited: Root microbiomics. Front. Plant Sci. 4:1–7

Bally, J., Jung, H., Mortimer, C., Naim, F., Philips, J. G., Hellens, R., Bombarely, A., Goodin, M. M., and Waterhouse, P. M. 2018. The rise and rise of nicotiana benthamiana: A plant for all reasons. Annu. Rev. Phytopathol. 56:405–426

Becquer, A., Guerrero-Galán, C., Eibensteiner, J. L., Houdinet, G., Bücking, H., Zimmermann, S. D., and Garcia, K. 2019. The ectomycorrhizal contribution to tree nutrition. Adv. Bot. Res. 89:77–126

Berendsen, R. L., Pieterse, C. M. J., and Bakker, P. A. H. M. 2012. The rhizosphere microbiome and plant health. Trends Plant Sci. 17:478–486

Berg, R. H., and Beachy, R. N. 2008. Fluorescent Protein Applications in Plants. Methods Cell Biol. 85:153–177

Bertani, G. 1951. Studies on lysogenesis. I. The mode of phage liberation by lysogenic Escherichia coli. J. Bacteriol. 62:293–300

Bhullar, S., Chakravarthy, S., Pental, D., and Burma, P. K. 2009. Analysis of promoter activity in transgenic plants by normalizing expression with a reference gene: Anomalies due to the influence of the test promoter on the reference promoter. J. Biosci. 34:953–962

Biłas, R., Szafran, K., Hnatuszko-Konka, K., and Kononowicz, A. K. 2016. Cis-regulatory elements used to control gene expression in plants. Plant Cell. Tissue Organ Cult. 127:269–287

Bradshaw, H. D., Ceulemans, R., Davis, J., and Stettler, R. 2000. Emerging model systems in plant biology: Poplar (Populus) as a model forest tree. J. Plant Growth Regul. 19:306–313

Brundrett, M. C. 2009. Mycorrhizal associations and other means of nutrition of vascular plants: Understanding the global diversity of host plants by resolving conflicting information and developing reliable means of diagnosis. Plant Soil. 320:37–77

Brunner, A. M., Busov, V. B., and Strauss, S. H. 2004. Poplar genome sequence: Functional genomics in an ecologically dominant plant species. Trends Plant Sci. 9:49–56

Buée, M., Reich, M., Murat, C., Morin, E., Nilsson, R. H., Uroz, S., and Martin, F. 2009. 454 Pyrosequencing analyses of forest soils reveal an unexpectedly high fungal diversity.

New Phytol. 184:449–456

Buée, M., Vairelles, D., and Garbaye, J. 2005. Year-round monitoring of diversity and potential metabolic activity of the ectomycorrhizal community in a beech (Fagus silvatica) forest subjected to two thinning regimes. Mycorrhiza. 15:235–245

Butler, J. E. F., and Kadonaga, J. T. 2002. The RNA polymerase II core promoter: A key component in the regulation of gene expression. Genes Dev. 16:2583–2592

Cevallos, M. A., Cervantes-rivera, R., Gutiérrez-ríos, R. M., Htcca, R., Htccb, R., and Htccc, R. 2008. Plasmid The repABC plasmid family. 60:19–37

Chalfie, M., Tu, Y., Euskirchen, G., Ward, W., and Prasher, D. 1994. Green fluorescent protein as a marker for gene expression. Science (80-.). 263:802–805

Chambers, S. M., Cairney, J. W. G., Dahlberg, A., Finlay, R. D., Kropp, B. R., Mueller, G. M., Marmeisse, R., Grypta, H., Jargeat, P., Fraissinet-Tachet, L., Gay, G., Debaud, J.-C., Molina, R., Trappe, J. M., Grubisha, L. C., and Spatafora, J. W. 1999. *Ectomycorrhizal Fungi: Key Genera in Profile*. J.W.G. Cairney and S.M. Chambers, eds. Springer-Verlag Berlin Heidelberg.

Chen, S., Songkumarn, P., Liu, J., and Wang, G. L. 2009. A versatile zero background T-vector system for gene cloning and functional genomics. Plant Physiol. 150:1111–1121

Chen, W. H., de Meaux, J., and Lercher, M. J. 2010. Co-expression of neighbouring genes in Arabidopsis: Separating chromatin effects from direct interactions. BMC Genomics. 11

Chow, C. N., Zheng, H. Q., Wu, N. Y., Chien, C. H., Huang, H. Da, Lee, T. Y., Chiang-Hsieh, Y. F., Hou, P. F., Yang, T. Y., and Chang, W. C. 2016. PlantPAN 2.0: An update of Plant Promoter Analysis Navigator for reconstructing transcriptional regulatory networks in plants. Nucleic Acids Res. 44:D1154–D1164

Chudakov, D. M., Matz, M. V., Lukyanov, S., and Lukyanov, K. A. 2010. Fluorescent proteins and their applications in imaging living cells and tissues. Physiol. Rev. 90:1103–1163

Collier, R., Fuchs, B., Walter, N., Lutke, W. K., and Taylor, C. G. 2005. Ex vitro composite plants: An inexpensive, rapid method for root biology. Plant J. 43:449–457

Cope, K. R., Bascaules, A., Irving, T. B., Venkateshwaran, M., Maeda, J., Garcia, K., Rush, T. A., Ma, C., Labbé, J., Jawdy, S., Steigerwald, E., Setzke, J., Fung, E., Schnell, K. G., Wang, Y., Schleif, N., Bücking, H., Strauss, S. H., Maillet, F., Jargeat, P., Bécard, G., Puech-Pagès, V., and Ané, J. M. 2019. The ectomycorrhizal fungus laccaria bicolor produces lipochitooligosaccharides and uses the common symbiosis pathway to colonize populus roots. Plant Cell. 31:2386–2410

Curtis, T. P., Sloan, W. T., and Scannell, J. W. 2002. Estimating prokaryotic diversity and its limits. Proc. Natl. Acad. Sci. U. S. A. 99:10494–10499

Daguerre, Y., Levati, E., Ruytinx, J., Tisserant, E., Morin, E., Kohler, A., Montanini, B., Ottonello, S., Brun, A., Veneault-Fourrey, C., and Martin, F. 2017. Regulatory networks underlying mycorrhizal development delineated by genome-wide expression profiling and functional analysis of the transcription factor repertoire of the plant symbiotic fungus Laccaria bicolor. BMC Genomics. 18:1–23

Dauphin, A., Gérard, J., Lapeyrie, F., and Legué, V. 2007. Fungal hypaphorine reduces growth and induces cytosolic calcium increase in root hairs of Eucalyptus globulus. Protoplasma. 231:83–88

Dauphin, A., De Ruijter, N. C. A., Emons, A. M. C., and Legué, V. 2006. Actin organization during Eucalyptus root hair development and its response to fungal hypaphorine. Plant Biol. 8:204–211

Day, R. N., and Davidson, M. W. 2009. The fluorescent protein palette: Tools for cellular

imaging. Chem. Soc. Rev. 38:2887–2921

Delaux, P. M., Radhakrishnan, G. V., Jayaraman, D., Cheema, J., Malbreil, M., Volkening, J. D., Sekimoto, H., Nishiyama, T., Melkonian, M., Pokorny, L., Rothfels, C. J., Sederoff, H. W., Stevenson, D. W., Surek, B., Zhang, Y., Sussman, M. R., Dunand, C., Morris, R. J., Roux, C., Wong, G. K. S., Oldroyd, G. E. D., and Ane, J. M. 2015. Algal ancestor of land plants was preadapted for symbiosis. Proc. Natl. Acad. Sci. U. S. A. 112:13390–13395

Doyle, J., and Doyle, J. 1987. A rapid DNA isolation procedure for small quantities of fresh leaf tissue. Phytochem. Bull. 19:11–15

Eszterhas, S. K., Bouhassira, E. E., Martin, D. I. K., and Fiering, S. 2002. Transcriptional Interference by Independently Regulated Genes Occurs in Any Relative Arrangement of the Genes and Is Influenced by Chromosomal Integration Position. Mol. Cell. Biol. 22:469–479

Field, K. J., and Pressel, S. 2018. Unity in diversity: structural and functional insights into the ancient partnerships between plants and fungi. New Phytol. 220:996–1011

Frank, A. B. 1885. Ueber die auf Wurzelsymbiose beruhende Ernaehrung gewisser Baeume durch unterirdische Pilze. Ber Dtsch Bot Ges. 3:128–145

Fürner, I. J., Huffmann, G. A., Amasino, R. M., Garfinkel, D. J., Gorden, M. P., and Nester, E. W. 1986. An Agrobacterium transformation in the evolution of the genus Nicotiana. Nature. 319:422–427

Gahan, J., and Schmalenberger, A. 2014. The role of bacteria and mycorrhiza in plant sulfur supply. Front. Plant Sci. 5:1–7

Gearing, M. 2018. Plasmids 101: Inducible Promoters. Available at: https://blog.addgene.org/plasmids-101-inducible-promoters.

Gelvin, S. B. 2003. Agrobacterium -Mediated Plant Transformation®: the Biology behind the " Gene-Jockeying " Tool. Microbiol. Mol. Biol. Rev. 67:16–37

Gelvin, S. B. 2017. Integration of Agrobacterium T-DNA into the Plant Genome. Annu. Rev. Genet. 51:195–217

Gelvin, S. B., and Kim, S. I. 2007. Effect of chromatin upon Agrobacterium T-DNA integration and transgene expression. Biochim. Biophys. Acta - Gene Struct. Expr. 1769:410–421

Geml, J., Laursen, G. A., O'Neill, K., Nusbaum, H. C., and Taylor, D. L. 2006. Beringian origins and cryptic speciation events in the fly agaric (Amanita muscaria). Mol. Ecol. 15:225–239

Geml, J., Tulloss, R. E., Laursen, G. A., Sazanova, N. A., and Taylor, D. L. 2008. Evidence for strong inter- and intracontinental phylogeographic structure in Amanita muscaria, a wind-dispersed ectomycorrhizal basidiomycete. Mol. Phylogenet. Evol. 48:694–701

Geurts, R., Xiao, T. T., and Reinhold-Hurek, B. 2016. What Does It Take to Evolve A Nitrogen-Fixing Endosymbiosis? Trends Plant Sci. 21:199–208

Goodin, M. M., Zaitlin, D., Naidu, R. A., and Lommel, S. A. 2008. Nicotiana benthamiana: Its history and future as a model for plant-pathogen interactions. Mol. Plant-Microbe Interact. 21:1015–1026

Gordon, J. E., and Christie, P. J. 2014. The Agrobacterium Ti Plasmids. Microbiol. Spectr. 2:1–18

Guerrero-Galán, C., Calvo-Polanco, M., and Zimmermann, S. D. 2019. Ectomycorrhizal symbiosis helps plants to challenge salt stress conditions. Mycorrhiza. 29:291–301

Handa, Y., Nishide, H., Takeda, N., Suzuki, Y., Kawaguchi, M., and Saito, K. 2015. RNA-seq Transcriptional Profiling of an Arbuscular Mycorrhiza Provides Insights into Regulated

and Coordinated Gene Expression in Lotus japonicus and Rhizophagus irregularis. Plant Cell Physiol. 56:1490–1511

Hansen, G., and Wright, M. S. 1999. Recent advances in the transformation of plants. Trends Plant Sci. 4:226–231

Hansen, J., Jørgensen, J. E., Stougaard, J., and Marcker, K. A. 1989. Hairy roots - a short cut to transgenic root nodules. Plant Cell Rep. 8:12–15

van der Heijden, M. G. A., Martin, F. M., Selosse, M. A., and Sanders, I. R. 2015. Mycorrhizal ecology and evolution: The past, the present, and the future. New Phytol. 205:1406–1423

Hellens, R. P., Anne Edwards, E., Leyland, N. R., Bean, S., and Mullineaux, P. M. 2000. pGreen: A versatile and flexible binary Ti vector for Agrobacterium-mediated plant transformation. Plant Mol. Biol. 42:819–832

Hernandez-Garcia, C. M., and Finer, J. J. 2014. Identification and validation of promoters and cis-acting regulatory elements. Plant Sci. 217–218:109–119

Hiltner, L. 1904. Über neuere Erfahrungen und Probleme auf dem Gebiete der Bodenbakteriologie unter besonderer Berücksichtigung der Gründüngung und Brache. Arb. der Dtsch. Landwirtschafts-Gesellschaft. 98:59–78

Hobbie, E. A. 2006. Carbon Allocation to Ectomycorrhizal Fungi Correlates with Belowground Allocation in Culture Studies Author (s): Erik A . Hobbie Published by : Wiley Stable URL : http://www.jstor.org/stable/20068977 CARBON ALLOCATION TO ECTOMYCORRHIZAL FUNGI CORRELATES. Ecology. 87:563–569

Hobbie, J. E., and Hobbie, E. A. 2006. N in Symbiotic Fungi and Plants Estimates Nitrogen. Ecology. 87:816–822

Hohnjec, N., Vieweg, M. F., Pühler, A., Becker, A., and Küster, H. 2005. Overlaps in the transcriptional profiles of Medicago truncatula roots inoculated with two different Glomus fungi provide insights into the genetic program activated during arbuscular mycorrhiza. Plant Physiol. 137:1283–1301

Jansson, S., and Douglas, C. J. 2007. Populus : A Model System for Plant Biology . Annu. Rev. Plant Biol. 58:435–458

Jefferson, R. A. 1987. Assaying chimeric genes in plants: The GUS gene fusion system. Plant Mol. Biol. Report. 5:387–405

Jiang, W., Sun, L., Yang, X., Wang, M., Esmaeili, N., Pehlivan, N., Zhao, R., Zhang, H., and Zhao, Y. 2017. The Effects of Transcription Directions of Transgenes and the gypsy Insulators on the Transcript Levels of Transgenes in Transgenic Arabidopsis. Sci. Rep. 7:1–12

Johnsen, N. C., and Gehring, C. A. 2007. CHAPTER 4 - Mycorrhizas: Symbiotic Mediators of Rhizosphere and Ecosystem Processes. Pages 73–100 in: The Rhizosphere: An Ecological Perspective, Z.G. Gardon and J.L. Whitbeck, eds. Elsevier.

Kan, W. 2006. *Agrobacterium Protocols*. Second Edi. W. Kan, ed. Humana Press, New Jersey.

Kang, H., Chen, X., Kemppainen, M., Pardo, A. G., Veneault-Fourrey, C., Kohler, A., and Martin, F. M. 2020. The small secreted effector protein MiSSP7.6 of Laccaria bicolor is required for the establishment of ectomycorrhizal symbiosis. Environ. Microbiol. 00

Kohler, A., Kuo, A., Nagy, L. G., Morin, E., Barry, K. W., Buscot, F., Canbäck, B., Choi, C., Cichocki, N., Clum, A., Colpaert, J., Copeland, A., Costa, M. D., Doré, J., Floudas, D., Gay, G., Girlanda, M., Henrissat, B., Herrmann, S., Hess, J., Högberg, N., Johansson, T., Khouja, H. R., Labutti, K., Lahrmann, U., Levasseur, A., Lindquist, E. A., Lipzen, A., Marmeisse, R., Martino, E., Murat, C., Ngan, C. Y., Nehls, U., Plett, J. M., Pringle, A., Ohm, R. A., Perotto, S., Peter, M., Riley, R., Rineau, F., Ruytinx, J., Salamov, A., Shah, F.,

Sun, H., Tarkka, M., Tritt, A., Veneault-Fourrey, C., Zuccaro, A., Tunlid, A., Grigoriev, I. V., Hibbett, D. S., and Martin, F. 2015. Convergent losses of decay mechanisms and rapid turnover of symbiosis genes in mycorrhizal mutualists. Nat. Genet. 47:410–415

Koncz, C., and Schell, J. 1986. The promoter of TL-DNA gene 5 controls the tissue-specific expression of chimaeric genes carried by a novel type of Agrobacterium binary vector. MGG Mol. Gen. Genet. 204:383–396

Kottke, I., Guttenberger, M., Hampp, R., and Oberwinkler, F. 1987. An in vitro method for establishing mycorrhizae on coniferous tree seedlings. Trees. 1:191–194

Krenek, P., Samajova, O., Luptovciak, I., Doskocilova, A., Komis, G., and Samaj, J. 2015. Transient plant transformation mediated by Agrobacterium tumefaciens: Principles, methods and applications. Biotechnol. Adv. 33:1024–1042

Kumari, S., and Ware, D. 2013. Genome-wide computational prediction and analysis of core promoter elements across plant monocots and dicots. PLoS One. 8

Kutach, A. K., and Kadonaga, J. T. 2000. The Downstream Promoter Element DPE Appears To Be as Widely Used as the TATA Box in Drosophila Core Promoters . Mol. Cell. Biol. 20:4754–4764

Landschulz, W. H., Johnson, P. F., and Mcknight, S. L. 1988. The Leucine Zipper: A Hypothetical Structure Common to a New Class of DNA Binding Proteins The authors are in the Department of Embryology, Carnegic Institution of Washing-ton. Science (80-.). 240:1759–64

Van Larebeke, N., Engler, G., Holsters, M., Van Den Elsacker, S., Zaenen, I., Schilperoort, R. A., and Schell, J. 1974. Large plasmid in agrobacterium tumefaciens essential for crown gall-inducing ability. Nature. 252:169–170

Lee, L.-Y., and Gelvin, S. B. 2007. T-DNA Binary Vectors and Systems. Plant Physiol. 146:325–332

Lerouge, P., Roche, P., Faucher, C., Maillet, F., Truchet, G., Promé, J. C., and Dénarié, J. 1990. Symbiotic host-specificity of Rhizobium meliloti is determined by a sulphated and acylated glucosamine oligosaccharide signal. Nature. 344:781–784

Lescot, M. 2002. PlantCARE, a database of plant cis-acting regulatory elements and a portal to tools for in silico analysis of promoter sequences. Nucleic Acids Res. 30:325–327

Li, X. 2011. Infiltration of Nicotiana benthamiana Protocol for Transient Expression via Agrobacterium. Bio-Protocol. 53:1689–1699

Lindsey, K., Pullen, M. L., and Topping, J. F. 2003. Importance of plant sterols in pattern formation and hormone signalling. Trends Plant Sci. 8:521–525

Luginbuehl, L. H., and Oldroyd, G. E. D. 2017. Understanding the Arbuscule at the Heart of Endomycorrhizal Symbioses in Plants. Curr. Biol. 27:R952–R963

Ma, J., Wan, D., Duan, B., Bai, X., Bai, Q., Chen, N., and Ma, T. 2019. Genome sequence and genetic transformation of a widely distributed and cultivated poplar. Plant Biotechnol. J. 17:451–460

Mader, M., Le Paslier, M. C., Bounon, R., Bérard, A., Rampant, P. F., Fladung, M., Leplé, J. C., and Kersten, B. 2016. Whole-genome draft assembly of Populus tremula x P. Alba clone INRA 717-1B4. Silvae Genet. 65:74–79

Marand, A. P., Zhang, T., Zhu, B., and Jiang, J. 2017. Towards genome-wide prediction and characterization of enhancers in plants. Biochim. Biophys. Acta - Gene Regul. Mech. 1860:131–139

Martin, F., Aerts, A., Ahrén, D., Brun, A., Danchin, E. G. J., Duchaussoy, F., Gibon, J., Kohler, A., Lindquist, E., Pereda, V., Salamov, A., Shapiro, H. J., Wuyts, J., Blaudez, D., Buée,

M., Brokstein, P., Canbäck, B., Cohen, D., Courty, P. E., Coutinho, P. M., Delaruelle, C., Detter, J. C., Deveau, A., DiFazio, S., Duplessis, S., Fraissinet-Tachet, L., Lucic, E., Frey-Klett, P., Fourrey, C., Feussner, I., Gay, G., Grimwood, J., Hoegger, P. J., Jain, P., Kilaru, S., Labbé, J., Lin, Y. C., Legué, V., Le Tacon, F., Marmeisse, R., Melayah, D., Montanini, B., Muratet, M., Nehls, U., Niculita-Hirzel, H., Secq, M. P. O. Le, Peter, M., Quesneville, H., Rajashekar, B., Reich, M., Rouhier, N., Schmutz, J., Yin, T., Chalot, M., Henrissat, B., Kües, U., Lucas, S., Van De Peer, Y., Podila, G. K., Polle, A., Pukkila, P. J., Richardson, P. M., Rouzé, P., Sanders, I. R., Stajich, J. E., Tunlid, A., Tuskan, G., and Grigoriev, I. V. 2008. The genome of Laccaria bicolor provides insights into mycorrhizal symbiosis. Nature. 452:88–92

Martin, F. M., Uroz, S., and Barker, D. G. 2017. Ancestral alliances: Plant mutualistic symbioses with fungi and bacteria. Science (80-.). 356

McCullen, C. A., and Binns, A. N. 2006. Agrobacterium tumefaciens and Plant Cell Interactions and Activities Required for Interkingdom Macromolecular Transfer . Annu. Rev. Cell Dev. Biol. 22:101–127

Melo, B. P. de, Moura, S. M. de, Morgante, C. V., Pinheiro, D. H., Alves, N. S. F., Rodrigues-Silva, P. L., Lourenço-Tessutti, I. T., Andrade, R. V., Fragoso, R. R., and Grossi-de-Sa, M. F. 2021. Regulated promoters applied to plant engineering: an insight over promising soybean promoters under biotic stress and their cis-elements. Biotechnol. Res. Innov. 5:e2021005

Mohammadi, K., Shiva Khalesro, Sohrabi, Y., and Heidari, G. 2011. A Review : Beneficial Effects of the Mycorrhizal Fungi for Plant Growth. J. Appl. Environ. Biol. Sci. :310–319

Molina, C., and Grotewold, E. 2005. Genome wide analysis of Arabidopsis core promoters. BMC Genomics. 6:1–12

Müller, F., and Tora, L. 2014. Chromatin and DNA sequences in defining promoters for transcription initiation. Biochim. Biophys. Acta - Gene Regul. Mech. 1839:118–128

Murashige, T., and Skoog, F. 1962. A Revised Medium for Rapid Growth and Bio Assays with Tobacco Tissue Cultures. Physiol. Plant. 15:473–497

Mysore, K. S., Nam, J., and Gelvin, S. B. 2000. An Arabidopsis histone H2A mutant is deficient in Agrobacterium T-DNA integration. Proc. Natl. Acad. Sci. U. S. A. 97:948–953

Neb, D. 2017. Bedeutung von SWEET-Genen für den pflanzlichen Zuckerexport in einer Ektomykorrhizasymbiose.

Neb, D., Das, A., Hintelmann, A., and Nehls, U. 2017. Composite poplars: a novel tool for ectomycorrhizal research. Plant Cell Rep. 36:1959–1970

Newell, C. A. 2000. Plant Transformation Technology: Developments and Applications. Mol. Biotechnol. 16:53–66

O'Shea, E. K., Klemm, J. D., Kim, P. S., and Alber, T. 1991. X-ray structure of the GCN4 leucine zipper, a two-stranded, parallel coiled coil. Science (80-.). 254:539–544

Ogbourne, S., and Antalis, T. M. 1998. Transcriptional control and the role of silencers in transcriptional regulation in eukaryotes. Biochem. J. 331:1–14

Oliveira, P., Barriga, J., Cavaleiro, C., Peixe, A., and Potes, A. Z. 2003. Sustained in vitro root development obtained in Pinus pinea L. inoculated with ectomycorrhizal fungi. Forestry. 76:579–587

Padidam, M., and Cao, Y. 2001. Elimination of Transcriptional Interference between Tandem Genes in Plant Cells. Biotechniques. 31:328–334

Pardo, A. G., Kemppainen, M., Valdemoros, D., Duplessis, S., Martin, F., and Tagu, D. 2005. T-DNA transfer from Agrobacterium tumefaciens to the ectomycorrhizal fungus

Pisolithus microcarpus. Rev. Argent. Microbiol. 37:69–72

Pellegrin, C., Daguerre, Y., Ruytinx, J., Guinet, F., Kemppainen, M., Frey, N. F. dit, Puech-Pagès, V., Hecker, A., Pardo, A. G., Martin, F. M., and Veneault-Fourrey, C. 2019. Laccaria bicolor MiSSP8 is a small-secreted protein decisive for the establishment of the ectomycorrhizal symbiosis. Environ. Microbiol. 21:3765–3779

Permyakova, N. V., Shumnyi, V. K., and Deineko, E. V. 2009. Agrobacterium-mediated transformation of plants: Transfer of vector DNA fragments in the plant genome. Russ. J. Genet. 45:266–275

Pieterse, C. M. J., de Jonge, R., and Berendsen, R. L. 2016. The Soil-Borne Supremacy. Trends Plant Sci. 21:171–173

Plett, J. M., Daguerre, Y., Wittulsky, S., Vayssierès, A., Deveau, A., Melton, S. J., Kohler, A., Morrell-Falvey, J. L., Brun, A., Veneault-Fourrey, C., and Martin, F. 2014a. Effector MiSSP7 of the mutualistic fungus Laccaria bicolor stabilizes the Populus JAZ6 protein and represses jasmonic acid (JA) responsive genes. Proc. Natl. Acad. Sci. U. S. A. 111:8299–8304

Plett, J. M., Kemppainen, M., Kale, S. D., Kohler, A., Legué, V., Brun, A., Tyler, B. M., Pardo, A. G., and Martin, F. 2011. A secreted effector protein of laccaria bicolor is required for symbiosis development. Curr. Biol. 21:1197–1203

Plett, J. M., Khachane, A., Ouassou, M., Sundberg, B., Kohler, A., and Martin, F. 2014b. Ethylene and jasmonic acid act as negative modulators during mutualistic symbiosis between Laccaria bicolor and Populus roots. New Phytol. 202:270–286

Plett, J. M., and Martin, F. 2012. Poplar root exudates contain compounds that induce the expression of MiSSP7 in Laccaria bicolor. Plant Signal. Behav. 7:12–15

Plett, J. M., Tisserant, E., Brun, A., Morin, E., Grigoriev, I. V., Kuo, A., Martin, F., and Kohler, A. 2015. The mutualist Laccaria bicolor expresses a core gene regulon during the colonization of diverse host plants and a variable regulon to counteract host-specific defenses. Mol. Plant-Microbe Interact. 28:261–273

Plett, J. M., Yin, H., Mewalal, R., Hu, R., Li, T., Ranjan, P., Jawdy, S., De Paoli, H. C., Butler, G., Burch-Smith, T. M., Guo, H. B., Ju Chen, C., Kohler, A., Anderson, I. C., Labbé, J. L., Martin, F., Tuskan, G. A., and Yang, X. 2017. Populus trichocarpa encodes small, effector-like secreted proteins that are highly induced during mutualistic symbiosis. Sci. Rep. 7:1–13

Plett, K. L., Singan, V. R., Wang, M., Ng, V., Grigoriev, I. V., Martin, F., Plett, J. M., and Anderson, I. C. 2020. Inorganic nitrogen availability alters Eucalyptus grandis receptivity to the ectomycorrhizal fungus Pisolithus albus but not symbiotic nitrogen transfer. New Phytol. 226:221–231

Porto, M. S., Pinheiro, M. P. N., Batista, V. G. L., Dos Santos, R. C., De Albuquerque Melo Filho, P., and De Lima, L. M. 2014. Plant promoters: An approach of structure and function. Mol. Biotechnol. 56:38–49

Read, D. J. 1991. Mycorrhizas in ecosystems. Experientia. 47:376–391

Read, D. J., and Perez-Moreno, J. 2003. Mycorrhizas and nutrient cycling in ecosystems - A journey towards relevance? New Phytol. 157:475–492

Riker, A. J., Banfield, W. M., Wright, W. G., Keitt, G. W., and Sagen, H. E. 1930. Studies on infectious hairy root of nursery apple trees. J. Agric. Res. 41

De Rybel, B., van den Berg, W., Lokerse, A. S., Liao, C.-Y., van Mourik, H., Moller, B., Llavata-Peris, C. I., and Weijers, D. 2011. A Versatile Set of Ligation-Independent Cloning Vectors for Functional Studies in Plants. Plant Physiol. 156:1292–1299

Saravanan, R. S., Slabaugh, E., Singh, V. R., Lapidus, L. J., Haas, T., and Brandizzi, F. 2009. The targeting of the oxysterol-binding protein ORP3a to the endoplasmic reticulum relies on the plant VAP33 homolog PVA12. Plant J. 58:817–830

Savka, M. A., Ravillion, B., Noel, G. R., and Farrand, S. K. 1990. Induction of Hairy Roots on Cultivated Soybean Genotypes and Their Use to Propagate the Soybean Cyst Nematode. Phytopathology. 80:503

Saxonov, S., Berg, P., and Brutlag, D. L. 2006. A genome-wide analysis of CpG dinucleotides in the human genome distinguishes two distinct classes of promoters. Proc. Natl. Acad. Sci. U. S. A. 103:1412–1417

Schnakenberg, J. 2020. Analysis of ectomycorrhiza induced gene expression of selected poplar genes expressed in poplar fine roots.

Schuler, I., Milon, A., Nakatani, Y., Ourisson, G., Albrecht, A. M., Benveniste, P., and Hartmann, M. A. 1991. Differential effects of plant sterols on water permeability and on acyl chain ordering of soybean phosphatidylcholine bilayers. Proc. Natl. Acad. Sci. U. S. A. 88:6926–6930

Shimomura, O., Johnson, F. H., and Saiga, Y. 1962. Extraction, Purification and Properties of Aequorin, a Bioluminescent Protein from the Luminous Hydromedusan,Aequorea. J. Cell. Comp. Physiol. 59:223–239

Smith, E. F., and Townsend, C. O. 1907. A plant tumor of bacterial origin. Science (80-.). 25:671–673

Smith, S., and Read, D. 2008. *Mycorrhizal Symbiosis*. 3rd ed. Academic Press.

Takada, S., and Jürgens, G. 2007. Transcriptional regulation of epidermanl cell fate in the Arabidopsis embryo. Development. 134:1141–1150

Tepfer, D. 1984. Transformation of several species of higher plants by agrobacterium rhizogenes: Sexual transmission of the transformed genotype and phenotype. Cell. 37:959–967

Teste, F. P., Jones, M. D., and Dickie, I. A. 2020. Dual-mycorrhizal plants: their ecology and relevance. New Phytol. 225:1835–1851

Trappe, J. M. 2005. A.B. Frank and mycorrhizae: The challenge to evolutionary and ecologic theory. Mycorrhiza. 15:277–281

Trappe, J. M. 1987. Phylogenetic and ecologic aspects of mycotrophy in the angiosperms from an evolutionary standpoint. Pages 5–25 in: Ecophysiology of VA mycorrhizal plants, G.R. Safir, ed. CRC Press, Boca Raton.

Tuominen, H., Sitbon, F., Jacobsson, C., Sandberg, G., Olsson, O., and Sundberg, B. 1995. Altered Growth and Wood Characteristics in Transgenic Hybrid Aspen Expressing Agrobacterium tumefaciens T-DNA Indoleacetic Acid-Biosynthetic Genes. Plant Physiol. 109:1179–1189

Tuskan, G. A., DiFazio, S., Jansson, S., Bohlmann, J., Grigoriev, I., Hellsten, U., Putnam, N., Ralph, S., Rombauts, S., Salamov, A., Schein, J., Sterck, L., Aerts, A., Bhalerao, R. R., Bhalerao, R. P., Blaudez, D., Boerjan, W., Brun, A., Brunner, A., Busov, V., Campbell, M., Carlson, J., Chalot, M., Chapman, J., Chen, G.-L., Cooper, D., Coutinho, P. M., Couturier, J., Covert, S., Cronk, Q., Cunningham, R., Davis, J., Degroeve, S., Dejardin, A., DePamphilis, C., Detter, J., Dirks, B., Dubchak, I., Duplessis, S., Ehlting, J., Ellis, B., Gendler, K., Goodstein, D., Gribskov, M., Grimwood, J., Groover, A., Gunter, L., Hamberger, B., Heinze, B., Helariutta, Y., Henrissat, B., Holligan, D., Holt, R., Huang, W., Islam-Faridi, N., Jones, S., Jones-Rhoades, M., Jorgensen, R., Joshi, C., Kangasjarvi, J., Karlsson, J., Kelleher, C., Kirkpatrick, R., Kirst, M., Kohler, A., Kalluri, U., Larimer, F.,

Leebens-Mack, J., Leple, J.-C., Locascio, P., Lou, Y., Lucas, S., Martin, F., Montanini, B., Napoli, C., Nelson, D. R., Nelson, C., Nieminen, K., Nilsson, O., Pereda, V., Peter, G., Philippe, R., Pilate, G., Poliakov, A., Razumovskaya, J., Richardson, P., Rinaldi, C., Ritland, K., Rouze, P., Ryaboy, D., Schmutz, J., Schrader, J., Segerman, B., Shin, H., Siddiqui, A., Sterky, F., Terry, A., Tsai, C.-J., Uberbacher, E., Unneberg, P., Vahala, J., Wall, K., Wessler, S., Yang, G., Yin, T., Douglas, C., Marra, M., Sandberg, G., Van de Peer, Y., and Rokhsar, D. 2006. The Genome of Black Cottonwood, Populus trichocarpa (Torr. & Gray). Science (80-.). 313:1596–1604

Tzfira, T., and Citovsky, V. 2008. *Agrobacterium: From Biology to Biotechnology*. T. Tzfira and V. Citovsky, eds. Springer New York, New York, NY.

Umate, P. 2011. Oxysterol binding proteins (OSBPs) and their encoding genes in Arabidopsis and rice. Steroids. 76:524–529

Varma, A., Prasad, R., and Tuteja, N. 2017. Mycorrhiza - function, diversity, state of the art: Fourth edition. Mycorrhiza - Funct. Divers. State Art Fourth Ed. :1–394

Veena, V., and Taylor, C. G. 2007. Agrobacterium rhizogenes: recent developments and promising applications. Vitr. Cell. Dev. Biol. - Plant. 43:383–403

Voß, U., Larrieu, A., and Wells, D. M. 2013. From jellyfish to biosensors: The use of fluorescent proteins in plants. Int. J. Dev. Biol. 57:525–533

Weake, V. M., and Workman, J. L. 2010. Inducible gene expression: Diverse regulatory mechanisms. Nat. Rev. Genet. 11:426–437

Wolfe, B. E., Tulloss, R. E., and Pringle, A. 2012. The irreversible loss of a decomposition pathway marks the single origin of an ectomycorrhizal symbiosis. PLoS One. 7

Xiao, Y., Niu, G., and Kozai, T. 2011. Development and application of photoautotrophic micropropagation plant system. Plant Cell. Tissue Organ Cult. 105:149–158

Yamamoto, Y. Y., Yoshioka, Y., Hyakumachi, M., and Obokata, J. 2011. Characteristics of core promoter types with respect to gene structure and expression in arabidopsis thaliana. DNA Res. 18:333–342

Yan, D., and Olkkonen, V. M. 2008. Characteristics of Oxysterol Binding Proteins. Int. Rev. Cytol. 265:253–285

Yu, K., Pieterse, C. M. J., Bakker, P. A. H. M., and Berendsen, R. L. 2019. Beneficial microbes going underground of root immunity. Plant Cell Environ. 42:2860–2870

Zangi, M., Amini-bayat, Z., Ehsani, P., and Ofoghi, H. 2019. Original Research Article Replication of pgR107 binary Ti vector without pSoup helper plasmid in disarmed Agrobacterium tumefaciens LBA4404. 3:19–28

Zuo, Y. C., and Li, Q. Z. 2011. Identification of TATA and TATA-less promoters in plant genomes by integrating diversity measure, GC-Skew and DNA geometric flexibility. Genomics. 97:112–120

9 List of abbreviations

µm	Mikrometer
35S promoter	Promoter of the cauliflower mosaic virus
ATP	Adenosine triphosphate
bp	base pair
BRE	Transcription factor II B recocnition element
BSA	Bovine serum albumin
CAS	CRISPR Associated
cDNA	complementary DNA
cis	Latin for "on this side"
cLSM	Confocal laser scanning microscope
CRISPR	Clustered regularly interspaced short palindromic repeats
CTAB	Hexadecyltrimethyl ammoniumbromide
dCTP	Deoxycytidine triphosphate
ddH_2O	double distilled water
DEPC	Diethyl dicarbonate
dGTP	Deoxyguanosine triphosphate
DNA	Desoxy ribonucleic acid
DTT	Dithiothreitol
ECM	Ectomycorrhiza
EDTA	Ethylenediaminetetraacetic acid
gDNA	Genomic DNA
GFP	Green fluorescent protein
HCL	Hydrochloric acid
kb	Kilo base pair
kDA	Kilodalton
LB	Lysogeny broth
LIC	Ligase independent cloning
MES	2-(N-morpholino)ethanesulfonic acid
MISSP	Mycorrhizal induced small secreted proteins
MMN	Minimal medium nitrogen
MOPS	3-(N-Morpholino)propansulfonicacid
NLS	Nuclear localisation sequence
NOS	nopaline synthase
NptII	Kanamycine resistance gene
NRE	Negative regulatory element
nt	Nucleotide
OCS	Octopine synthase gene
OD	Optical densitiy
ori	Origin of replication
OSBP	Oxysterol binding protein
P	Promoter

PCR	Polymerase chain reaction
pmol	Picomol
P$_{UBQ}$	Arabidopsis ubiquitin promoter
qPCR	Quantitiative real time polymerase chain reaction
Ri	Root inducing
RNA	Ribonucleotide
rol	Root oncogenic loci
SDS	Sodium dodecyl sulfate
seq	sequencing
SNL	Peroxisomal localisation sequence
T	Terminator
TBP	TATA binding protein
tDNA	transfer DNA
Ti	Tumour inducing
Tm	Melting temperature
vir	virulence
YFP	Yellow fluorescent protein

10 Eidesstattliche Erklärung

Universität Bremen | Fachbereich 02 | Postfach 33 04 40, 28334 Bremen

Universität Bremen

Fachbereich 2

Prüfungsamt Chemie

z. Hd. Frau Frauke Ernst

Leobener Straße

Prüfungsamt
Chemie

Frauke Ernst
Geschäftsstelle
Fachbereich 02
Leobener Str. / NW2
D-28359 Bremen

Verwaltungspavillon 06
Tel. 0421 218-62802
Fax 0421 218-9862802
frauke.ernst@uni-bremen.de
www.fb2.uni-bremen.de

Versicherung an Eides Statt

Ich, Jana Müller,

versichere an Eides Statt durch meine Unterschrift, dass ich die vorstehende Arbeit selbständig und ohne fremde Hilfe angefertigt und alle Stellen, die ich wörtlich dem Sinne nach aus Veröffentlichungen entnommen habe, als solche kenntlich gemacht habe, mich auch keiner anderen als der angegebenen Literatur oder sonstiger Hilfsmittel bedient habe.
Ich versichere an Eides Statt, dass ich die vorgenannten Angaben nach bestem Wissen und Gewissen gemacht habe und dass die Angaben der Wahrheit entsprechen und ich nichts verschwiegen habe.
Die Strafbarkeit einer falschen eidesstattlichen Versicherung ist mir bekannt, namentlich die Strafandrohung gemäß § 156 StGB bis zu drei Jahren Freiheitsstrafe oder Geldstrafe bei vorsätzlicher Begehung der Tat bzw. gemäß § 161 Abs. 1 StGB bis zu einem Jahr Freiheitsstrafe oder Geldstrafe bei fahrlässiger Begehung.

Bremen,

Ort, Datum / Unterschrift

11 Supplemented data

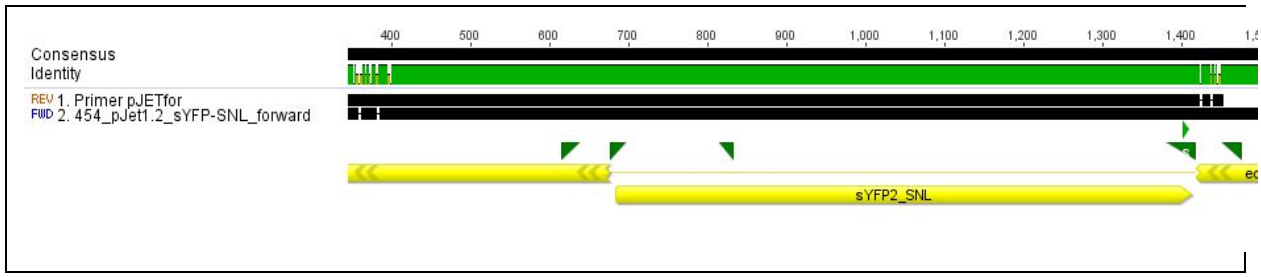

Figure 36: Sequencing result of pJET_1.2_sYFP-SNL. All sequencing reactions were performed by Macrogen (Amsterdam, Netherlands). Sequencing confirmed the correct sequence of sYFP-SNL and revealed integration in forward orientation.

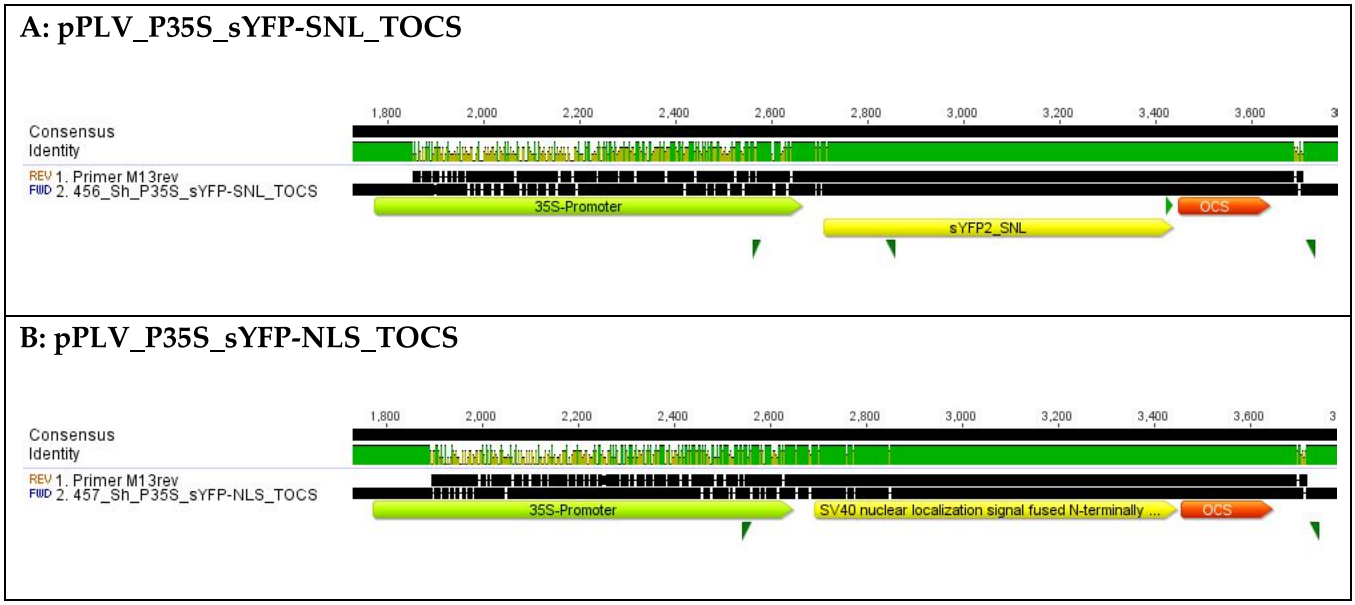

Figure 37: Sequencing results of pPLV_P35S_sYFP-SNL_TOCS (**A**) & pPLV_P35S_sYFP-NLS_TOCS (**B**) confirming correct integration of the respective YFP constructs.

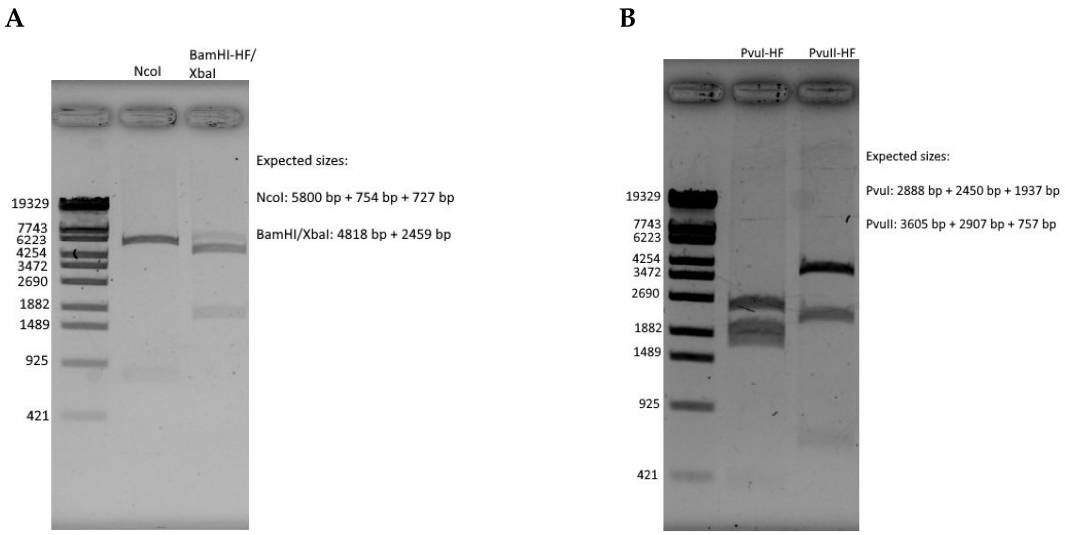

Figure 38: pPLV04 digested with different endonucleases. . **A:** pPLV04 digested with NcoI (lane 1) and a combination of BamHI-HF and XbaI (lane 2). **B:** pPLV04 digested with PvuI-HF (lane 1) and PvuII-HF (lane 2). Lambda DNA digested with StyI was used as a molecular marker.

A

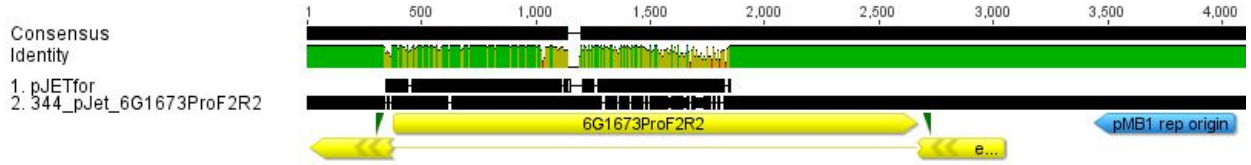

B

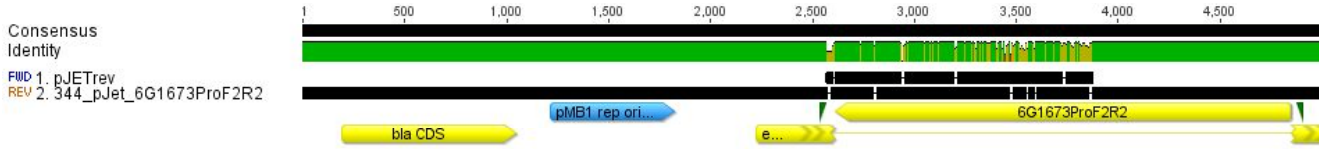

C

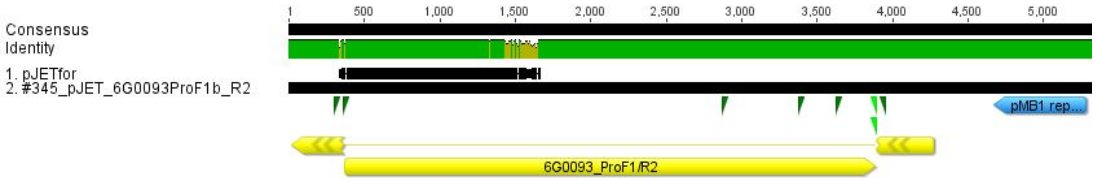

D

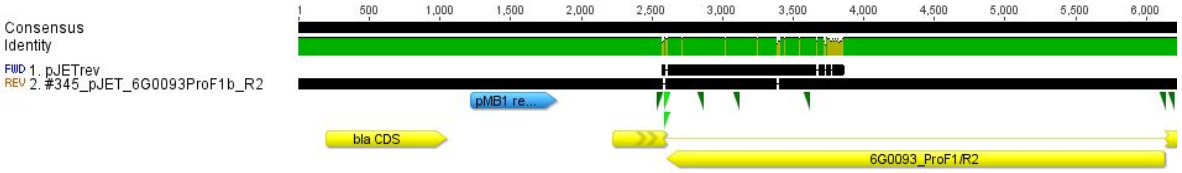

E

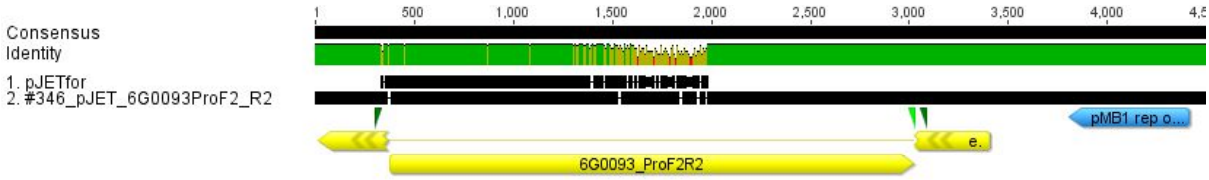

F

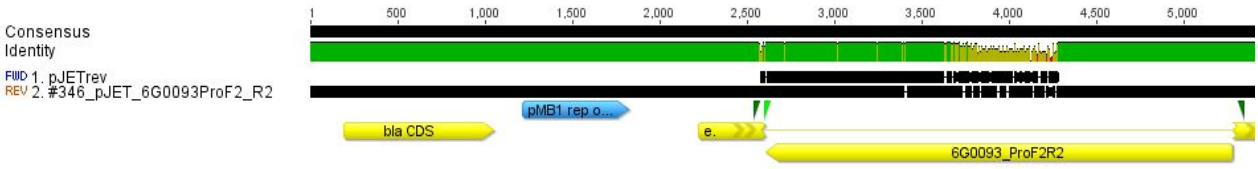

Figure 39: Sequencing results of different pJET_promoter constructs. All sequencing reactions were performed by Macrogen (Amsterdam, Netherlands). A & B: Sequencing results of pJET1.2_6G1673ProF2_R2 with pJETfor (A) and pJETrev (B). C & D: Sequencing results of pJET1.2_6G0093ProF1b/R2 with pJETfor (C) and pJETrev (D). E & F: Sequencing results of pJET1.2_6G0093ProF2/R2 with pJETfor (E) and pJETrev (F).

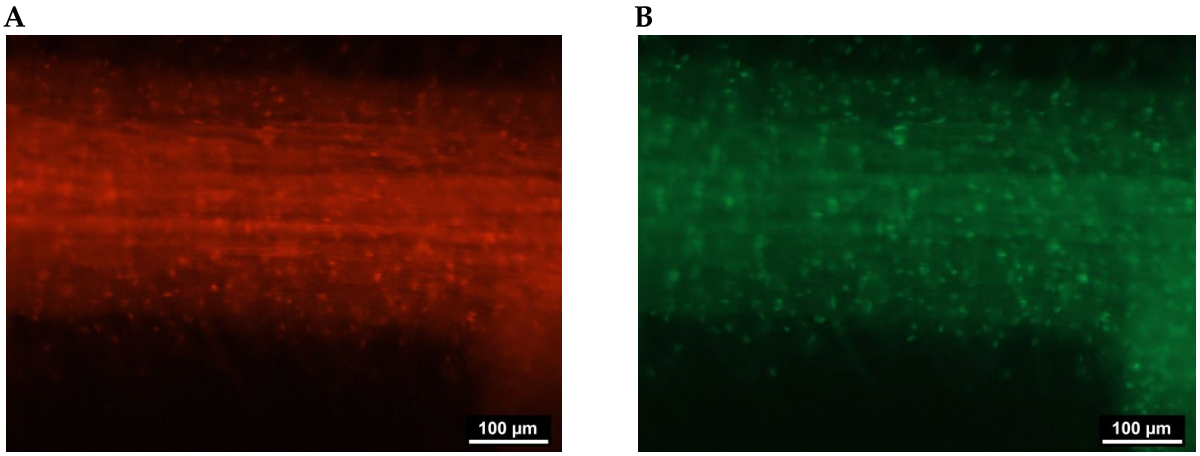

pCXUN_6G1673_1kb in *P. tremula x tremuloides*

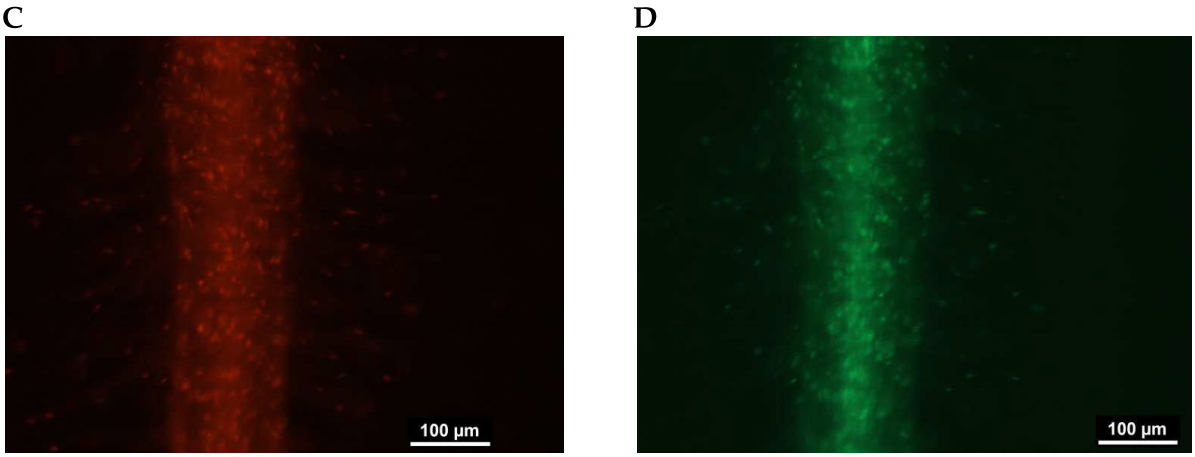

pCXUN_6G1673_500bp in *P. tremula x tremuloides*

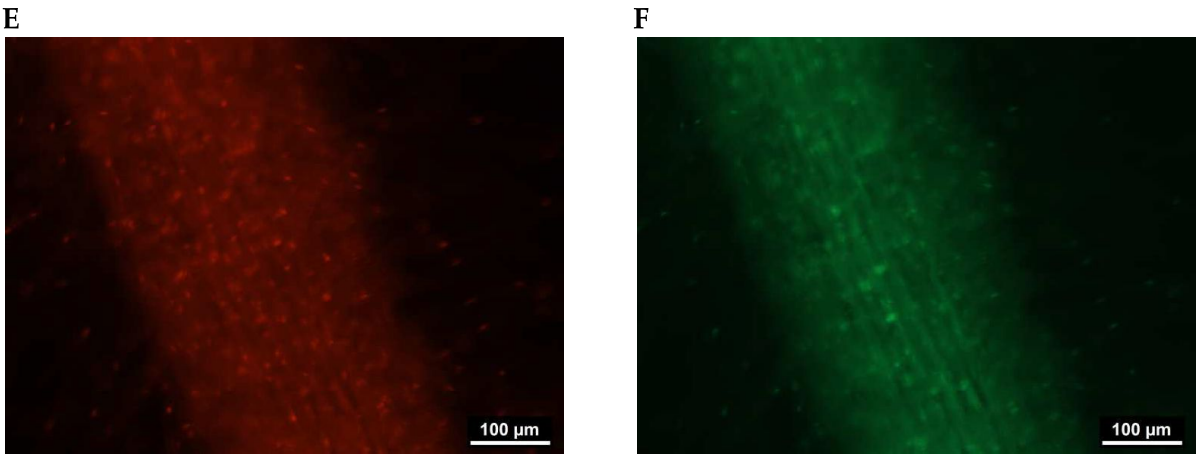

pCXUN_6G1673_250bp in *P. tremula x tremuloides*

Figure 40: Fluorescence microscopy of *P. tremula x tremuloides* roots transformed with different promoter fragments of pCXUN_6G1673. Both fluorescence markers were targeted to the nucleus. The pictures were taken 4 weeks after transforming the roots with *A. rhizogenes K599*. **A/B:** pCXUN_6G1673_2.2kb. A: red channel, 2 sec exposure time. B: GFP channel, 1 sec exposure time. **C/D:** pCXUN_6G1673_1kb C: red channel, 2 sec exposure time and D GFP channel with 2 sec exposure time. **E/F:** pCXUN_6G1673_500bp. E: red channel with 2 sec exposure time and F: GFP channel with 2 sec exposure time. **G/H:** pCXUN_6G1673_250bp. G: red channel with 3 sec exposure time and H: GFP channel with 3 sec exposure time.

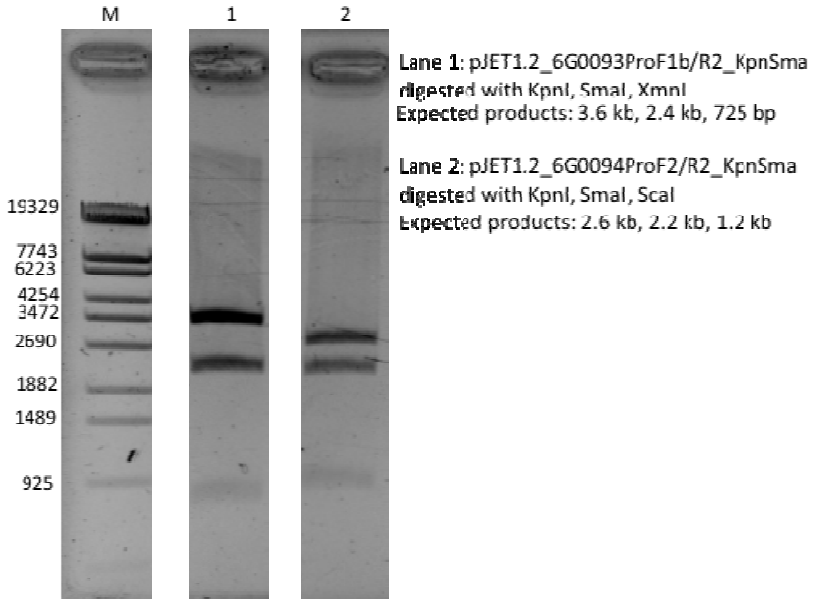

Figure 41: Verification of pJET_6G0093 promoter constructs with additional KpnI and SmaI recognition sites.

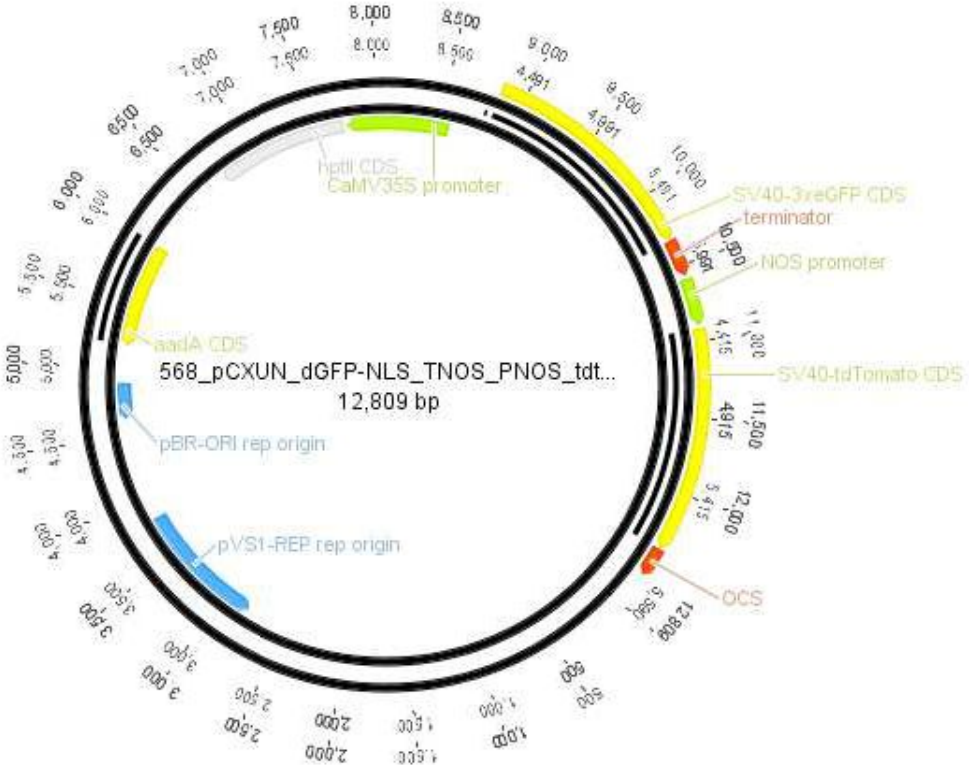

Figure 42: Vector map of pCXUN_dGFP-NLS_TNOS_PNOS_tdtomato-NLS_TOCS.

12 Acknowledgement

Der Weg ist das Ziel.

Konfuzius (551 – 479 v. Chr.)

Ich möchte mich an dieser Stelle bei allen bedanken, die mich auf meinem Dissertationsweg begleitet und unterstützt haben.